DISSERTATION

BIOCHEMICAL AND BIOLOGICAL ROLES OF RIBOSOME-INACTIVATING PROTEIN

Submitted by

Sang-Wook Park

Department of Horticulture and Landscape Architecture

In partial fulfillment of the requirements
For the Degree of Doctor of Philosophy
Colorado State University
Fort Collins, Colorado
Spring 2004

COLORADO STATE UNIVERSITY

May 5, 2004

WE HEREBY RECOMMEND THAT THE DISSERTATION PREPARED UNDER OUR SUPERVISION BY SANG-WOOK PARK ENTITLED BIOCHEMICAL AND BIOLOGICAL ROLES OF RIBOSOME-INACTIVATING PROTEIN BE ACCEPTED AS FULFILLING IN PART REQUIREMENTS FOR THE DEGREE OF DOCTOR OF PHILOSOPHY.

Committee on Graduate Work

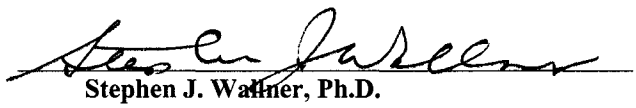

Stephen J. Wallner, Ph.D.

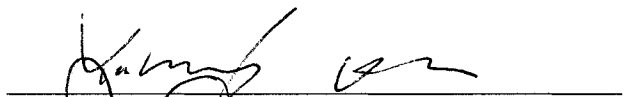

Yaling Qian, Ph.D.

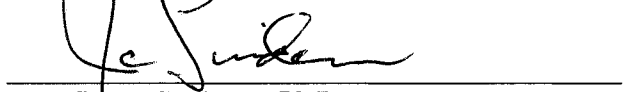

James C. Linden, Ph.D.

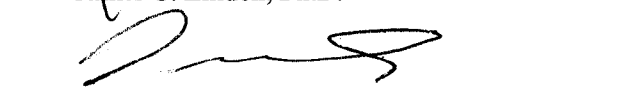

Jorge M. Vivanco, Ph.D. (Advisor)

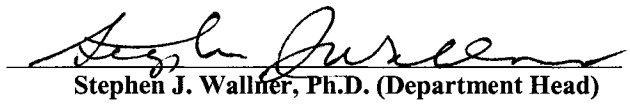

Stephen J. Wallner, Ph.D. (Department Head)

ABSTRACT OF DISSERTATION

BIOCHEMICAL AND BIOLOGICAL ROLES OF RIBOSOME-INACTIVATING PROTEINS

Ribosome-inactivating proteins (RIPs) are a group of plant cytotoxic *N*-glycosidases that specifically cleave nucleotide N-C glycosidic bonds. It has been proposed that RIPs inhibit protein synthesis by virtue of their enzymatic activity, selectively removing a specific adenine residue from the highly conserved and surface-exposed α-sarcin/ricin (S/R) loop in the large rRNA. This enzymatic cleavage prevents the binding of the EF-2/GTP complex to the ribosome, with the subsequent arrest of protein synthesis, and, eventually, cell death.

In the present study, a novel type-1 RIP, termed PAP-H, was purified from *Agrobacterium rhizogenes*-transformed hairy roots of *Phytolacca americana*, and biochemically characterized. PAP-H was determined to be 29.5 kD, and its full-length cDNA sequence has 1,125 nucleotides with an open reading frame of 1074 nucleotides representing 339 amino acids (Genebank, accession number AY071928). Further, PAP-H was found to be localized in the cell walls of hairy roots and root border cells using immuno-fluorescence microscopy, and was determined to be constitutively secreted as part of the root exudates, with its secretion enhanced by a mechanism mediated by ethylene induction. By secretion into the rhizosphere, PAP-H penetrates and inhibits the growth of soil-borne fungi by a synergetic combination of chitinase, *β*-1,3-glucanase, and protease within root exudates. To further understand the antifungal mechanism of RIPs, I have examined three type I RIPs to determine their substrate specificities on fungal ribosomes, and I have correlated the data with their antifungal activity. The results provide experimental evidence that the enzymatic activity and specificity of RIPs are separated from their

cytotoxicity. In addition, using protein-fluorescence labeling technology, I have found that RIPs selectively recognize, interact with, and are internalized into fungal cells to exert cytotoxicity.

The final stage of this research focused on investigating the enzymatic interaction of the RIP ME_1 (from *Mirabilis expansa*) with non-ribosomal substrates upon their structural modification. The RIP-RNA/ RIP-DNA interactions was found to depend on the secondary structure of substrates, and did not require any sequence or structure motif. RIP targeted only single-stranded regions of nucleic acid, removing adenine and, to a lesser extent, guanine residues. In addition, RIP was capable of recognizing and depurinating a pathogenic RNA transcript, completely abolishing its infectivity. Subsequently, we examined the activity of ME_1 toward *M. expansa* ribosomes in the presence of increasing concentrations of small synthetic oligonucleotides ($^{23}SSO\text{-}A_{12}$), indicating that the long-considered only substrate of RIP, the ribosome, is unlikely be the primary target in plant systems.

Sang-Wook Park

Department of Horticulture and Landscape Architecture

Colorado State University

Fort Collins, CO 80526

Spring 2004

ACKONWLEDGEMENTS

I would like to express my appreciation to my dissertation advisor Dr. Jorge M. Vivanco for giving me the opportunity to pursue my Ph.D. experiment in his laboratory. I would also like to thank Drs. Stephen J. Wallner, Yaling Qian, and James C. Linden for feely sharing their time, kind consideration, and expertise as members of my graduate committee.

I am thankful to co-authors of my studies, Drs. Ramarao Vepachedu, Robert A Owens, and Christopher B. Lawrence, for their great amount of personal and scientific advice, guidance, and their willingness to lend a helping hand whenever I needed it. I would like to express special appreciation to Dr. Ramarao Vepachedu for his every support and guidance. I am also deeply grateful to Travis S. Walker for his understanding, help and friendship. I would like to acknowledge other members of the Vivanco's laboratory (Hope Gruszewske and Drs. Neelam Sharma and Harsh P. Bais) for making this time a memorable experience in my life.

I would like to express my gratitude to my greatest friend and the mentor of my life, Richard J. Cernek, for his support and encouragement during all of my endeavors. I would also appreciate my family, most notably my mother-in-law, Young-Sook Cheon, for her endless understanding and encouragement.

DEDICATION

I dedicate this research in loving memory to my wife, Sang-Mi Lee.

TABLE OF CONTENTS

LIST OF TABLES

LIST OF FIGURES

CHAPTER 1

Revisiting Ribosome-Inactivating Proteins in Plant Biology

INTRODUCTION

Ribosome-inactivating proteins (RIPs) are cytotoxic enzymes identified in plants, fungi and bacteria, which act as *N*-glycosidases that specifically cleave nucleotide N-C glycosidic bonds (Endo et al., 1987). It has been proposed that RIPs inhibit protein synthesis by virtue of their enzymatic activity, selectively removing a specific adenine residue from the highly conserved and surface-exposed α-sarcin/ricin (S/R) loop in the large rRNA (Endo et al., 1987; Endo and Tsurugi, 1987; Hartley et al, 1991). This enzymatic cleavage prevents the binding of the EF-2/GTP complex to the ribosome, with the subsequent arrest of protein synthesis, and, eventually, cell death (Osborn and Hartley, 1990). For the last few decades, RIPs have been the subject of much biological and biochemical research due to their unique properties and activities, which could potentially lead to diverse applications in veterinary and medical research (for a comprehensive review, see van Damme et al., 2001).

Apart from *in vitro* characterized ribosome-inactivating (RI) activity, the biological function and role of RIPs *in planta* remains open to speculation. There has been no unequivocal answer, so far, to the question of why plants synthesize and accumulate RIPs. One possible answer could be their defensive role against various pathogenic invasions (for review, see Nielsen and Boston, 2001). Although several lines of evidence support this hypothesis, this subject is also largely unexplored. This chapter will summarize the recent research progress on RIPs in order to further our understanding of the biological significance and relevance in plant systems.

STRUCTURE CLASSIFICATION

RIPs are regarded as either single-chain (Type I) or double-chain proteins (Type II). Type II RIPs, such as ricin (from *Ricinus communis*) and abrin (from *Abrus precatorius*), contain a B-chain with a galactose-binding domain linking to a biologically active A-chain through a disulfide bond (Stirpe et al., 1992). The galactose-binding domain enables the attachment of type II RIPs to galactose receptors on the cell membrane and the internalization of the active chain (Steeves et al., 1999). The type I RIPs PAP (from *Phytolacca americana*) and saporin (from *Saponaria officinalis*) are monomeric and basic proteins with approximate molecular weights of

30,000; they contain a number of highly conserved amino acid residues (Funatsu et al., 1991; Barbieri et al., 1993). However, they do not possess sequence homology overall, and also have differences at the posttranslational modification level (Hartley and Lord, 1993).

OCCURRENCE OF RIPS IN PLANTS

RIPs have been found in about one hundred plant species covering twenty families. RIPs have been identified not only in several exotic plants, but also in crop plants such as wheat, maize, and barley (for review, see van Damme et al., 2001). Originally, however, it was thought that RIPs did not occur universally among plant species (for review, see Peumans et al., 2001). This was evidenced by the failure to identify RIPs in several plants used as so-called model systems, such as *Arabidopsis thaliana* and *Nicotiana tabacum*, in spite of repeated attempts to do so.

The biochemical properties of RIPs have been well characterized, more so than their biological functions *in planta*. A critical reason why the biological role of RIPs *in planta* has been poorly elucidated is, again, the lack of information about this group of enzymes from any model plant system. Recently, a 26 kDa RIP-like protein termed TRIP containing *N*-glycosidase activity was isolated and characterized from *N. tabacum* (Sharma et al., 2004). TRIP was found to be expressed at very low levels in the leaf (0.01% of total starting materials). This low level of expression could be a reason for the long-standing failure to identify an RIP from this model plant system. The identification of TRIP could raise the possibility that all plant systems, including *A. thaliana*, possess one or more *N*-glycosidases, and could thus accelerate the understanding of RIPs by allowing us to bring the abundance of biological information available from a model system to bear on the question of RIPs' biological role in plants.

CLASSICAL ENZYMATIC ACTIVITY

RIPs are presently classified as rRNA *N*-glycosidases in the enzyme nomenclature [EC 3.2.2.22]. Several studies using the ricin A-chain (RTA) have suggested that RIPs specifically cleave the N-C glycosidic bond of the adenine base in the tetra loop sequence (GAGA) located on the sarcin/ricin (S/R) loop of eukaryotic and prokaryotic ribosomes. The universally conserved

adenine residue A_{4324} of the eukaryotic 28S rRNA (and A_{2660} in the prokaryotic 23S rRNA) has long been considered the only enzymatic target site for RIPs (Endo et al., 1987; Endo and Tsurugi, 1997), but several lines of evidence have recently revealed alternative substrates to the S/R loop (discussed below in the section titled "Alternative Roles of RIPs").

Several studies have suggested that RIP catalytic activity requires a specific substrate structure such as a tetraloop with the sequence $^{(1)}G^{(2)}A^{(3)}G^{(4)}A$ (Endo and Tsurugi, 1988; Marchant and Hartley, 1995; Orita et al., 1993). The stem of this structure possesses tilted Watson-Crick base-paring in the stem with an unusual $^{(1)}G$:$^{(4)}A$ base-pairing in the loop region (Orita et al., 1993; Szewczak et al., 1993). The depurination-site adenine ($^{(2)}A$) occupies an exposed position external to the solvent-accessible loop, while the other nucleotide bases are buried within the phosphodiester backbone by hydrogen-bonding and base-stacking.

The RI activity of RIPs is substrate-specific against intact ribosomes isolated from different sources (Endo and Tsurugi, 1997; Krawetz and Boston, 2000; Park et al., 2002b). These substrate specificities of RIPs are thought to be due to the ribosomal proteins, as the rRNA target loop is universally conserved. Later studies have suggested that the ribosomal protein L3 is a critical element for the binding of RIPs to ribosomes, and the subsequent depurination of rRNA (Hudak et al., 1999). It has been shown that a mutation in the L3 protein, a highly conserved protein located at the peptidyl transferase center of ribosomes, results in failure of the RI activity of PAP (Uchiumi et al., 1999).

NOVEL ENZYMATIC ACTIVITIES

During recent years, there has been an increasing controversy as to whether or not some RIPs possess enzymatic activities in addition to *N*-glycosidase. Most of these novel enzymatic activities of RIPs are RNase and DNase activities (for reviews, see Peumans et al., 2001). In addition to these, some RIPs have been shown to have superoxide dismutase (SOD, Li et al., 1997), phospholipase (Helmy et al., 1999), and chitinase (Remi Shih et al., 1997) activities. At first all of these novel enzymatic activities were thought to be due to impurities (for review, see Peumans et al., 2001). Finally, however, working despite such controversial reports (Day et al.,

1998, Valbonesi et al., 1999, Barbieri et al., 2000), Tumer and her colleagues (1999; 2000) re-examined and confirmed DNase and RNase activities in PAP using highly purified protein, minimizing the chances of contamination. The DNase activity of the cinnamomin A-chain (from *Cinnamomum camphora*, Ling et al., 1994, 1995) has been also re-confirmed using *Escherichia coli*-expressed recombinant RIP (He and Liu, 2004). The deletion mutants of the cinnamomin A-chain further demonstrated that *N*-terminal 52 or/and *C*-terminal 51 amino acid residues are responsible for both *N*-glycosidase and DNase activities. Calcaelin (from *Calvatia caelata*) is somewhat different from RIPs in its sequence, but was found to inhibit translation in rabbit reticulocyte lysate in assumption of *N*-glycosidase activity, and to display a heat-labile RNase activity (Ng et al., 2003). The SOD activity reported for the camphorin (type I RIP from *Cinnamomum camphora*) was not possible to prove, due to the lack of conclusive information about the sequence studies (Li et al., 1997). Interestingly, TRIP has SOD activity in addition to *N*-glycosidase activity, and its internal amino acid sequence showed exact sequence homology with the Fe-SOD found in *Nicotiana plumbaginifolia, Solanum tuberosum*, and Arabidopsis (Sharma et al., 2004). Although TRIP has RI activity, it did not show any sequence homology with well-known RIPs. Conversely, Fe-SOD isolated from *E. coli* also showed *N*-glycosidase activity toward *Saccharomyces cerevisiae* ribosomes along with its superoxide scavenging activity, which unequivocally proves that some RIPs showing SOD activity could not be the result of contamination as described by Peumans et al. (2001); rather, we need to look into all existing data about these proteins to fully understand their biological functions. Taken together, these observations suggest that RIPs may possess dual biochemical activities and multiple biological roles. These novel insights have renewed biological interest in RIPs because of the potential for diverse functions *in planta* of the possible primary/secondary roles of RIPs.

ANTIMICROBIAL ACTIVITY

In plants, RIPs are considered to be defense-related proteins because RIPs deadenylate ribosomes from all organisms tested. Furthermore, the expression of several RIPs in transgenic plants provides resistance against several plant pathogens.

Antiviral Activity

Despite differences in virus infection mechanisms, a number of RIPs show broad-spectrum antiviral activity against both plant and animal viruses including a human immunodeficiency virus (HIV). Since McGrath and coworkers provided evidence in 1989 that trichosanthin (TCS from *Trichosanthes kirilowii*) is a potent inhibitor of HIV-1 replication, GAP31 (from *Gelonium multiflorum*) and MAP30 (from *Momordica charantia*) have also been identified as having inhibitory action against HIV-1 (Lee-Huang et al., 1994; 1995). Au and coworkers (2000) finally demonstrated strong anti-HIV-1 activity using several common plant RIPs including saporin, TCS, agrostin, gelonin, luffin, and α-momorcharin.

Among RIPs, antiviral activity has been best described for PAP. Since PAP-containing extracts from the leaves of *P. americana* was shown to have potent antiviral activities against cucumber mosaic virus and influenza virus (Tomlinson et al., 1974), several researchers have gone on to discover various viral targets for PAP, including poliovirus (Ussery et al., 1977), herpes simplex virus (Aron et al., 1980), HIV (Zarling et al., 1990), and tobacco mosaic virus (Taylor et al., 1994). Furthermore, transgenic tobacco expressing PAP and its mutants has offered the possibility of developing a plant's resistance to a broad spectrum of plant viruses (Lodge et al., 1993), and a recent study provides direct evidence that three different PAP isoforms (PAP from spring leaves, PAP-II from early summer leaves, and PAP-III from late summer leaves) cause concentration-dependent depurination of genomic RNA purified from HIV-I, TMV, and bacteriophage (MS 2) (Rajamohan et al., 1999a). Further experiments revealed that PAP is able to directly depurinate selective viral mRNA that have a 5' terminal m^7GpppG cap; in contrast, PAP has no significant effect on uncapped mRNAs (Hudak et al. 2000, 2002). From these observations, the authors hypothesized that during viral infection, PAP may target selective viral RNAs by binding to the cap analog.

Antifungal Activity

Several RIPs have shown inhibitory activity against the growth of various pathogenic and non-pathogenic fungi such as *Alternaria solani*, *A. alternaria*, *Botrytis cinerea*, *Fusarium oxysporum*, *F. proliferatum*, *Mycosphaerella arachidicola*, *Neurospora crassa*, *Phycomyces*

blakesleeanus, *Pythium irregulare*, *Physalospora piricola*, *Trichomera reesei*, and *Verticillium dahliae* (for review, see Nielsen and Boston, 2001). Although the antifungal activity of RIPs has been explained by their potent RI activity toward fungal ribosomes (Tumer et al., 1997), the actual action mechanism has not yet been understood.

Some RIPs such as hypsin (from *Hypsizigus marmoreus*) and lyophyllin (from *Lyophyllum shimeji*) interestingly showed synergism in their antifungal effects together with other antifungal proteins (e.g. *Lyophyllum* antifungal protein, Lam et al., 2001 a,b). The recently isolated PAP-H (from *Agrobacterium rhizogenes*-transformed hairy roots of *P. americana*) also showed the traces of inhibitory activity against several fungal pathogens by virtue of a synergetic effect in the presence of other PR proteins (chitinase and β-1,3-glucanase, Park et al., 2002a). Facilitating this possible synergetic effect, disease resistance in transgenic tobacco plants was manifested by enhanced antifungal activity when the barley RIP was constitutively co-expressed with barley class II chitinase (Jach et al., 1995). The combination of barley endosperm RIP with barley class II chitinase produced a significant increase in resistance to *Rhizotonia solani* in transgenic tobacco. Both transgenic proteins (RIP + chitinase) accumulated in the intercellular spaces of transgenic tobacco, and it was postulated that the cytotoxic effect of the barley RIP on fungal cells was enhanced by chitinase action resulting in an increased amount of RIP entering fungal cells. Maize RIP, b-32, under control of the potato *wun1* gene promoter, also increased the tolerance of transgenic tobacco to *R. solani* (Maddaloni et al., 1997).

Antibacterial Activity

The biological activity of RIPs against bacteria has been suggested but not well characterized (Vivanco et al., 1999). ME_1 and ME_2 (type I RIPs from *Mirabilis expansa*) were tested against 27 soil-borne bacterial species, and inhibitory activity was found against eight of them. Among these bacteria, there were nonpathogenic species, such as *Bacillus subtilis*, *Rhizobium leguminosarum*, and *Serratia marcescens*, and pathogenic species, *Pseudomonas syringae*, *A. tumerfaciens*, *A. rhizogenes* R100nal, *Xanthomonas campestris* pv *versicatoria*, and *Erwinia carotovora*. It is believed that the antibacterial activity of RIPs is similar to RIP-mediated fungal inhibition.

CLASSIC THEORY OF ANTIMICROBIAL MECHANISM

The defense mechanism of RIPs in plants was explained previously by the so-called "suicide model" similar to the hypersensitive response (HR) (for review, see Tumer et al., 1997). The inhibitory mechanism of RIPs against microbial-pathogens has been postulated based on the evidence and mechanistic information available from PAP and its isoform (Ready et al., 1986; Park et al., 2002a). Based on the RI activity and the extracellular localization of PAP, it has been described that RIPs are synthesized in an inactive form, sequestered in the cell wall matrix, and re-enter the cytoplasm along with the pathogen at the infection sites (Fig.1.1). Thus, RIPs inhibit pathogen multiplication by inactivating host ribosomes and causing host cell death. However, the antimicrobial activity and mechanism of RIPs are gaining new attention through recent studies.

REVISITING ANTIMICROBIAL MECHANISM

As discussed, the widely accepted mechanism for antimicrobial action identifies host ribosomes as the target of RIP activity. However, no evidence has been discovered that would prove this suicidal mechanism. Several experiments with transgenic plants expressing RIPs also do not exhibit HR or other symptoms of spontaneous cell death in response to microbial infection - even though they are resistant to a wide range of pathogens. In addition, no pathogen has been reported to evoke the suicidal machinery in any plant system producing RIP(s).

Several independent studies suggest that the antimicrobial activity of RIPs can be independent from the enzymatic activity of RIPs inactivating ribosomes of the plant host. The earliest demonstrations were made by Tumer and her colleagues who assayed deletion mutants of PAP in transgenic tobacco plants (Zoubenko et al., 1997; 2000, Tumer et al., 1997). Although PAPc ($PAP_{W327stop}$) and PAPn (PAP_{G75D}) were unable to depurinate the S/R loop, they still conferred resistance against plant viral and fungal pathogens. Further experiments revealed that PAP is able to directly depurinate selective viral mRNA that have a 5' terminal m^7GpppG cap; in contrast, PAP has no significant effect on uncapped mRNAs (Hudak et al., 2000, 2002). From these observations, the authors hypothesized that during viral infection, PAP may target selective

viral RNAs by binding to the cap instead of inactivating host ribosomes. Recently, the inhibitory mechanism of RIPs against HIV replication that has generally been believed to relate to RI activity was also readdressed (Wang et al., 2003). Site-directed mutagenesis approaches using TCS demonstrated that the classical RI activity of TCS is not adequate to explain the anti-HIV action of TCS. In this study, an exception was demonstrated such that TCS mutants with a C-terminal deletion or addition of amino acids retained almost all RI activity, but were devoid of anti-HIV activity. This result demonstrates that the C-terminus region of TCS is responsible for anti-HIV activity, and suggests that the defensive mechanism of RIPs against pathogens can be separated from RI activity.

As for the inhibitory mechanism of RIPs against fungal pathogens, more and more evidence has shown that RIPs can directly target and inhibit fungal growth rather than depurinating host plant ribosomes and causing cell death. The type I $RIPs_x$ ME_1, hypsin, lyophyllin, and hispin (*Benincasa hispida*) have demonstrated a direct inhibitory activity against an array of pathogenic and nonpathogenic fungi (Vivanco et al., 1999; Lam and Ng, 2001 a, b; Park et al., 2002b; Ng and Parkash, 2002). This fungal cytotoxicity has also been shown to be independent from RI activity (Park et al., 2002b). Comparing three different RIPs, ME_1, RTA, and saporin-S6 (isoform of saporin), the latter two showed approximately 10 to 50-fold higher enzymatic activity against isolated fungal ribosomes than did ME_1. Nevertheless, ME_1 showed higher inhibitory activity against fungal growth itself compared to RTA and saporin-S6. A study with transgenic tobacco plants expressing PAP and its mutants also demonstrated that the RI activity of RIP is not sufficient for host resistance to the fungal pathogen (Zoubenko et al., 1997). To further understand the antifungal mechanism of RIPs, ME_1 and saporin-S6 were labeled with NHS-fluorescein and the interaction between labeled RIPs and fungal cells was monitored (Park et al., 2002b). A labeled ME_1 showed strong interaction with fungal hyphae, translocated within the septa, and presumably penetrated into the cytosolic region, in contrast to no interaction observed between labeled saporin-S6 and fungi. This indicates that some type I RIPs, lacking any known carbohydrate-binding domain, are capable of interacting with the target cell surface. Taken together, these results (Fig.1.1) indicate that i) the RI activity of RIPs does not adequately explain

their defensive action against pathogens, ii) the defensive action of RIPs is independent from their enzymatic specificity, iii) some RIPs are able to recognize and target selective pathogens by possibly binding to cell membrane components, and finally iv) the defense mechanism of RIPs could proceed by directly targeting invading pathogens rather than host ribosomes.

CROSS-TALK BY RIPS IN PLANT DEFENSE SIGNALING

Plants employ complex responses to cope with biological and environmental stresses. Wounds on host plants may provide an entry for pathogens, especially for viruses and bacteria that could not otherwise penetrate the plant cell wall. Upon wounding, plants respond by inducing a diverse array of defense-related genes to protect themselves against pathogenic infection (Bowles, 1990). It has been suggested that the wound-related signaling pathway involves a number of signaling molecules, such as systemin, jasmonic acid (JA), methyl-jasmonate (MeJA), abscisic acid (ABA), benzoic acid (BA), salicylic acid (SA), ethylene, lipoxygenase (LOX), lipid peroxides, and other phytoalexins (Schaller and Ryan, 1995; Hammond-Kosack and Jones, 1996; Koiwa et al., 1997; Wasternack and Parthier, 1997; Dong, 1998; Reymond and Farmer 1998; Ryan and Pearce, 1998, Ohme-Takagi et al., 2000). These signaling molecules induce synthesis of PR proteins leading to plant resistance and systemic acquired resistance (SAR) (Hammond-Kosack and Jones, 1996). Although a number of signaling molecules that accompany pathogen recognition and defense responses of plants have been recognized to induce PR proteins, only a minimal amount has been determined about the induction of RIPs. Since plants mostly share the same signaling pathways for pathogen-defense and for stress-related responses, some studies have addressed the induction of RIPs caused by stress and stress-related compounds such as JA, osmotic stress or heat shock, salt shock, and abscisic acid (Reinbothe S. et al., 1994, Reinbothe C. et al., 1997; Stripe et al., 1996; Rippmann et al., 1997).

In barley, four groups of prominent jasmonate-induced proteins (JIPs) were identified (Andresen et al., 1992; Becker and Apel, 1992; Reinbothe S. et al. 1992 ab; Reinbothe C. et al., 1994). Among these JIPs, JIP60 was identified as an RIP involved in the general down-regulation of the protein biosynthetic machinery in long-term MeJA-treated or long-term-stressed leaf tissues

(Becker and Apel, 1992; Chaudhry et al., 1994; Reinbothe S. et al., 1994; Reinbothe C. et al., 1997; Dunaeva et al., 1999). JIP60 was found to be located in the cytosol and to target translational machinery leading to a decay of cytoplasmic polysomes in response to long-term MeJA-treatment of barley leaves (Reinbothe C. et al., 1997; Dunaeva et al., 1999). Interestingly, pathogen attack induced the synthesis of MeJA as a signal molecule, thus depressing protein synthesis at the initial transaltion step (Reinbothe S. et al., 1993).

Recently, Song et al. (2000) reported that *P. incularis* antiviral protein 2 (PIP2) is induced by mechanical wounding. Furthermore, the wound induction of the PIP2 gene was systemic as a general PR, and the PIP2 gene was increased in a systemic manner after treatment with JA and ABA. Therefore, although the expressional induction of RIPs has not been well characterized, we believe that the production of RIPs is systemically induced upon several environmental and biological stresses including pathogen-related signal transduction. Interestingly, root-specific PAP-H was enhanced in its secretion into the rhizosphere by ethylene (Park et al., 2002a). Exogenous challenge as well as endogenous production of ethylene caused a significant enhancement in the root-secretion of PAP-H. This evidence suggests that the secretion of PAP-H from plant roots into the rhizosphere may be induced under ethylene regulation. Ethylene is rapidly induced in response to environmental stress, including infection by pathogens, and is biologically active at a very low concentration (Taiz and Zeiger, 1991; for a review, see Ohme-Takagi, 2000). Chen et al. (2001) has recently reported that the ethylene receptor-like protein ETR1 is located in the endoplasmic reticulum (ER) membrane. Since PAP-H shows strong secretory induction by ethylene treatment and is assumed to be secreted through the ER, it has been suggested that ethylene induced by biological stresses binds to the receptor protein at the ER membrane initiating a downstream signaling cascade to activate the PAP-H secretory pathway as a defense mechanism.

ALTERNATIVE ROLES FOR RIPS

In contrast to the possibility of a defensive role, a recent research has suggested that the biological role of RIPs may be strictly to inactivate host ribosomes in response to potential

exogenous challenges. The identification of a novel enzyme, named ribosomal RNA apurinic site specific lyase (RALyase), re-emphasized the RI activity of RIPs (Ogasawara et al., 1999). It has been reported that RALyase specifically cleaves the phosphodiester bond at the 3' side of the apurinic site introduced by RIPs into the S/R loop of rRNA. The presence of RALyase for the complete termination of the elongation step after RIP action hypothetically proves that RIPs are biologically designed to inhibit protein synthesis in their own organ. The authors proposed that the cleavage of the plant S/R loop induces some apoptosis-like responses, including the degradation of the ribosomes (depurinated or not) and/or down-regulation of other cellular functions, which could prevent the infecting pathogen, if any, from growing (Ozawa et al., 2003).

Other possible explanations of the biological role of RIPs could be derived from the increasing evidence for their ability to interact with non-ribosomal substrates. As previously mentioned, the universally conserved adenine residue from sequence GAGA located on S/R loop of large ribosomes was long considered to be the only enzymatic site of RIPs, but several lines of recent research have revealed alternative substrates to the S/R loop. For instance, it has been shown that several RIPs can release adenine from multiple sites in rRNA (Barbieri et al., 1992). Furthermore, saporin-L1 can release adenine residues from a variety of nucleic acid substrates - poly(A), mRNA, tRNA, and DNA (Barbieri et al., 1994, 1996). More than fifty other RIPs are active on DNA (Barbieri et al., 1997). In addition to nucleic acid molecules, several RIPs exhibited activity against poly(ADP-ribosyl)ated poly(ADP-ribose) polymerase (auto modified enzyme, Barbieri et al., 2003). This ability to affect various substrates could allow RIPs to control important cellular functions, as well as ensure the survival of the tissue expressing them.

PROGRESS ON THERAPEUTIC APPLICATION OF RIPS AGAINST CANCER

The target specificity of monoclonal antibodies has induced the development of immunotoxins which deliver toxins, such as RIPs, to specific cells. PAP has been used to generate an immunotoxin which prevents the growth of leukemia cells (Ramakrishnan and Houston, 1984). Human CD19+ mixed lineage leukemia cells (RS4-11) proliferate in the hematopoietic tissues and other organs of mice with severe combined immunodeficiency in a manner similar to human acute

leukemia. PAP was linked to specific antibodies (anti-CD19-Pokeweed antiviral protein immunotoxin) selectively inhibited clonegenic RS4,11 cells *in vitro*. This immunotoxin was able to extend the life span of the mice inoculated with RS4,11 cells (Jansen et al., 1992). Furthermore, studies with the anti-CD19(B-43)-PAP immunotoxin on human B-cell precursor leukemia in SCID mice indicate that it provides significant protection (Messinger et al., 1996). When this immunotoxin was used along with ara-C, an arabinose nucleoside anologue of deoxycytidine against human B-cell precursor leukemia in SCID mice, it produced 100% long-term event free survival from an otherwise invariably fatal leukemia (Messinger et al., 1996). Preclinical trials with anti anti-CD-19(B-43)-PAP in cynomolgus monkeys have shown that monkeys exhibited a dose dependent immune response to both IgG and PAP moieties of the immunotoxin. However, (B-43)-PAP is well tolerated with no significant clinical or laboratory toxicity effects at dose levels between 0.007 to 0.7 $mg \cdot kg^{-1}$. At higher dose levels (3.5–7.0 $mg \cdot kg^{-1}$), the immunotoxin caused renal toxicity as a result of renal tubular necrosis (Uckun et al., 1997).

Another relatively successful immunotoxin is TP3-PAP. This antibody (TP3) is reactive against an antigen on human and canine osteosarcoma. This tumor-associated antigen is expressed at very high levels on the surface membrane of human osteosarcoma cells (Bruland et al., 1988), and the antibody (IgG2b anti-P80, TP3) reacts with mesenchymal tumors like osteosarcomas, hemangiopericytomas, chondrosarcomas, malignant fibrous histiocytomas and synovial cell sarcomas (Bruland et al., 1986). Studies with TP3 attached to PAP (TP3-PAP) showed high activity against osteosarcoma cells *in vitro*, killing all the culture cells after 48 hours. When this immunotoxin was given i.p. (intraperitoneal) after three to five days of tumor inoculation in mice, a dose dependent reduction of lung metastases was observed (Anderson et al., 1995). Studies by Ek et al. (1998) on the clinical potential of TP3-PAP have indicated that toxicity in BALB/c mice can be observed at doses of 3 $mg \cdot kg^{-1}$ (LD50) and higher. The histopathological lesions were dose dependent and appear above 2 $mg \cdot kg^{-1}$ dose levels. The lesions include necrosis of cardiac and skeletal muscle fibers and mineralization of muscle fibers. Mild kidney damage with necrotic tubules was also seen. Antitumor studies of TP3-PAP in mice have shown that 1 $mg \cdot kg^{-1}$ cumulative doses gave excellent protection and none of the SCID (severe combined

immunodeficient) mice treated with TP3-PAP at this dose level developed tumors for up to 110 days after inoculation with OHS (human osteosarcoma cells). In contrast mice treated with chemotherapeutic agents like adriamycin, methotrexate or cyclophosphamide developed tumors within 45 days. Neither the TP3 nor PAP individually could give any protection under similar conditions.

Finally, studies with immunotoxins prepared by linking momordin 1, PAP-S and saporin-s6 to the monoclonal antibodies 48-127, which recognize a glycoprotein (gp54) expressed in human bladder carcinomas, have shown that RIPs linked to those antibodies are effective against bladder tumor cell lines (T24) (Battellinet et al., 1996). The same three RIPs linked to Ber-H2 monoclonal antibodies directed against CD30 antigen of human lymphocytes induced apoptosis in CD30 cell lines (Bolognesi et al., 1996). Further RIP gelanin was also shown to be effective on malarial parasites when linked to human transferin (Surolia and Misquith, 1996). These studies indicate that RIPs have the potential to be very effective antitumor drugs when linked to proper targeting antibodies.

SUMMARY

In spite of being investigated for decades as a tool to facilitate toxicity, the role and function of RIPs in plants and their distribution in nature remain enigmatic. Using a recently identified RIP from the model system *N. tabacum* in corroboration with biotechnological approaches, such as mutagenesis and silencing, and genomic approaches, could be an effective way to bridge the gaps in our knowledge. Furthermore, the discovery of novel enzymatic activities could indicate some RIPs' dynamic participation in various cellular mechanisms in response to various exogenous environments. New insights into the defense mechanisms of RIPs and their additional non-ribosomal substrates have also begun to increase our understanding of properties important for protecting organs and regulating cellular functions of host cells. Such varied approaches will likely accelerate our knowledge of the biological function of RIPs and establish their fundamental significance for medicinal applications in the next few years.

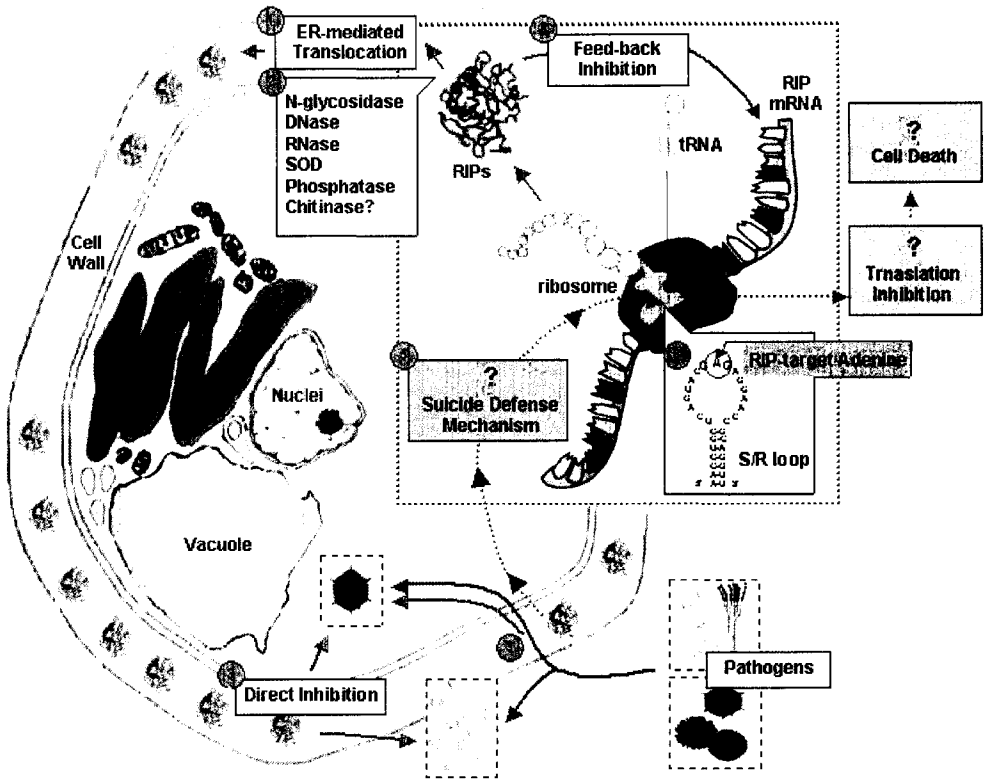

Figure 1.1. Proposed model showing the direct defensive mechanism of RIPs against invasive viral and fungal pathogens. **1.** RIPs are compartmentalized into cell walls via ER-mediated translocation. **2.** Some RIPs possess dual enzymatic activities: the classical *N*-glycosidase activity and a novel enzymatic activity. **3.** Upon infection, RIPs directly target the pathogens either in cytosolic or extracellular regions, and inhibit the growth of pathogens. The defense mechanism is separated from the classic RI activity of RIPs. **4.** RIPs are able to destabilize their own mRNA after their levels are up-regulated by a mechanism that occurs independently of rRNA depurination and translation, probably by direct depurination of mRNA. **5.** The originally proposed suicidal defense mechanism of RIPs. Pathogen infection is thought to alter the structure of the host cell, allowing RIPs to gain access to the ribosomes and leading to the arrest of protein synthesis and cell death. **6.** The enzymatic target site of RIPs in the S/R loop. The universally conserved adenine residue A_{4324} of the eukaryotic 28S rRNA was long considered to be the only enzymatic substrate of RIPs, but several lines of evidence have recently revealed alternative substrates to the S/R loop.

CHAPTER 2

Isolation and Characterization of a Novel Ribosome-Inactivating Protein from Root Cultures of *Phytolacca americana* and Its Mechanism of Secretion from Roots

ABSTRACT

In the present study, a novel type-1 RIP, termed PAP-H, was purified from *A. rhizogenes*-transformed hairy roots of *P. americana*. The protein was purified by anion and cation exchange chromatography. PAP-H has a molecular weight of 29.5 kD as detected by sodium dodecyl sulfate polyacrylamide gel electrophoresis (SDS-PAGE), and its isoelectric point was determined to be 7.8. Yeast ribosomes incubated with PAP-H released the 360-nucleotide diagnostic fragment from the 26S rRNA upon aniline treatment, an indication of its ribosome-inactivating activity. Using immuno-fluorescence microscopy, PAP-H was found to be located in the cell walls of hairy roots and root border cells. PAP-H was determined to be constitutively secreted as part of the root exudates, with its secretion enhanced by a mechanism mediated by ethylene induction. Purified PAP-H did not show *in vitro* antifungal activity against soil-borne fungi. In contrast, root exudates containing PAP-H as well as additional chitinase, β-1,3-glucanase, and protease activities did inhibit the growth of soil-borne fungi. I found that PAP-H depurinates fungal ribosomes *in vitro* and *in vivo,* suggesting an additive mechanism that enables PAP-H to penetrate fungal cells.

INTRODUCTION

P. americana (pokeweed) produces a suite of constitutive and induced RIPs in its leaves and seeds. For instance, PAP is a 29 kDa constitutive RIP found in pokeweed leaves and localized in the cell wall matrix of leaf mesophyll cells (Irvin, 1975, 1980; Ready et al., 1986; Lin et al., 1991). PAP II is a seasonal 30 kDa RIP found in pokeweed leaves harvested in late summer (Irvin et al., 1980), and PAP-S (29.8 kDa) is expressed in seeds (Barbieri et al., 1982). Amino acid comparisons show 80% homology of PAP with PAP-S, and 33% homology of PAP with PAP II. Accordingly, PAP-S cross-reacts with PAP antibodies, but PAP II does not react with PAP antibodies (Barbieri et al., 1982). PAP is thought to play a defense role since it depurinates ribosomes from all organisms tested, and because its expression in transgenic tobacco plants leads to resistance against viral and fungal infection (Lodge et al., 1993, Zoubenko et al., 1997). However, a clear understanding of the role of PAP in *P. americana* has not been achieved.

To better understand the functional significance of RIPs in *P. americana,* I developed a hairy root system for the expression and manipulation of constitutive RIPs. Hairy roots show stable expression of root-specific biosynthetic pathways, and thus have been used as an experimental system to study the biology and biochemistry of underground organs (Flores and Curtis, 1992; Flores et al., 1999). Plant roots synthesize and store various macromolecules, including storage and defense-related proteins such as chitinase and β-1,3-glucanase, to cope with pathogenic challenge (Mauch et al., 1988; Linthorst, 1991; Savary and Flores, 1994; Savary et al., 1997). Here I report the identification of a novel RIP, termed PAP-H, located in the cell walls of hairy roots and root border cells of *P. americana.* PAP-H was also found to be constitutively secreted as part of the root exudates, and its secretion was enhanced by elicitation with ethylene. Hairy root exudates of *P. americana* containing PAP-H and other defense-related proteins showed strong antifungal activity against fungi causing root rot. We have previously reported that *in vitro* root secretions of secondary metabolites and proteins compare with root secretions under natural settings (Flores et al., 1999), suggesting that *P. americana* may secrete RIPs into the soil. This paper reveals a new mechanism by which roots are able to secrete RIPs into the rhizosphere to prevent pathogen infection.

MATERIALS AND METHODS

Plant Material

Seeds of *P. americana* were collected in New Brunswick (New Jersey). Seeds were washed five times with sterile water and germinated on filter papers on a petri-dish. The seeds were then transferred to pots and placed in the greenhouse.

Establishment of *A. rhizogenes*-Transformed Hairy Roots of *P. americana*

Shoots from *P. americana* were collected from greenhouse-grown plants and surface-sterilized with 10% (v/v) commercial bleach for 15 min and then washed 4 times with sterile water. Shoot cultures were placed separately in Magenta GA-7 vessels containing Murashige and Skoog (MS) basal medium (Murashige and Skoog, 1962) solidified with 0.3% Phytagel (Sigma).

Cultures were kept in a light chamber maintained at 24 °C with a light intensity of 100 μmole $m^{-2}s^{-1}$ PAR. In order to produce hairy root cultures, one-month-old *in vitro* plants were infected with a 3-d old culture of *A. rhizogenes* (ATCC 15834) grown in TY medium at 30 °C (Verveliet et al., 1975). Briefly, stems of *P. americana* were punctured in several places with *A. rhizogenes* and then placed in a light chamber. Roots that developed at the infection sites were transferred to petri dishes containing solid MS medium supplemented with 250 $\mu g \cdot ml^{-1}$ Claforan (Hoechst-Roussel Pharmaceuticals) and kept in the dark chamber at 24 °C. After 14 d, 1 cm root tips were subcultured twice to eradicate excess bacteria before transferring them to fresh medium in the absence of antibiotic. Clonal root lines established after serial transfers of root tips to fresh MS medium were subcultured into 125 ml Erlenmeyer flasks containing 50 ml liquid MS medium and placed on a gyratory shaker set at 90 rpm in a dark chamber.

Protein Extraction from Hairy Roots

Hairy roots of *P. americana* were immersed in liquid N_2 and ground to a powder using a mortar and pestle. Ground root tissue was dissolved into two volumes of extraction buffer (25 mM $NaPO_4$, pH 7.0 with 250 mM NaCl, 10 mM EDTA, 5 mM DTT, 1 mM PMSF, and 1.5% [w/v] PVPP), homogenized, and centrifuged for 30 min at 10,000g. The supernatant was brought to 20% (w/v) ammonium sulfate, and centrifuged again for 20 min at 10,000g. The supernatant was dialyzed against 20 mM $NaPO_4$ buffer (pH 7.0) until it was free from sulfate ion. All extraction procedures were conducted at 4 °C, and the crude extract was stored at 4 °C until use.

Electrophoresis and Western-Blot Analysis

SDS-PAGE gel electrophoresis was performed with 12% (v/v) acrylamide discontinuous gels (Laemmli, 1970) using an electrophoresis cell (Mini-Protein® 3 Cell; Bio-Rad), according to manufacturer's instructions. Low molecular weight protein markers (21.1~110 kD; Bio-Rad) were run simultaneously for each electrophoresis gel. The gel was stained with Coomasie® brilliant blue R-250 (EM Science). Proteins were electroblotted to Immun-Blot™ PVDF membranes (Bio-Rad) using a Mini Trans-Blot® Electrophoretic Transfer Cell (Bio-Rad, Hercules,

CA). The blot was then probed with protein A-purified polyclonal rabbit anti-PAP antibody obtained from Dr. Nilgun Tumer (Rutgers University), and the membranes were developed using Opti-4CN™ Detection Kit purchased from Bio-Rad, following the manufacturer's instructions. An antiserum titer of 1:1000 was used for all experiments.

Chromatography and Isoelectric Focusing

Ion exchange separation was performed using Sep-Pack® Plus Cartridges (Waters). Waters Accell™ Plus QMAs were equilibrated with 20 mM Na_3PO_4 buffer (pH 7.0), and the flow-through solution containing unretained (basic) proteins was collected. Basic proteins were applied to Waters Accell™ Plus CMs equilibrated with 20 mM $NaPO_4$ buffer (pH 7.0), and unbound (acidic) proteins were collected. Basic proteins were eluted with step gradients from 40 to 600 mM of NaCl. The target protein was resolved in the 80 mM fraction. The 80 mM fraction was dialyzed against 20 mM $NaPO_4$ buffer (pH 7.0) and subsequently separated by cation-exchange chromatography using a UNO™ S1 column (Bio-Rad). Diluted protein solutions and fractions were concentrated by ultrafiltration using a Stirred Ultrafiltration Cell 8050 (Amicon, Millipore). Protein purity and peak size were confirmed by SDS-PAGE stained with Coomasie® brilliant blue R-250 (EM Science) and Silver Stain Plus (Bio-Rad). Protein concentration was determined by the Bradford method (1976) using a protein assay kit purchased from Bio-Rad.

The pI of purified PAP-H was estimated by isoelectric focusing (IEF) using a Mini-Protean® II 2-D Cell (Bio-Rad) with Bio-Lyte® ampholytes (pH range 3 to 10; Bio-Rad) following manufacturer's instructions. Second dimension was performed in an SDS-PAGE gel with 12% (v/v) acrylamide gel using a Mini-Protein® 3 Cell (Bio-Rad), and stained with Silver Stain Plus (Bio-Rad).

N-terminal Sequencing and Amino Acid Analysis

The purified protein was N-terminally sequenced on a Precise Protein Sequencer System (Applied Biosystems) at the Macromolecular Resources Facility in the Department of

Biochemistry (Colorado State University). Amino acid analysis and composition were obtained by the Protein Structure Core Facility at the University of Nebraska.

Isolation of Ribosomes and rRNA Depurination Assay

Yeast (*Saccharomyces cerevisiae*) strain YPH500 (Sikorski and Hieter, 1989) was grown in YPD medium, and fungi, *T. reesei* and *R. solani*, were grown in potato dextrose media. Yeast was then pelleted by centrifugation and mycelial tissue of *T. reesei* and *R. solani* were collected by vacuum-filtration. To isolate ribosomes, 10 g of pelleted yeast and fungal hyphae were ground in a mortar with liquid N_2, and dissolved in 100 ml of extraction buffer (200 mM KCl, 25 mM $MgCl_2$, 25 mM EGTA, 200 mM Sucrose and 25 mM β-mercaptoethanol in 200 mM Tris-HCl, pH 9.0). The supernatant, collected by centrifugation at 10,000 g for 20 min at 4 °C, was pipetted onto a sucrose cushion (1 M sucrose, 20 mM KCL and 5 mM $MgCl_2$ in 25 mM Tris-HCl, pH 7.6) in 70 Ti tubes (Beckman), and centrifuged at 55,000 rpm for 4 h at 4 °C (L-70 Ultracentrifuge, Beckman). The pellets were resuspended in 25mM Tris-HCl buffer (pH 7.6) with 25mM KCl and 5mM $MgCl_2$, and stored at –80 °C.

The depurination assay was conducted according to Tumer et al. (1997). Briefly, ribosomes were resuspended in RIP buffer (167 mM KCl, 100 mM $MgCl_2$, 100 mM Tris-HCl, pH 7.2,) and incubated with RIPs at 30 °C for 30 min in a total volume of 100μl. RNA incubated in the absence of RIPs served as a negative control. Following incubation, the RIPs were removed from the mixture by phenol:chloroform extraction and the RNA was divided in half. Half of the extracted RNA was incubated on ice for 30 min with 1 M of aniline acetate (pH 4.5) and precipitated with ethanol. Both aniline- treated and untreated RNAs were subjected to electrophoresis in a 7 M urea/ 6% polyacrylamide gel and stained with ethidium bromide.

cDNA Cloning of PAP-H

Total RNA was isolated from hairy roots of *P. americana* using RNeasy® Plant Mini Kit (QIAGEN) according to manufacturer's instructions. cDNA was cloned by the RACE PCR method using the SMART™ RACE cDNA Amplification kit following the manufacturer's

instructions (Clontech). To amplify the 3' end of the PAP-H cDNA(s), two gene specific primers (GSPs, 5'-CCT TCG ATG TTG GAA GTG CAA CCA TTA GC, and 5'-GGA AGT GCA ACC ATT AGC AAG TAT ACC ACC) were designed based on the N-terminal amino acid sequence of the purified PAP-H protein and considering codon preferences in previously cloned PAP-related genes from *P. americana*. PCR reactions were performed in a GeneAmp System 2400 (Applied Biosystems) as follows: 94 °C for 1 min; 30 cycles of 94 °C for 5 sec, 68 °C for 10 sec, and 72 °C for 3 min. The nucleotide sequences of the GSPs used for 5'-RACE (5'-TGG CAA CCA ATA GGA ATC CTG CCT CGG and 5'-TGG CAA CCA ATA GGA ATC CTG CCT CGG) were designed based on the nucleotide sequences derived from the 3'-RACE product. The second PCR was performed as follows: 32 cycles of 94 °C for 5 sec, 60 °C for 10 sec, and 72 °C for 3 min. Each PCR product was purified using Quantum Prep Gel Slice Kit (Bio-Rad), and cloned into pCR®4Blunt-TOPO® or pCR®4TA-TOPO® (Invitrogen) for sequencing. The DNA sequencing was performed using an ABI Prism 377 DNA Sequencer (Applied Biosystems) at the Macromolecular Resources Facility in the Department of Biochemistry (Colorado State University).

Microscopy

The tips of hairy root tissues were cut into 2 mm segments and fixed for 1 hr at 4 °C with 1.5% formaldehyde in Sorenson's phosphate buffer [SPB] (0.03M of sodium phosphate monobasic and 0.12M of sodium phosphate dibasic, pH 7.5). Samples were placed into gelatin capsules containing 15% gelatin solution, and overlaid with one or two drops of the gelatin solution by gentle pipetting. The gelatin capsules containing samples were incubated for 24 hr at 4 °C to be polymerized. After the resins were completely polymerized, gelatin blocks were removed from the capsules, and sections were cut 30 to 50 μm thick in pre-chilled SPB using a Vibratome (Sorvall MT2-B, Porter Blum). The sections were placed on slides and allowed to adhere for a few seconds. A drop of 50mM glycine was added and sections were incubated for approximately 10 min. After washing twice with SPB, the sections were incubated with blocking buffer [LBB] (10% goat serum and 1% triton-x) for 30min at 4 °C, and incubated overnight with

diluted PAP primary antibody (1:1000) in LBB at 4 °C in dark. Negative controls were incubated with only LBB under the same conditions. After 17 hr, the sections were rinsed with LBB 4 times for 10 min at 4 °C, and incubated with fluorescein goat anti-rabbit IgG (1:1000 dilution in LBB; Molecular Probes, Eugene, OR) for 4 hr in dark at 4 °C. The sections were washed with LBB again and SPB was used as a final wash. The sections were then mounted with antifade reagent (SlowFade® Antifade Kit; Molecular Probes, Eugene) in glycerol/PBS and sealed, and fluorescent images were taken using a microscope (JEOL 2000 EXII). PAP antibodies were obtained from Dr. Nilgun Tumer (Rutgers University).

Preparation of Proteins from Liquid Media

Root cultures grown in liquid media were vacuum filtered with a 0.8 μm Cellulose Nitrate Membrane filter (Whatman®), and the media were supplementary filtered to avoid debris using 0.22 μm Millex-GP syringe-driven filter (Millipore). The samples were precipitated with trichloroacetic acid (TCA) according to the method of Peterson (1977). Briefly, to each 1 ml of sample containing approximately 5 to 100 mg of protein, 100 μl of Na-deoxycholate was added and incubated for 10 min at room temperature. Then, 100 μl of 72% TCA was dispensed, mixed and incubated on ice for 15 min and centrifuged for 10 min. The supernatants were immediately removed, and the pellets were washed three times with ice-cold acetone. Pellets were then dissolved in SDS-PAGE sample buffer (Laemmli, 1970).

Elicitation Experiments and Ethylene Measurement

Hairy roots of *P. americana* grown for 30 d were transferred into 50 ml of fresh MS media, and treated with air, ethylene, and air + methylcyclopropane (MCP, Biotechnologies for Horticulture). Air treatment was performed using an air-permeable-silicon cap, and ethylene treatment was conducted by feeding 10 ppm ethylene gas into a flask connected to a gas mixing apparatus (Mirjalili and Linden, 1995) at a total flow rate of 15 $ml \cdot min^{-1}$; air was used as the balance gas. These flasks were connected by means of a second tubing to remove effluent gas outside of the incubator. MCP was added as powder at a final concentration of 20 ppm. Each

treatment was incubated on a gyratory shaker in a dark chamber for a week and 2 ml of each culture media was collected daily for 6 d. Collected samples were stored at 4 °C and concentrated using TCA precipitation (Peterson, 1977).

Ethylene was measured on a Hewlett Packard model 5840A gas chromatography system equipped with a flame ionization detector (FID). An Alltech Porapak N (6 ft, 0.2 mm i.d., Stainless Steel) column was used at 75 °C. The injection port and detector temperatures were 90 °C and 180 °C, respectively; the mobile gas was helium at 20 $ml \cdot min^{-1}$; sample size was 0.1 ml.

Antifungal Assay

Antifungal activity of purified and exudated proteins was determined by a radial growth-inhibition assay adapted from the method of Schlumbum et al. (1986). Various fungal plugs were placed in the center of potato-dextrose-agar plates, and sterile paper discs were placed next to the fungal plugs. 50 μg of each protein, which was sterilized using Ultrafree-MC Sterile (0.22 μm GV Durapore, Millipore), was pipetted onto the discs. The plates were then incubated in the dark at room temperature. Antifungal activity was observed as a crescent-shaped zone of inhibition at the mycelial front. The effect on fungal growth was expressed qualitatively, according to the procedure of Schlumbaum et al. (1986).

Enzyme Activity Determinations

A colorimetric assay for chitinase and β–1,3-glucanase activities in root exudates, with chitinase azure and laminarin azure as substrates, was performed as described by Qiu et al. (1997). The reaction mixture contained 550 μl of H_2O, 200 μl of substrate (4 $mg \cdot ml^{-1}$ in 0.2 M sodium acetate buffer, pH 5.0), and 50 μl of root exudates (1 $mg \cdot ml^{-1}$). After incubating the mixtures at 37 °C for 5 min, 200 μl of 1 N HCl was added, placed on ice for 10 min, and centrifuged for 5 min at 12,000 g. The resulting supernatants (900 μl) were measured spectrophotometrically at 550 nm. All assays were performed in triplicate, and blanks were prepared without the addition of root exudates during incubation. Enzymatic activities were calculated according to Wirth and Wolf

(1992) and expressed as international units per milligram protein. One international unit (U) is defined as the amount of enzyme required to catalyze the formation of 1 nmol product per minute.

Zymogram Ready Gel was used for proteolytic activity. A 10% SDS-PAGE gel containing gelatin (Bio-Rad, Hercules, CA) was used and electrophoresis was performed according to the manufacture's instructions. Following electrophoretic separation, the gel was incubated at room temperature for 30 min in 100 ml of 2.5% Triton X-100 with agitation, and incubated overnight at 37 °C in 100 ml of development buffer (50 mM of Tris-base, 200 mM of NaCl, 5 mM of $CaCl_2$ anhydrous, and 0.02% of Brij-35, pH 7.5). The gel was then stained with 0.5% Coomasie® brilliant blue R-250 (EM Science).

RESULTS

Development of *P. americana* Hairy Roots

The transformation of *P. americana* with *A. rhizogenes* ATCC No. 15834 was accomplished. Several hairy root clones were established and selected based on growth and stability, and root cultures were established in 125 ml flasks as indicated in Materials and Methods (Fig.2.1A). *P. americana* root cultures showed stable growth and phenotype, producing a substantial biomass yield. As shown in Figure 2.1B, *P. americana* hairy roots showed a biphasic root growth until day 30, which contained two periods of exponential growth. Maximum tissue accumulation under these conditions was approximately 180 g fresh weight·L^{-1} medium, representing about a 900-fold increase in biomass starting from a single root tip inoculum. Root intracellular (in organ) and extracellular (secreted) proteins which accumulated in the culture medium during the time course were also examined by SDS-PAGE followed by western blotting using a PAP-specific antibody (Fig.2.1C). Cross-reactivities with the PAP antibody were found in both the intracellular and the extracellular protein fractions. In the intracellular protein fraction, PAP-antibody cross-reactivity increased during very early stages of growth, and maximum protein accumulation occurred before the end of exponential root growth phase at approximately 20 d.

PAP cross-reactivity developed in culture media (extracellular proteins) after day 8, and increased through the time course.

Identification and Purification of RIP from Hairy Roots of *P. americana*

To ascertain whether PAP expressed in established hairy roots is similar to PAP isoforms produced in leaves, seeds and roots of *P. americana*, the protein profiles of these different organs were probed with a PAP antibody by western blotting. Total protein was extracted from 40-d old hairy root cultures of *P. americana*, and from *P. americana* leaves, seeds and roots (Fig.2.2A). Western blot analysis indicated slight differences in molecular weight among immuno-detected proteins from different extracts. The immuno-reactive band observed in hairy roots by western blotting was slightly larger in size than that of PAP (from leaves) but smaller than that of PAP-S (from seeds). It also differed in size from the immuno-reactive bands of RIPs detected in storage roots, but was of a similar size to that of an RIP from primary roots. Based on these results, I concluded that RIP is produced in the transformed hairy roots of the pokeweed plant. Interestingly, RIP production was also detected as part of the root exudates secreted both *in vitro* from hairy root cultures and from whole plant cultures.

To biochemically purify the RIP from hairy roots of *P. americana*, total proteins were subjected to ion-exchange chromatography as outlined in Materials and Methods. Because RIPs are mostly basic proteins, the unretained protein solution from the anion-exchange column was applied to a cation-exchange column (Sep-Pack®), and basic proteins were eluted with NaCl step gradients from 40mM to 600mM. A 29.5 kD protein corresponding to the RIP detected in hairy roots was resolved in the 80mM fraction and analyzed by western blotting (Fig.2.2B). The RIP was further resolved using UNO™ S1 cation-exchange column chromatography. The RIP was determined to have a molecular mass of 29.5 kD as determined by SDS-PAGE.

Characterization and Enzymatic Activity of PAP-H

The N-terminal region of the RIP purified from hairy roots of *P. americana* was sequenced and compared with those from PAP isoforms and other RIPs (Fig.2.3A). The data

showed that the N-terminal amino acid sequence of the hairy root RIP differed from those of all known PAP isoforms and other RIPs. The N-terminal regions of the hairy root RIP had 61% homology with PAP, and 56% homology with PAP-S. The N-terminal region of the hairy root RIP also showed a significant homology with PAP-□(Lin et al., 1991), as well as PIP 2 from *P. insularis* (Song et al., 2000) and PD-S2 from *P. dioica* (Del Vecchio Blanco et al., 1997). Importantly, the data indicated that highly conserved hydrophobic residues reported in the N-terminal region of all other RIPs, such as a ^{14}Tyr (Y) and ^{17}Phe (F) (Funatsu et al., 1991), were found in the N-terminal region of the hairy root RIP. Based on these results, we concluded that the RIP purified from transformed hairy roots of *P. americana* is a novel type of PAP, and named it PAP-H. PAP-H was determined to be, unexpectedly, a neutral protein with an isoelectric point (pI) of 7.8 by IEF-PAGE (Fig.2.3B), and amino acid composition analysis showed that the amino acid distribution of PAP-H was similar to that of other RIPs (Fig.2.3C).

The RNA *N*-glycosidase activity of PAP-H was tested using yeast ribosomes as a substrate. When depurinated rRNAs are treated with aniline, cleavage occurs at the depurinated site and a small nucleotide fragment is released from the 26S rRNA (Stirpe et al., 1986). Yeast ribosomes were incubated with PAP-H and with ME_1, saporin-S6, and RTA. As shown in Figure 2.4, PAP-H dupurinated the rRNAs and released the 367-nucleotide fragment upon treatment with aniline (Stirpe et al., 1986). These results demonstrate the enzymatic activity of PAP-H as a ribosome-inactivating protein.

PAP-H is Localized at the Cell Wall Matrix in the Hairy Roots and Root Border Cells of *P. americana*

I examined the location of PAP-H in hairy roots of *P. americana* using fluorescent microscopy. As shown in Figure 2.5A, thin-longitudinal sectioned hairy roots were treated with an anti-PAP antibody and a fluorescein-labeled secondary antibody as described in Materials and Methods. Green fluorescence, which indicates PAP-H presence as measured by the fluorescent tag-antibody interaction, was observed in the walls of every cell in the hairy roots. According to the broad density of fluorescence imaging along the entire circumference of the cell wall, PAP-H is

most likely embedded in the cell wall matrix rather than bound to the cell wall (Fig.2.5A). Interestingly, I found that PAP-H was also located in the cell walls of root border cells released from the root cap as the root grows (Fig.2.5B). This observation suggested a possible secretion mechanism of PAP-H from the roots into the rhizosphere.

cDNA Cloning of PAP-H

Total RNA was isolated from hairy roots of *P. americana* using RNeasy® Plant Mini Kit (QIAGEN) (see Materials and Methods). In order to clone the cDNA corresponding to the PAP-H protein, two gene specific primers (GSPs) were designed for rapid amplification of cDNA ends (RACE). The sequences of these primers were formulated based upon the partial amino acid sequence of the N-terminus region of PAP-H as well as the codon preferences of several previously cloned PAP-related genes from *P. americana*. One outer primer covered amino acids 6-14 including the first absolutely conserved hydrophobic residue, ^{14}Tyr (Y), while a second primer was designed from amino acids 9-18, overlapping the outer primer and covering the two absolutely conserved hydrophobic residues, ^{14}Tyr (Y) and ^{17}Phe (F). A 968-bp fragment obtained by 3'-RACE was cloned into the pCR®4Blunt-TOPO® and pCR®4TA-TOPO® (Invitrogen), and its nucleotide sequence was determined as addressed in "Materials and Methods". A 3' untranslated region of 51 bp with a polyadenylation site was found downstream from the stop codon. To obtain a 5' sequence of PAP-H, 5'-RACE was performed using two GSPs designed from the fragments produced by 3'-RACE. These primers were designed so that a full-length cDNA clone sequence could be assembled from sequences of overlapping 5'- and 3'-RACE amplification products. A GSP of 27 bp was designed; it corresponded to the DNA sequence located approximately 100 bp downstream from the GSPs used for 3'-RACE. A second GSP of 29 bp was designed, corresponding to the DNA sequence located approximately 200 bp downstream of the 3'-RACE GSPs. 5'-RACE was performed and amplification products were cloned and sequenced as described for the 3'-RACE procedures.

Following DNA sequencing of the multiple clones for each amplification product produced with the various GSPs, the PAP-H cDNA sequence was assembled using the Jellyfish 1.5

Gene Analysis software package (http://www.biowire.com) and found to be 1125 bp in length with an open reading frame (ORF) of 1074 bp (Fig.2.6A, Genebank, accession number AY071928). The deduced translated amino acid sequence indicated that PAP-H cDNA has a putative signal peptide sequence of 47 amino acids, and a coding sequence of 292 amino acid residues. The first 18 amino acid residues from the deduced mature PAP-H polypeptide were found to be identical to those obtained by N-terminal sequencing of the purified PAP-H protein (Fig.3C). A polyadenylation signal (AATAAA) was found between 10 and 30 bases upstream of the polyadenylation site, as found in most plant and animal mRNA (Joshi, 1987). Using the gene analysis software package mentioned above, the coding region of the PAP-H cDNA was found to be slightly longer than that of PAP (Genebank, accession number X55383), especially on the 5' upstream region. When compared with the previously cloned PAP cDNA, PAP-H was found to contain an additional 25 amino acids upstream of the N-terminal sequence. Approximately 50% amino acid sequence homology was found to exist between PAP-H and PAP in the amino-terminal extension region. Analysis also indicated that the carboxyl-terminal extension region of PAP-H may be comprised of 28 amino acids instead of 29 amino acids as found in PAP, with six amino acids differing between the two translated sequences. The cDNA sequence of the ORF region from PAP-H has 59.1% homology with PAP, 69.7% with PAP-S, 64.7% with PAP-□ and 52.1% with PAP II (Genebank, accession numbers X55383, X98079, D10600 and X78628). The analysis also shows that the predicted mature protein from PAP-H cDNA has 66.8% identity with PAP, 64.4% with PAP-S, 58.4% with PAP-□ and 36.0% with PAP II. Highly conserved hydrophobic residues reported by Funatsu et al. (1991) were found in the deduced amino acid sequences of the PAP-H cDNA (^{14}Y, ^{17}F, ^{22}R, ^{74}Y, ^{125}Y, ^{143}G, ^{166}A, ^{178}E, ^{179}A, ^{181}R, ^{207}E, and ^{210}W), and the relatively well-conserved region (^{172}AIQMVSEAARFKYI^{186}) thought to be the active site of enzymatic activity of RIPs (Frankel et al., 1989; Lin et al., 1991) was also found in PAP-H (Fig.2.6B).

Ethylene Enhances the Secretion of PAP-H into the Rhizosphere

Based on PAP-H cell wall localization and on the observation that PAP-H was secreted as part of the root exudates (Fig.2.2A), I decided to study the exudation mechanism of PAP-H. Upon closer examination, I observed exudates resembling water drops that were secreted from the root hairs of *P. americana* root cultures growing in solid culture media (Fig.2.7A). The exudate was collected using a pipette, filtered to avoid collecting root border cells, and run on an SDS-PAGE gel (Fig.2.7B). The exudate showed slight differences in protein patterns compared to the proteins expressed in hairy roots. To determine if PAP-H was also secreted as a part of the root exudates, the intra- (in organ) and extracellular (in exudate) proteins of *P. americana* hairy roots were probed with the PAP antibody (Fig.2.7B). The antibody strongly cross-reacted with both intra- and extracellular proteins and showed the same band, PAP-H (29.5 kD), which indicated that PAP-H is secreted as part of the root exudates as well as with the root border cells. Accordingly, *in vitro*-grown *P. americana* plants growing in liquid media also released PAP-H, presumably through roots (Fig.2.2A).

To analyze the biological significance of PAP-H exudation, hairy root cultures of *P. americana* were challenged with the stress-related chemical ethylene. As shown in Figure 2.7C, an enhanced induction of PAP-H was observed in the root exudates when the hairy roots were treated with ethylene. The secretion of PAP-H was induced shortly after beginning the ethylene treatment, and constantly increased through day 6 of ethylene treatment. On day 6, the secretion of PAP-H was increased up to 8 fold compared to a control, which consisted of roots secreting PAP-H for 30 d without any treatment. Air treatment showed no induction of PAP-H until 3 d after culture transfer, showing PAP-H secretion on day 4. In contrast, treatment with an ethylene inhibitor (MCP) suppressed the natural secretion of PAP-H. This result suggested that MCP blocked the binding of the endogenous ethylene and thus PAP-H secretion. The concentration of ethylene in the headspace of the flask was measured in replicates of all three treatments. Endogenous ethylene produced in the hairy roots treated with air began to increase in day 4, and reached 5 ppm at day 6, a level similar to the concentration supplied in the ethylene treatment (Fig.2.7D). The increase of endogenous ethylene concentration correlates to the increase of PAP-H production starting on day 4, as detected by western blotting. The result shown in Figure 2.7D

indicated that MCP also blocked the production of endogenous ethylene. Thus our results clearly show that PAP-H is secreted under natural conditions by a mechanism mediated by ethylene induction. Interestingly, the western blot analysis of intracellular PAP-H indicates that its concentration inside the hairy roots slightly decreased upon ethylene treatment, which correlates to increasing PAP-H accumulation in the media (Fig.2.7E). These results suggest that ethylene induces secretion of PAP-H rather than the *novo* production of this RIP. Taken together, these results suggest that ethylene induces secretion of PAP-H into the rhizosphere but does not induce production of PAP-H.

Antifungal Activity of PAP-H

To explore the biological significance of PAP-H, I examined the *N*-glycosidase activity of PAP-H against fungal ribosomes. The depurination experiment described for PAP-H against yeast ribosomes was repeated using ribosomes isolated from *T. reesei*. Following aniline treatment, a small fragment of about 360 nucleotides was detected by urea-acrylamide gel electrophoresis (Fig.2.8A). This result indicates that PAP-H may be involved in inhibiting fungal growth by actively depurinating the fungal ribosomes. Based on this result, I tested the antifungal activity of PAP-H against an array of fungi (see Materials and Methods). However, PAP-H did not show fungal inhibitory activity in plate assays. Subsequently, I tested the total secreted proteins (exudates) from *P. americana* hairy roots for fungal inhibition to check any possible antifungal effect with other pathogenesis-related (PR) proteins that may allow PAP-H entrance onto fungal cells. As shown in figure 2.8B, 50 μg of total secreted proteins produced a significant inhibition of the growth of *R. solani* as well as of *T. reesei* (data not shown). These data indicate that PAP-H may participate in an active defense mechanism of roots against rhizosphere microbes. Thus I studied whether fungal inhibition was due to the direct effect of PAP-H on fungal ribosomes. I co-cultured *R. solani* with hairy roots of *P. americana* which were grown for 2 weeks prior to co-culture in MS basal media (Fig.2.8Ca). Fungal hyphae growing in the proximity of the roots were collected after a week of co-culture and washed briefly with H_2O to cleanse of medium (solids) attached to hyphae, and ribosomes were then isolated from collected fungal mycelium tissues.

Interestingly, a small fragment appeared when the rRNA derived from these ribosomes was run on SDS-PAGE, indicating rRNA cleavage due to RIP depurination after RNA extraction and aniline treatment (Fig.2.8Cbcd). This result demonstrated that PAP-H entered into the cytosolic region of fungal cells, and depurinated fungal ribosomes.

Enzymatic Activity Assay of PR Proteins in Root Exudates of *P. americana*

Based on previous results, I hypothesized that root exudates of *P. americana* contained other PR proteins which could facilitate the entry of PAP-H into fungal cells by lysing fungal cell walls. Chitinase, β–1,3-glucanase, and protease enzymatic activities were tested as possible candidates as described in "Materials and Methods". As shown in Figure 2.8D, the root exudates demonstrated chitinase and β–1,3-glucanase (10.18 U and 16.82 U per mg of total protein) activities, as well as protease activities detected by zymogram gel analysis. Correlating the concentration of chitinase and β–1,3-glucanase in *P. americana* root exudates with previously reported enzymatic activity for these enzymes in other plants (approximately 14 $U \cdot mg^{-1}$ for chitinase and 18.5 $U \cdot mg^{-1}$ for β–1,3-glucanase) (Kombrink et al., 1988; Vögeli et al., 1988; Kragh et al., 1990; Wyatt et al., 1991; Qiu et al., 1997), I conclude that the concentration of these PR proteins in the root exudates is sufficient to damage fungal cell walls. These results suggest that these PR proteins in root exudates may generate an additive effect to facilitate entrance of PAP-H into fungal cells.

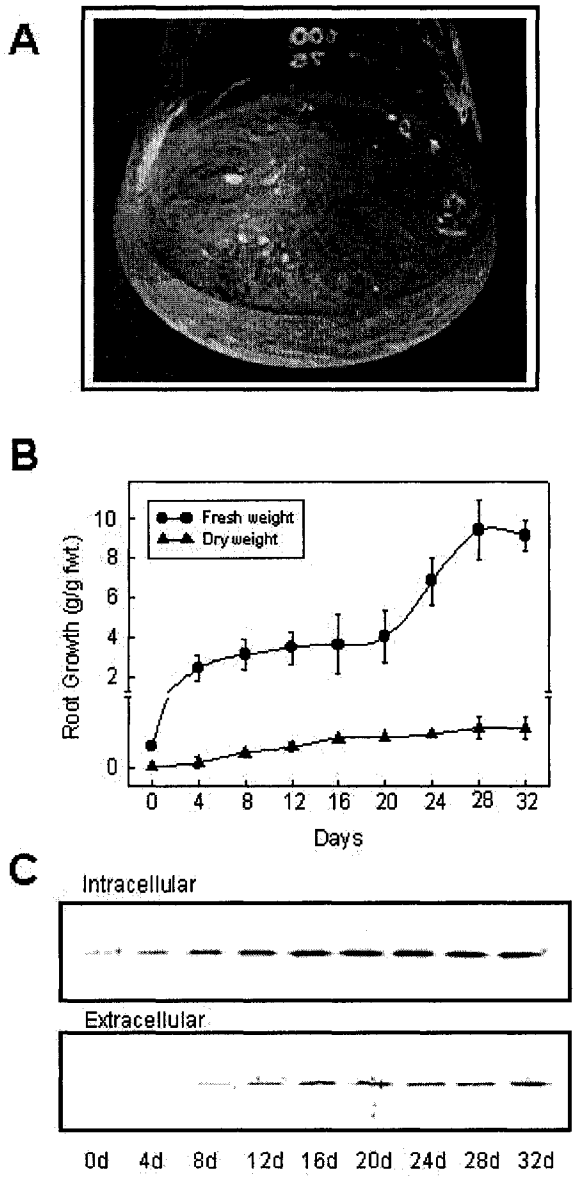

Figure 2.1. Establishment of *P. americana* hairy roots, and time course of root growth and PAP-H accumulation. **A**, Developed hairy roots of *P. americana* as described in "Materials and Methods". **B**, Growth curve of fresh and dry weight accumulation over 32 d. **C**, Western blot analysis of intra- and extracellular PAP-H accumulation over 32 d. The same amount (0.2g fresh wt) of hairy roots from each sample was harvested to extract total proteins, and 1 ml of media from each sample was collected to concentrate the root secreted proteins followed by TCA precipitation as described in "Materials and Methods".

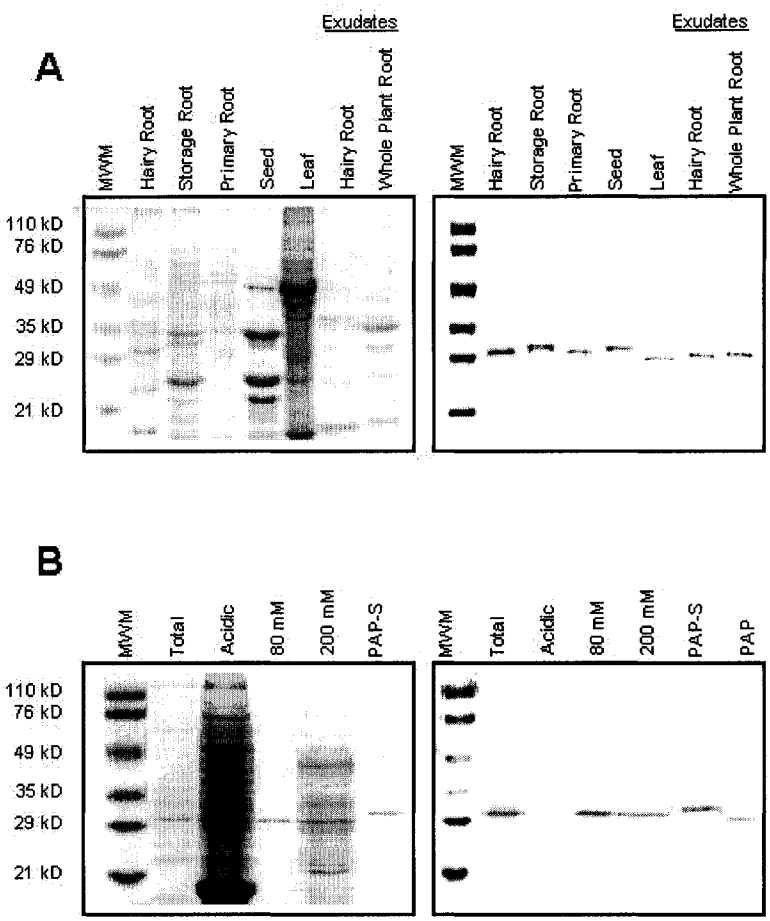

Figure 2.2. Identification and purification of PAP-H. **A**, Profiling of SDS-PAGE and western blot. Total proteins prepared from different organs of the pokeweed plant, and media where the hairy roots and whole pokeweed plant were grown were concentrated and run through 12% SDS-PAGE. The antibody raised against PAP was used for western blotting. Approximately, 25 μg of protein was loaded per lane. **B**, Cation-exchange chromatography of the total hairy root proteins from *P. americana*. Total protein and samples of each fraction were run in 12% SDS-PAGE, and western blot was performed using the PAP antibody. Approximately 5 μg of total, basic fractions, PAP-S and PAP, and 15 μg of acidic fraction were loaded per lane.

A

```
PAP-H:                                  IISFDVGSATISKYTTFQ
PAP:              MKSMLVVTISIWLILAPTSTWAVNTIIYNVGSTTISKYATFL
PAP-R:    (N-terminus)-                 VNTIIYNVGSTTISKYATFL
PAP-S:       MKVMLVVVVTLIAWLIAAPTSTCAINTITFDAGNATINKYATFM
PAPII:       MKMKVLEVVGLAISIWLMLTPPASSN-IVFDVENATPETYSNFL
PAP-α:        KMMVVVVVMMLSWLILKPPSTWAINTITFDVGNATINKYATFM
PIP 2:     MKMMVVLVMTITAWLIFAPASTWAASPNPITFEVGNATINKYATFM
PD-S2:                                  VSTITFDVGSATISKYTTFL
ME1:                                 APPT---LATLDDTAIANYPPFM
ME2:                                 APSALDKLATLDLNMPTTYLLFN
MAP: MLTTTKVFFLLLTTWITWYAIVNPQSRAAP-TLETIASLDLNNPTTYLSFI
SAP:          MKIYVVAYIAWILLQFSAWTTTDAVTSITLDLVNPTAGQYSSFV
```

B

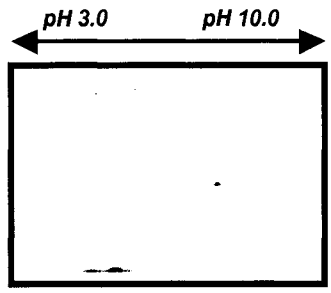

C

A.A	PAP-H	PAP	PAP-R	PAP-S	PAP II	MAP	ME 1	ME 2
Asx	23.2	31	18.0	34.3	26	27	33	30
Thr	13.3	17	1.6	13.9	18	27	25	28
Ser	18.2	18	10.0	15.0	16	19	14	13
Glx	20.6	26	32.3	29.0	25	20	15	16
Pro	8.0	14	17.7	12.1	12	8	12	8
Gly	14.1	16	17.0	17.9	21	12	15	15
Ala	12.7	15	20.7	16.4	19	20	26	31
Val	13.5	19	11.2	15.6	17	14	13	16
Cys	5.8	3	13.4	2.2	4	2	0	0
Met	1.0	4	12.8	5.9	8	4	3	3
Ile	10.7	17	3.4	19.6	15	20	14	15
Leu	16.8	24	17.0	26.6	23	21	23	20
Tyr	7.4	11	3.3	10.3	16	11	8	7
Phe	8.5	10	15.0	6.8	11	13	10	15
Lys	15.7	18	31.0	23.6	20	23	23	22
His	3.5	3	8.8	2.2	4	0	1	1
Arg	7.8	10	7.8	13.6	9	7	12	10

Figure 2.3. Characterization of PAP-H. **A**, Comparison of the N-terminal sequences of PAP-H. PAP (Genebank, accession number X55383); PAP-R (Bolognesi et al., 1990); PAP-S (X98079); PAP II (X78628); PAP-α, antiviral protein precursor from *P. americana* (D10600); PIP 2, ribosome inactivating protein 2 from *P. insularis* (AF141331); PD-S2, protein synthesis inhibitor from *P. dioica* (P34967); ME_1 and $_2$, *M. expansa* protein 1 and 2 (Vivanco et al., 1999); MAP, *M. jalapa* antiviral protein (D10227); SAP, saporin (CAA41948). Red characters represent two amino acids that are absolutely conserved in all RIPs (Funatsu et al., 1991). **B**, Determination of Isoelectric point (pI). SDS-PAGE of the purified PAP-H was performed as described in "Materials and Methods". pH range of the first dimension gel was pH 3 to pH 10 using Bio-Lyte® ampholytes (Bio-Rad). **C**, Amino acid composition of PAP-H, PAP (Irvin et al., 1980), PAP-R (Bolognesi et al., 1990), PAP-S (Barbieri et al., 1982), PAP II (Irvin et al., 1980), MAP (Wong et al., 1992), and ME_1 and ME_2 (Vivanco et al., 1999).

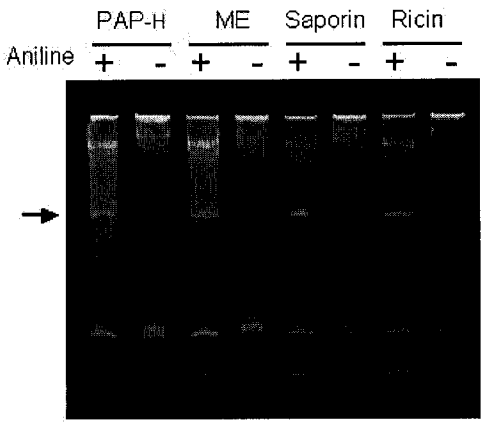

Figure 2.4. Enzymatic activity of PAP-H *in vitro*. Ribosomes were isolated from yeast and incubated with PAP-H, ME, saporin, and ricin as described in "Materials and Methods". rRNAs were extracted, treated with aniline, separated on a 4.5% urea-polyacrylamide gel, and stained with ethidium bromide. The presence (+) or absence (-) of aniline is denoted. The arrow shows the presence of the diagnostic 367-nucleotide cleavage product of rRNA.

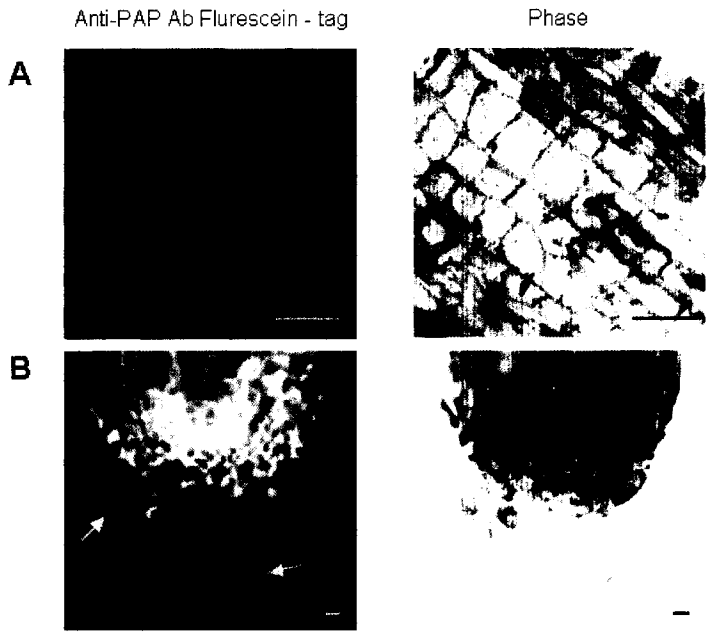

Figure 2.5. Localization of PAP-H in hairy roots of *P. americana.* The tips of hairy root tissues were cut into thin sections and fixed as described in "Materials and Methods". Sections of cells were then stained with PAP antibody, followed by fluorescein labeled secondary antibody reaction. Green fluorescence as observed in a fluorescent microscope indicates the presence of PAP-H in the cells. **A**, Longitudinal section of hairy roots. **B**, Longitudinal section of hairy roots showing root border cells (the arrows) near the root cap. Phase-images were taken by light microscopy. Control root images not incubated with PAP antibody and fluorescein labeled secondary antibody did not show fluorescent signal indicating no-root endogenous fluorescence (data not shown). (Bars = 20 μm).

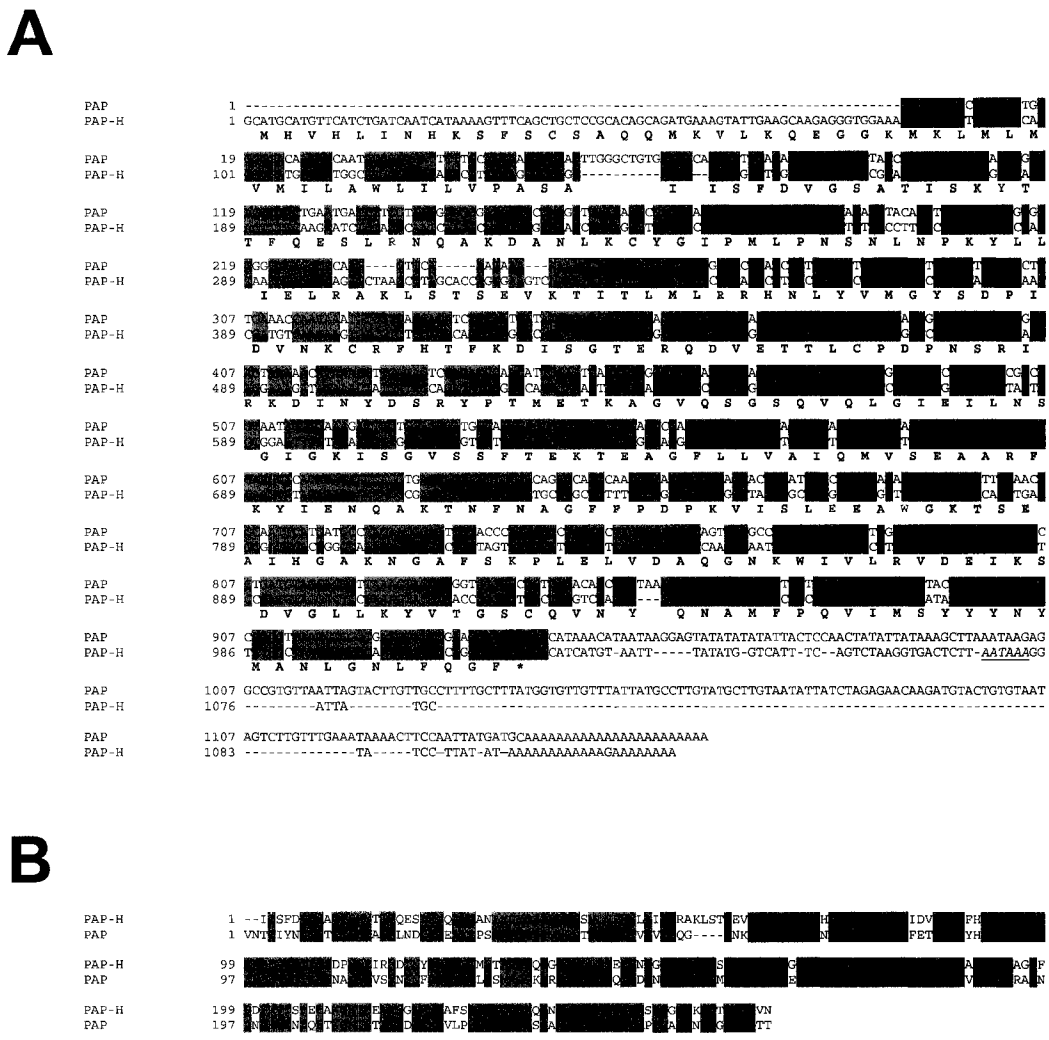

Figure 2.6. cDNA and deduced amino acid sequences of PAP-H. **A**, The amino acid sequence of the mature protein (PAP-H) is in dark bold and the absolutely conserved amino acid residues among RIPs (Funatsu et al., 1991) are in red. The blue and green characters represent amino and carboxyl-terminal extensions. The polyadenylation sites are indicated in italics and underlined. The cDNA sequence (X55358) of PAP is aligned along with PAP-H. **B**, Comparison of the mature proteins between PAP-H and PAP (X55358).

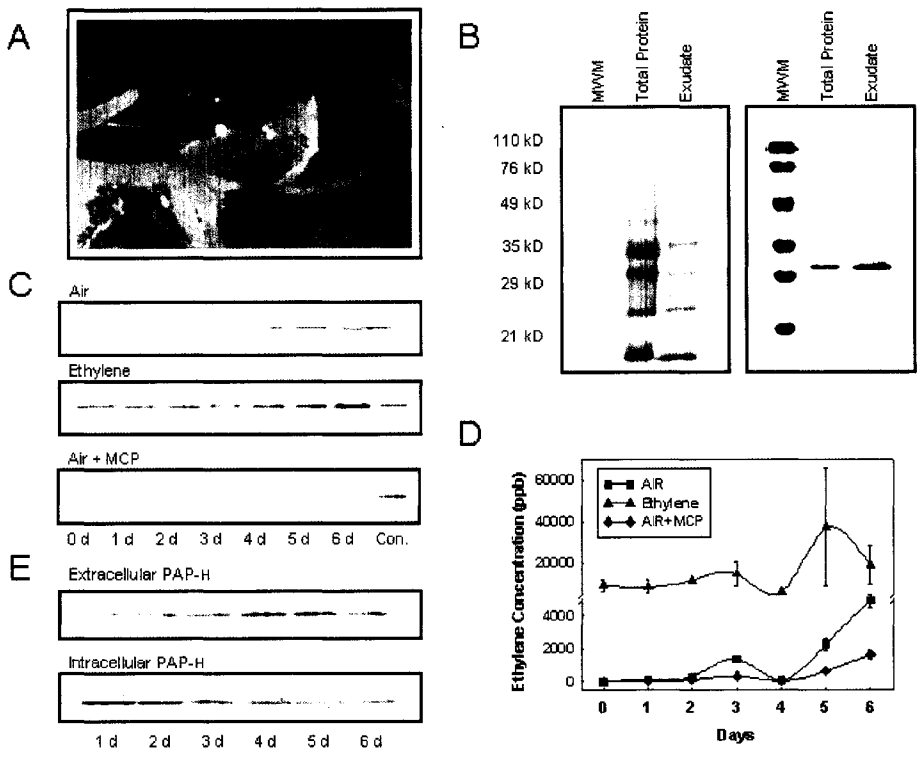

Figure 2.7. Identification and ethylene induction of extracellular PAP-H. **A**, Water-drop shaped exudates secreted from hairy roots of *P. americana* grown in solid culture media. **B**, SDS-PAGE and western blotting of total protein and exudates from hairy roots of *P. americana*. The PAP antibody strongly cross-reacted with intra- and extracellular proteins and showed the same band, PAP-H (29.5 kD), indicating that PAP-H was secreted as part of the root exudates. Approximately 20 μg of protein was loaded per lane. **C**, Western blot analysis of elicitation experimentation during one time course study. Hairy roots of *P. americana* grown for 30 d were transferred into 50 ml of fresh MS media, and treated with air (top), ethylene (middle), and air + MCP (bottom) through 6 d. The medium from which the hairy roots were grown for 30 d was used as control. One milliliter of media from each sample was collected to concentrate the root secreted proteins followed by TCA precipitation as described in "Materials and Methods", and subsequently the concentrated protein was loaded in each lane. **D**, Ethylene concentration in the headspace of flasks during the course of each treatment. **E**. Western blot analysis of intra- and extracellular PAP-H elicited by ethylene in the time course. One milliliter of media from each sample was collected, concentrated and loaded as described above.

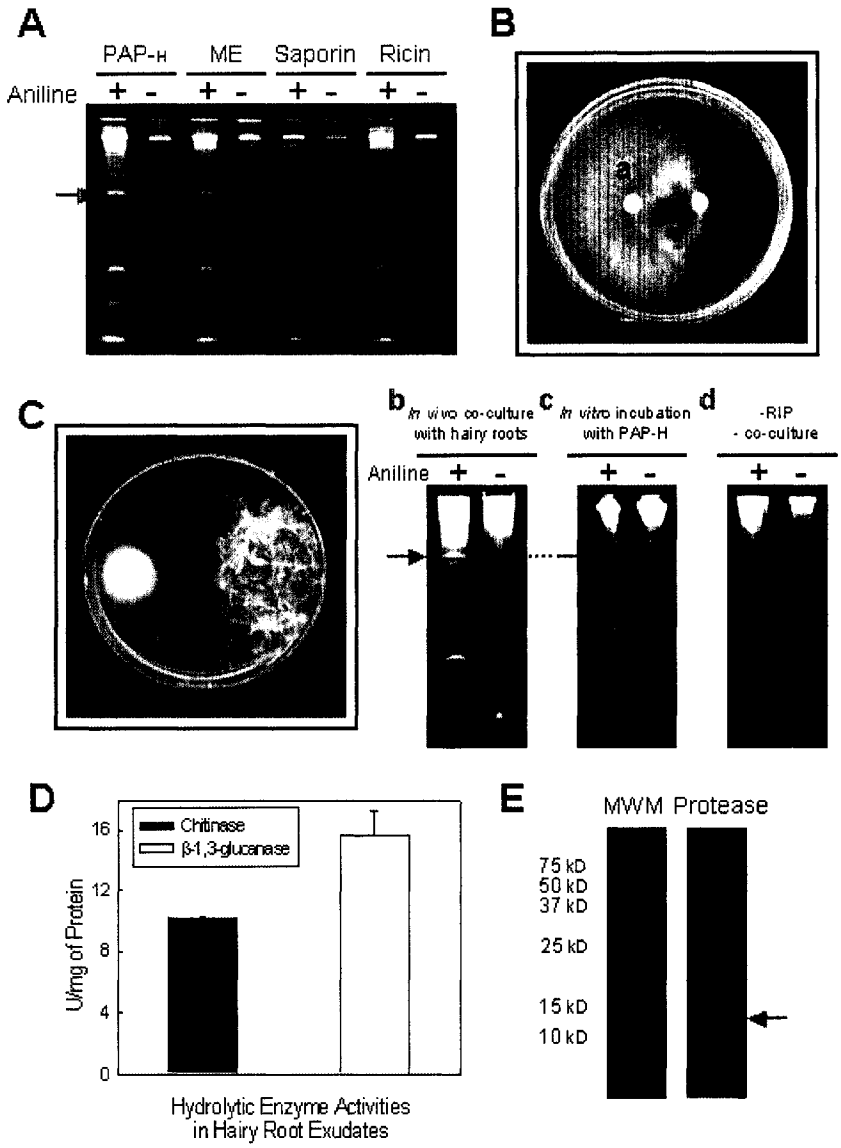

Figure 2.8. Antifungal activity of *P. americana* hairy root exudates. **A**, Depurination of *T. reesei* ribosomes *in vitro*. The arrow shows the presence of the diagnostic nucleotide cleavage product of rRNA. **B**, Radial growth-inhibition assay of *P. americana* hairy root exudates against *R. solani*. 25 mM $NaPO_4$ buffer, pH 7.5 (a) and filter-sterilized 50 µg of total root exudates (b) were applied to the discs, and tested for antifungal activity. **C**, Enzymatic activity of exudated PAP-H from hairy roots against *R. solani*. **D**, Enzymatic activities of chitinase and *ß*–1,3-glucanase in root exudates. **E**, Determination of proteolytic activity of root exudates. The arrow indicates protease activity in root exudates.

DISCUSSION

I established transformed root clones of *P. americana* with *A. rhizogenes* ATCC No. 15834. These transformed roots ("hairy roots") displayed similar morphological characteristics to primary roots including a well-developed cortex with new tissues developing from an apical meristem. The hairy roots of *P. americana* showed stable and fast growth, and produced PAP-H steadily and constitutively. Hairy roots of *P. americana* grew rapidly after day 20, and reached the stationary stage in approximately 30 d. The production of intracellular PAP-H increased during the very early stage, and remained constitutive after 15 d. In contrast, extracellular PAP-H accumulated to detectable levels in approximately 8 d, and continuously increased with the growth of roots. These results indicate that extracellular PAP-H accumulation occurs over time along with root growth while the expression of intracellular PAP-H is constant.

In this communication, I report the isolation of PAP-H, a new constitutively produced RIP, from *A. rhizogenes* – transformed hairy roots of *P. americana*. The isoelectric point (pI) of PAP-H was determined to be 7.8 by IEF-PAGE, suggesting that PAP-H is the first neutral and active protein among known RIPs (Fig.2.3B). As shown in Figure 2.3C, the lower levels of basic amino acids such as lysine and arginine in PAP-H compared with the levels in PAP and other isoforms may contribute to its lower pI. PAP-H showed N-terminal amino acid sequence similarity with other RIPs found in *P. americana*, such as PAP and PAP-S, and to a lesser extent with PAP-II (Irvin et al., 1980; Barbieri et al., 1982). PAP-H cross-reacts with PAP antibodies, but does not react with the PAP-II antibody (data not shown). Amino acid comparisons show 75.8% homology between PAP and PAP-S, and 33% homology between PAP and PAP II. Accordingly, PAP-S cross-reacts with PAP antibodies, but PAP II does not react with PAP antibodies (Barbieri et al., 1982). I suggest that since PAP, PAP-S and PAP-H are constitutively produced they share more sequence and antigenic specificity, in contrast to PAP II in which expression is environmentally regulated.

Comparing PAP isoforms detected among different types of roots (Fig.2.2A), PAP-H showed size differences with RIPs found in storage roots. However, PAP-H has a molecular

weight similar to the protein expressed in primary roots, which cross-reacted with the PAP antibody. *A. rhizogenes* – transformed hairy roots, in general, exhibit morphological and genetic similarity with fibrous primary roots (for review, see Vivanco and Flores, 2000; Bais et al., 2001). Savary and Flores (1994) have shown that secondary growth induction leading to storage root formation shifts the protein production and accumulation patterns of RIPs. Therefore, PAP-H may be considered a biochemically identical isoform to the protein found in the primary roots. Our results also showed that storage roots have two immuno-reactive bands which indicate a molecular weight (30 kDa) close to that of PAP-S isolated from seeds (Barbieri et al., 1982). Furthermore, hairy root and whole plant root exudates cross-reacted with the PAP antibody, and the immuno-reactive band produced by these exudates showed the same molecular weight as PAP-H, suggesting that PAP-H is released from roots to the rhizosphere as a part of the root exudates (Fig.2.2A, 2.7B).

The amino acid sequence of the PAP-H cDNA was deduced and found to be identical to the protein sequence corresponding to the N-terminus of the purified PAP-H protein (Fig.2.3C, 2.6A,B). Mature PAP-H contains 264 amino acid residues, which is similar to the 262 and 261 amino acid residues found in PAP and PAP-S (Monzingo et al., 1993). Although the numbers of amino acid residues from mature proteins are similar to each other, molecular weights of PAP-H, PAP, and PAP-S clearly showed differences (Fig.2.2A) suggesting that post-translational modification may occur in pokeweed RIPs. Recently, a number of mutagenesis studies using PAP have revealed certain specific sites important for its enzymatic activities. Transgenic plants expressing non-toxic mutated PAP forms such as PAPx (active site mutant), PAPn (N-terminal mutant), and PAPc (C-terminal mutant) have shown that ^{176}Glu, ^{75}Gly, and 25 C-terminal amino acids are critical amino acid residues involved in ribosome depurination (Zoubenko et al, 1997; Tumer et al., 1997; Smirnow et al., 1997; Hudak et al., 2000; Zoubenko et al., 2000). Comparison of cDNA sequences of PAP-H and PAP shows that PAP-H also contains those amino acid residues involved in ribosome depurination. The deduced amino acid sequences of PAP-H from its cDNA show ^{178}Glu and ^{77}Gly corresponding to ^{176}Glu and ^{75}Gly from PAP; the later amino acids are responsible for the N-glycosidase activity of PAP. PAP-H also has high sequence homology with

PAP in 25 C-terminus amino acid residues. Furthermore, the PAP active site residues (^{72}Tyr, ^{123}Tyr, and ^{179}Arg) directly participated in the catalytic deadenylation of RNA, and ^{208}Trp involved in the stabilization of ribosome binding (Rajamohan et al., 2000) may correspond to ^{74}Tyr, ^{125}Tyr, ^{181}Arg, and ^{210}Trp from PAP-H. These sequence analyses indicate that PAP-H shares with PAP amino acid residues involved in cytotoxicity, so that the *N*-glycosidic activity of PAP-H may be similar to that of PAP. Interestingly, the cDNA analysis demonstrates that PAP-H contains 75 amino acid residues corresponding to the amino- and carboxyl-terminal extensions (47 from N-terminus and 28 from C-terminus). The sequence comparison of both amino- and carboxyl-extension regions from PAP-H and PAP suggest that these regions from PAP-H may function as cell wall targeting sequences in hairy roots as was previously reported for PAP (Ready et al., 1986; Monzingo et al., 1993). However, the amino-terminal extension of PAP-H contains an additional 25 amino acids compared with PAP and PAP-S, and the sequences of these two proteins differ from each other. Therefore, the N-terminus sequence of PAP-H may include additional functions such as directing secretion of PAP-H to the rhizosphere under ethylene regulation.

I found that PAP-H is located in the cell wall matrix of hairy roots (Fig.2.5A), similar to PAP being localized in the cell wall matrix of leaf mesophyll cells (Ready et al., 1986). Since PAP is an exported protein, it may have an ER signal sequence at the N-terminus to enter the secretory pathway as reviewed by Lodish et al. (2000). As described above, PAP-H contains potentially functional amino-terminal extension residues, and shows localization similar to that of PAP. Accordingly, PAP-H may share the same processing mechanisms as PAP. Interestingly, PAP-H was also found to be localized in the cell walls of root border cells and released from the root tip as the root grew (Fig.2.5B). Root border cells are considered to be one of the key factors in root-microbe communication as they are programmed to be detached from the root and enter the rhizosphere (for review, see Hawes et al., 2000). Border cells are involved in triggering various responses by producing secondary metabolites, chemo-attractants, repellents and signals that can lead to agglutination against infesting microbes and root parasites. However, no specific enzyme has been isolated from root border cells. Recently, Hawes and co-workers have suggested the

production of a low-pH galactosidase in the root border cells of the pea (Hawes et al., 2000). Our data showed that *P. americana* root border cells produce and store RIPs. As mentioned above, I also found that hairy roots of *P. americana* constitutively secreted water-drop-shaped exudates while growing in solid media (Fig.2.7A). Western-blot analysis (Fig.2.7B) of filtered exudates collected from hairy roots indicated that PAP-H was released as part of the root exudates. To our knowledge, PAP-H is the first RIP shown to be secreted in the root exudates, as well as the first shown to be compartmentalized in secreted root border cells. These root specific functions may act as potential plant-defense mechanism against pathogen infection.

PAP is regarded as a defense-related protein because it can deadenylate ribosomes from all organisms, and its expression in transgenic plants leads to resistance to viral and fungal infection (Lodge et al., 1993; Zoubenko et al., 1997). Although many elicitors and signals that accompany pathogen recognition and defense responses of plants have been found to induce PR proteins, only limited information has been determined about the induction of RIPs. Some studies have addressed the induction of RIPs caused by stress and stress-related compounds such as jasmonate (Reinbothe S et al., 1994), osmotic stress or heat shock (Stripe et al., 1996), and salt-shock (Rippmann C et al., 1997). Reinbothe et al. (1997) reported that methyl jasmonate also rapidly induces and accumulates RIP in leaf tissues of barley at the transcriptional level. Ethylene is induced in response to environmental stress, including infection by pathogens (for review, see Ohme-Takagi, 2000). Ethylene has also been shown to be an important factor in plant cell culture systems, affecting the stimulation of secondary metabolites from various tissue and cell cultures (Cho et al., 1988; Phisalaphong and Linden, 1999). Thus, ethylene is biologically active at a very low concentration – less than 1 ppm (1 $\mu l \cdot L^{-1}$) - and its production is temporarily increased several-fold within 25-30 min when tissues are wounded or mechanically perturbed (Taiz and Zeiger, 1991). Exogenous application of ethylene has been shown to induce the transcription of several genes encoding basic-type PR proteins such as class I basic chitinases and class I β-1,3-glucanase (for review, see Ohme-Takagi et al., 2000). Chen et al. (2001) has recently reported that the ethylene receptor-like protein ETR1 is located in the endoplasmic reticulum (ER) membrane in *Arabidopsis*. Ethylene receptors such as ETR1 are two-component signaling

systems containing a receptor with histidine kinase activity and a response regulator (Schaller et al., 1995, 2000; Hall et al., 2000). In response to ethylene, the receptor is autophosphorylated and a phosphate is then transferred to the response regulator which mediates downstream responses (Schaller et al., 2000). Since PAP-H showed strong secretory induction by ethylene treatment and is assumed to be secreted through the ER, the ethylene receptor located in the ER membrane may be involved in activating the secretory mechanism of PAP-H. In conclusion, I feel that ethylene induced by biological stresses, such as pathogen attack, binds to the receptor protein at the ER membrane initiating a downstream signaling cascade to activate the PAP-H secretory pathway as a defense mechanism.

As part of a secretory root defense mechanism, PAP-H creates an antifungal scenario with the aid of other PR proteins secreted from hairy roots of *P. americana*. As shown in Figure 2.8A, PAP-H has *in vitro N*-glycosidase activity against fungal ribosomes, which indicates that PAP-H can recognize and depurinate fungal ribosomes; however, purified PAP-H did not show *in vitro* antifungal activity against *R. solani*. In contrast, total root exudates of *P. americana* showed inhibitory activity against fungi (Fig.2.8B). Upon close examination, the ribosomes isolated from *R. solani* grown in the presence of hairy roots of *P. americana* (Fig.2.8Ca) showed depurination traces (Fig.2.8Cc). I hypothesize that PAP-H depurinates fungal rRNA and inhibits fungal growth by disrupting protein synthesis in fungal cells. The penetration of PAP-H into the fungal cells may be facilitated by PR proteins such as chitinase, β-1,3-glucanase, and proteases (Fig.2.8D and E). Both chitinase and β-1,3-glucanase are widely distributed enzymes in higher plants, and have been hypothesized to function synergistically in plant defense against fungal pathogens (Abeles et al., 1971; for review, see Leubner-Metzger and Meins, 1999; Neuhaus, 1999).

I suggest that PAP-H is constitutively produced as a host defense protein, and secreted into the rhizosphere as a barrier against soil-borne microbe infection. The secretion of PAP-H is regulated in response to endo- and exogenous stresses. Based on our results, PAP-H may prevent the multiplication of pathogens in the soil, acting in an additive effect with other PR proteins. Another hypothesis is that PAP-H is constitutively secreted in order to produce organic matter in

the soil by depurinating the ribosomes of soil microorganisms. These and other hypotheses are currently being tested to shed light on the function of RIPs in the rhizosphere.

CHAPTER 3

Enzymatic specificity of three ribosome-inactivating proteins against fungal ribosomes, and correlation with antifungal activity

ABSTRACT

In the present study, I employed three RIPs to dissect the antifungal activity of RIPs as plant defense proteins. I measured the catalytic activity of RTA, saporin-S6, and ME_1 against intact ribosomal substrates isolated from various pathogenic fungi. I further determined the enzymatic specificity of these three RIPs against fungal ribosomes, from *R. solani*, *A. solani*, *T. reesei* and *C. albicans*, and correlated the data with antifungal activity. RTA showed the strongest toxicity against all tested fungal ribosomes, except for the ribosomes isolated from *C. albicans*, which were most susceptible to saporin. RTA and saporin showed higher enzymatic activity than ME_1 against ribosomes from all of the fungal species assayed, but did not show detectable antifungal activity. In contrast, ME_1 showed significant inhibitory activity against fungal growth. Using NHS-fluorescein labeling of RIPs and fluorescent microscopy, I determined that ME_1 was targeted to the surface of fungal cells and transferred into the cells. Thus, ME_1 caused ribosome depurination and subsequent fungal mortality. In contrast, saporin did not interact with fungal cells, correlating with its lack of antifungal activity.

INTRODUCTION

Several studies have demonstrated the specificity of RIPs towards different ribosomal substrates from sources including animal, plant and bacterial species. Ricin, for example, is highly active toward mammalian ribosomes, but shows less activity against wheat ribosomes (Cawley et al., 1977; Lord and Roberts, 1996). Maize RIP also shows higher activity against rabbit ribosomes than plant ribosomes (Bass et al., 1992; Hey et al., 1995). This enzymatic specificity suggests that RIP-ribosome interaction depends on the ribosomal conformation of the affected organism (Krawetz and Boston, 2000).

Apart from enzymatic activity and substrate specificity, very little is known about the biological function and role of RIPs. A potential RIP role as a plant defense protein has been deduced from its enzymatic activity and extracellular localization (Ready et al., 1986). It has been proposed that RIPs are synthesized as inactive proteins sequestered in the cell wall matrix, and re-enter the cytoplasm along with the pathogen at infection sites. Thus RIPs are thought to inhibit

pathogen multiplication by inactivating the host ribosomes (Ready et al., 1986). However, recent studies suggest that RIPs can directly inhibit pathogens by inactivating their ribosomes and causing cell death (Vivanco et al., 1999; Lam and Ng, 2001 a,b). MEs showed direct inhibitory activity against an array of fungal and bacterial plant pathogens (Vivanco et al., 1999), and hypsin and lyophyllin demonstrated the inhibition of mycelial growth in various fungal species (Lam and Ng, 2001 a,b). Furthermore, recent study indicates a direct RIP fungal inhibition by which RIPs inhibit fungal growth by entering fungal cells through synergism with other defense proteins such as chitinases, β-1,3-glucanases and proteases (Park et al., 2002a). However, the actual defense mechanism of RIPs has not been clearly defined. In this present experiment, I further the understanding of the enzymatic specificity of three RIPs, RTA, saporin-S6 and ME_1, by showing that RIPs have substrate specificity and that some RIPs, such as ME_1, exert fungicidal activity after internalization into fungal cells via an as-yet-unknown mechanism.

MATERIALS AND METHODS

Protein materials

ME_1 was purified by ion-exchange chromatography according to Vivanco et al. (1999), and saporin-S6 (SO-6) and RTA were purchased from Sigma. The proteins were dissolved in 25 mM phosphate buffer, pH 7.0, and the purity of the RIPs was confirmed by Coomassie and silver staining of SDS polyacrylamide gels, and the concentration was determined by the Bradford method (1976) using a protein assay kit purchased from Bio-Rad.

Ribosome isolation from fungi

Plant pathogenic fungi, *R.solani, A. solani* and *T. reesei*, and human pathogenic yeast, *C. albicans*, were grown in potato dextrose media. Mycelial tissues of fungi and yeast were collected by vacuum-filtration. The yeast and fungal hyphae were ground in a mortar with liquid N_2, and dissolved in 100 ml of extraction buffer (200 mM KCl, 25 mM $MgCl_2$, 25 mM EGTA, 200 mM sucrose and 25 mM β-mercaptoethanol in 200 mM Tris-HCl, pH 9.0). The supernatant was

collected by centrifugation at 10,000 g for 20 min at 4 °C, and carefully pipetted onto a sucrose cushion (1 M sucrose, 20 mM KCL and 5 mM $MgCl_2$ in 25 mM Tris-HCl, pH 7.6) in 70 Ti tubes, and centrifuged at 55,000 rpm for 4 h at 4 °C (L-70 Ultracentrifuge, Beckman). The pellets were resuspended in 25mM Tris-HCl buffer (pH 7.6) with 25mM KCl and 5mM $MgCl_2$, and stored at – 80 °C until use.

Enzymatic activity analysis of RIPs

The depurination assay was conducted according to Tumer et al. (1997). Briefly, fungal ribosomes were resuspended in RIP buffer (100mM Tris-HCl, 167 mM KCl, 100 mM $MgCl_2$, pH 7.2) and incubated with each RIP at 30 °C for 30 min in a total volume of 100μl. RNA incubated in the absence of RIPs served as a negative control. Following incubation, the RIPs were removed from the mixture by phenol:chloroform extraction and the RNA was divided in half. Half of the extracted RNA was incubated on ice for 30 min with 1 M of aniline acetate (pH 4.5) and precipitated with ethanol. Both aniline- treated and untreated RNAs were subjected to electrophoresis in a 7 M urea/ 6% polyacrylamide gel and stained with ethidium bromide.

Antifungal Assay

Antifungal activity of each RIP was determined by a radial growth-inhibition assay adapted from the method of Schlumbaum et al. (1986). Fungal plugs were placed in the center of potato-dextrose-agar (PDA) plates, and sterilized paper discs were placed around the fungal plugs. Subsequently, various amounts of sterilized RIPs ranging from 25 to 100 $\mu g \cdot ml^{-1}$ were pipetted onto the discs. Proteins were sterilized using Ultrafree-MC Sterile (0.22 μm GV Durapore, Millipore). The plates were incubated in the dark at room temperature. Antifungal activity was observed as a crescent-shaped zone of inhibition at the mycelial front. The effect on fungal growth was expressed qualitatively, according to the procedure of Schlumbaum et al. (1986).

Preparation of NHS-Fluorescein labeled proteins

ME_1 and saporin-S6 were fluorescence-labeled using NHS-Fluorescein (Pierce, Rockford, IL) according to the manufacturer's instructions. Briefly, 1 mg of each sample was dissolved in 100 µl of conjugation buffer (0.1 M phosphate, 0.15 M NaCl, pH 7.2). Subsequently, 50 µl of 2 M NHS-Fluorescein dissolved in dimethyl sulfoxide (DMSO, Sigma) was added dropwise in each protein sample, and mixed by stirring. Samples were placed on ice and incubated for 2 h. The unreacted NHS-fluorescein was then removed by dialysis, and the protein concentration was determined by the Bradford method (1976) using a protein assay kit purchased from Bio-Rad. Fluorescein-labeled proteins were stored at 4 °C in 0.1 % NaN_3 until use.

Fluorescent microscopy analysis

Fluorescence-labeled ME and saporin-S6 were applied to *R. solani* using the modified plate assay method (Schlumbum et al., 1986). Briefly, a fungal plug was placed in the center of a PDA plate, in all treatments, and sterilized paper discs were placed around the fungal plug. Subsequently, each labeled RIP was sterilized using Ultrafree-MC Sterile (0.22 µm GV Durapore, Millipore), and pipetted onto the discs. The plates were covered with aluminum foil to exclude light, and incubated at room temperature. After 96 h incubation, fungal hyphae were carefully collected from the halo where fungal growth inhibition occurred. Collected hyphae were briefly washed with 10 % glycerol, and placed on a glass plate. As a negative control, 100 µl of 2 M NHS-Fluorescein solution was applied in the antifungal assay using the same procedure used for the labeled proteins. Fluorescent images and phase images were taken using a fluorescent microscope (JEOL 2000 EXII).

RESULTS

Substrate specificity of RTA, saporin and ME_1 on the ribosomes isolated from *R. solani*, *A. solani*, *T. reesei* and *C. albicans*

The substrate specificity of three type I RIPs, RTA, saporin-S6 and ME_1, were examined against the fungal ribosomes isolated from *R. solani*, *A. solani*, *T. reesei* and *C. albicans*. When RIP-depurinated rRNA is treated with aniline, cleavage occurs at the depurinated site and a small nucleotide fragment is released (Fig.3.1). Ribosomes from the four fungi were individually incubated with five different concentrations of each RIP (RTA, saporin-S6 and ME_1). rRNAs were then extracted, treated with aniline, and analyzed by urea-polyacrylamide gel electrophoresis (PAGE). Figure 3.1 shows the RNA depurination of *R. solani* ribosomes incubated with RIPs. RTA showed the strongest activity against *R. solani* ribosomes. Efficient depurination was observed with as low as 1 $ng \cdot ml^{-1}$ of RTA. Saporin-S6 and ME_1 showed less depurination activity against *R. solani* ribosomes compared to RTA. The enzymatic activity of saporin was approximately 5-fold less against *R. solani* ribosomes and a dose of 5 $ng \cdot ml^{-1}$ showed the minimum enzymatic activity. ME_1 was approximately 50-fold less active compared to RTA, and a dose of 50 $ng \cdot ml^{-1}$ showed the minimum depurination activity.

A similar pattern of RIP activity profiles was observed against *A. solani* ribosomes as was seen against *R. solani* ribosomes (Table 3.1). However, the density and thickness of diagnostic fragments indicated that RTA was more active against *A. solani* than *R. solani* ribosomes (Table 3.1). In contrast, saporin-S6 showed enhanced depurination activity against *R. solani* ribosomes compared to *A. solani* ribosomes. Saporin-S6 showed depurination activity at concentrations as low as 5 $ng \cdot ml^{-1}$ against both *R. solani* (Fig.3.1B) and *A. solani* ribosomes (Table 3.1). However, the comparison of the diagnostic fragments indicated that saporin-S6 was more active against *R. solani* ribosomes than against *A. solani* ribosomes (Table 3.1). The enzymatic activity of ME_1 against *A. solani* ribosomes was lower than the activity of the other two RIPs, a finding similar to the results obtained with *R. solani* ribosomes. However, ME_1 exhibited enhanced enzymatic activity against *A. solani* ribosomes as determined by gel analysis. A sparse band was detected in *A. solani* ribosomes incubated with 10 $ng \cdot ml^{-1}$ of ME_1 (data not shown); the same amount of ME_1 did not produce a detectable fragment against *R. solani* ribosomes (Fig.3.1C).

Saporin-S6 showed enzymatic activity against *T. reesei* ribosomes with 10 $ng \cdot ml^{-1}$ as its lowest concentration, and RTA demonstrated the strongest enzymatic activity with 1 $ng \cdot ml^{-1}$ as its lowest concentration (Table 3.1). Nevertheless, diagnostic fragments observed by gel analysis indicated that *T. reesei* ribosomes were less susceptible to RTA than *A. solani* and *R. solani* ribosomes. Interestingly, *C. albicans* ribosomes were the most sensitive to saporin with doses as low as 5 $ng \cdot ml^{-1}$ causing depurination (Table 3.1). RTA was relatively less active against *C. albicans* ribosomes than against other fungal ribosomes, creating only faint aniline fragments at a concentration of 50 $ng \cdot ml^{-1}$ (Table 3.1). Unexpectedly, ME_1 showed no depurination activity against either *T. reesei* or *C. albicans* ribosomes upto 100 $ng \cdot ml^{-1}$ (Table 3.1).

Antifungal activity of RTA, saporin-S6 and ME_1

To explore the biological significance of the enzymatic activity of RIPs on fungal ribosomes, I tested the antifungal activity of RTA, saporin-S6 and ME_1 against *R. solani* and *T. reesei* (see Materials and Methods). Various concentrations of each enzyme were tested against the fungi, and the antifungal activity was observed as a crescent-shaped zone of inhibition at the mycelial front. RTA and saporin did not inhibit the growth of *R. solani* (Fig.3.2) nor that of *T. reesei* (data not shown) in plate assays. A number of different concentrations as high as 100 $\mu g \cdot ml^{-1}$ of RTA and saporin-S6 were tested against both *R. solani* and *T. reesei*, but no inhibitory activity was observed (data not shown). As summarized in Table 3.2, RTA and saporin-S6 had no antifungal activity even though these enzymes showed stronger enzymatic activity than that of ME_1 against intact ribosomes isolated from *R. solani* and *T. reesei* As shown in Figure 3.2A-C, 50 $\mu g \cdot ml^{-1}$ of ME_1 significantly inhibited the growth of *R. solani* during a time course. *R. solani* was treated with various doses of ME_1. As little as 10 $\mu g \cdot ml^{-1}$ of ME_1 showed inhibitory activity after 96 h of incubation, but ME_1 did not show growth inhibition against *T. reesei* (data not shown). These results indicate that ME_1 has selective inhibitory activity against certain fungi, and correlate with the gel depurination analysis result that ME_1 depurinated ribosomes from *R. solani* but not those isolated from *T. reesei* (Table 3.1).

ME_1 interactions with the fungal hyphae of *R. solani*

To dissect the antifungal activity of RIPs at the cellular level, ME_1 and saporin-S6 were labeled with a fluorescent dye using NHS-fluorescein (Pierce). Subsequently, the enzymatic activities of labeled RIPs were tested against *R. solani* ribosomes using depurination gel analysis. As shown in Figure 3.3A, 100 $ng \cdot ml^{-1}$ of labeled ME_1 and saporin-S6 were active against the ribosomes and released diagnostic fragments. Labeled RIPs were then applied to *R. solani* as described in Materials and Methods. *R. solani* was incubated with the labeled RIPs in an absolutely dark chamber to prohibit the light's effect on NHS-fluorescein. As shown in Figure 3.3B, NHS-fluorescein labeled ME_1 created an inhibitory zone against *R. solani* after 96 h of incubation, and this inhibition lasted up to 142 h (data not shown). However, labeled saporin-S6 up to 100 $\mu g \cdot ml^{-1}$ did not show any inhibitory activity, and the buffer solution containing 2 M NHS-fluorescein did not show fungal inhibition either (Fig.3.3B). Taken together, these results demonstrate that NHS-fluorescein did not interfere with the enzymatic activity of the proteins, and that antifungal activity was most likely the result of the biological function of the RIPs tested, and not the side effect of NHS-fluorescein.

To observe the RIP-fungus interaction, carefully collected hyphae growing in the proximity of applied labeled enzymes were used to detect the localization of fluorescence by fluorescent microscopy. As shown in Figure 3.4A and B, fluorescent signal indicated that ME_1 interacted with the fungal mycelium of *R. solani*. ME_1 showed strong interaction with the surface of hyphae in all collected samples. Interestingly, fluorescent signal was also detected in the region between hyphal cells, demonstrating that ME_1 could penetrate into the septa, or that ME_1, having penetrated the surface of cells, may move to the septa. Further, a dispersed staining pattern of fluorescent signal was observed in the cytoplasmic space of *R. solani* hyphae (Fig.3.4C-F). These images indicate that internalization of ME_1 occurs in the outer envelope after its interaction with the cell. As shown in Figure 3.4F, ME_1 then spreads out of hyphal cells, appearing as lysed fungal cells, suggesting that ME_1 depurinates ribosomes, and thus causes cell mortality. In contrast, hyphae collected after incubation with labeled saporin showed no fluorescent signal, indicating

that saporin did not interact with *R. solani* (Figure 3.4G and H), which correlates with its lack of antifungal activity.

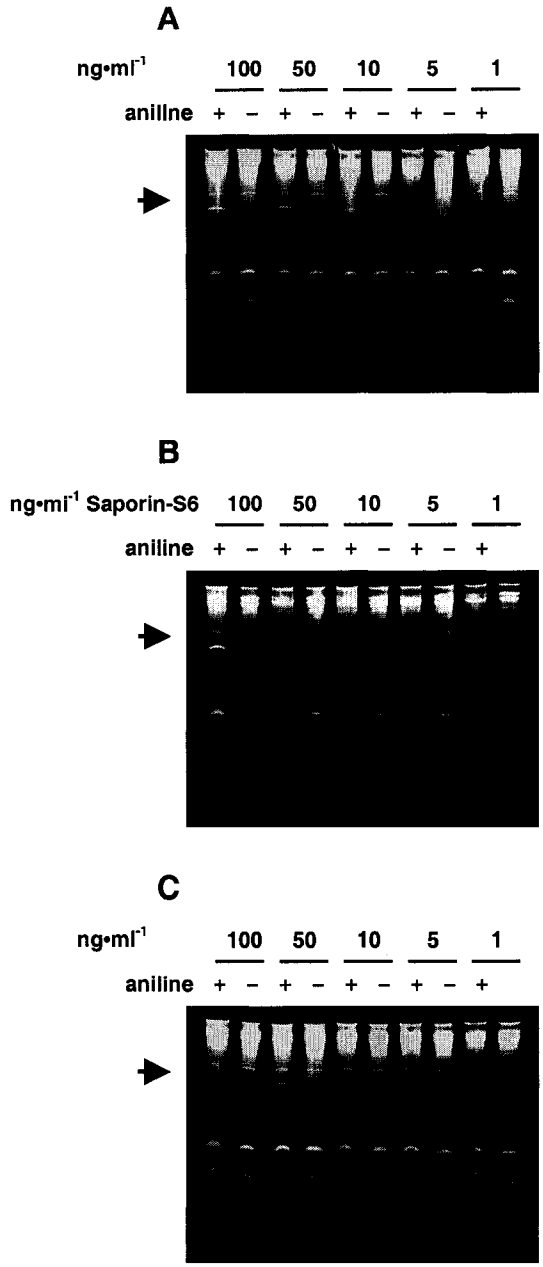

Figure 3.1. Enzymatic activity of RTA, Saporin-S6 and ME_1 on *R. solani* ribosomes. The ribosomes were isolated from *R. solani* and incubated with RTA (**A**), saporin-S6 (**B**) and ME_1 (**C**) as described in Materials and Methods. rRNAs were extracted, treated with aniline, separated on a 4.5% urea-polyacrylamide gel, and stained with ethidium bromide. RIP concentrations ($ng \cdot ml^{-1}$) are indicated above the lane, and the presence (+) or absence (-) of aniline is denoted. The arrow shows the presence of the diagnostic nucleotide cleavage product of rRNA.

Table 3.1. Comparison of enzymatic activity of RTA, saporin-S6 and ME_1. Enzymatic activity of RTA, saporin-S6 and ME_1 against ribosomes isolated from *A. solani, R. salani, T. reesei,* and *C. albicans*. Three RIPs in five different concentrations (100, 50, 10, 5, and 1 $ng \cdot ml^{-1}$) dissolved in 10 µl of 25 mM phosphate buffer (pH 7.0) were used for the determination of enzymatic activity. The RIP effect on fungal ribosomes is expressed in qualitative terms, in which + + + + + + + stands for the strongest activity, + for the weakest activity, and – for no activity. The activity was based on the relative intensity of the RIP-depurinated nucleotide fragments as observed in 4.5% urea-PAGE, and was analyzed using Gel Doc 2000 gel documentation system and Quantity One Quantitation Software (Bio-Rad).

Tested fungal pathogens	RTA	Saporin-S6	ME_1
		100, 50, 10 $ng \cdot ml^{-1}$	
R. solani	+ + + + + +	+ + + +	+
A. solani	+ + + + + + +	+ + +	+ +
T. reesei	+ + + + +	+ + +	–
C. albicans	+ +	+ + +	–
Tested fungal pathogens	RTA	Saporin-S6	ME_1
		5, 1 $ng \cdot ml^{-1}$	
R. solani	+ + +	+ +	–
A. solani	+ + + +	+	–
T. reesei	+ +	–	–
C. albicans	–	+	–

Table 3.2. Comparison between enzymatic and antifungal activity of RTA, saporin-S6 and ME_1. Enzymatic and antifungal activity of saporin-S6, RTA and ME_1 against *R. salani* and *T. reesei*. Ten $ng \cdot ml^{-1}$ of three RIPs dissolved in 10 µl of 25 mM phosphate buffer (pH 7.0) were used for the determination of enzymatic activity, and 50 $\mu g \cdot ml^{-1}$ of each RIP dissolved in 50 µl of 25 mM phosphate buffer (pH 7.0) was used for determination of antifungal activity. The effect on fungal ribosomes and growth is expressed in qualitative terms in which + + + + + stands for the strongest activity, + for the weakest activity, and – for no activity.

	Enzymatic activity of ribosomes			Inhibitory activity on fungal growth		
Tested fungi	RTA	Saporin-S6	ME_1	RTA	Saporin-S6	ME_1
R. solani	+ + + + +	+ + +	+	–	–	+ + + +
T. reesei	+ + + +	+ +	–	–	–	–

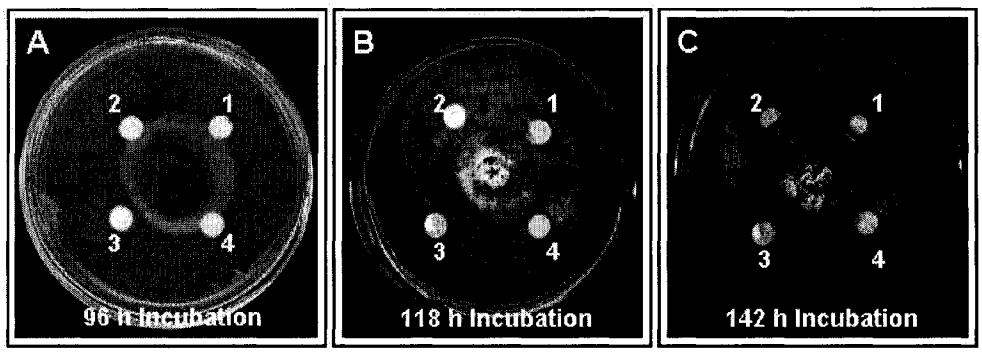

Figure 3.2. Radial growth-inhibition assay of RIPs against *R. solani* during a time course. Filter-sterilized 50 μg of saporin-S6 (**1**), RTA (**2**) and ME_1 (**3**) were applied to the discs, and tested for antifungal activities as described in Materials and Methods. The control (**4**) consisted of 25 mM $NaPO_4$ buffer, pH 7.5.

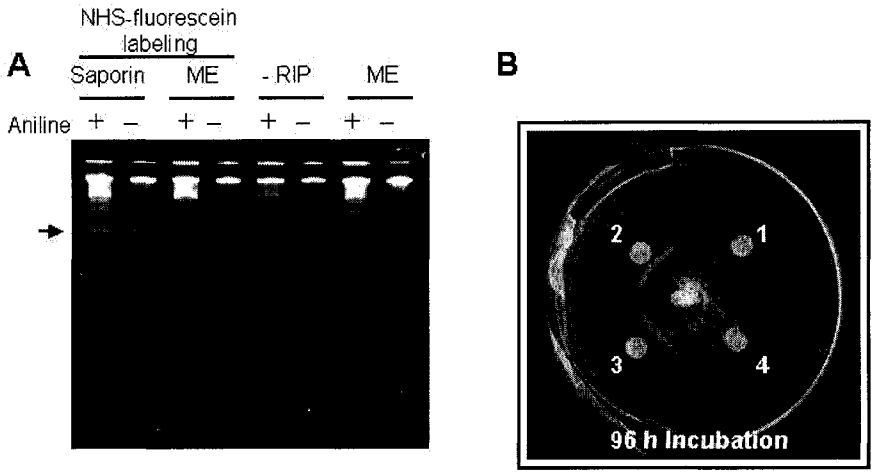

Figure 3.3. Enzymatic and antifungal activity of NHS-fluoresein labeled saporin-S6 and ME_1. **A,** The ribosomes were isolated from *R. solani* and incubated with 100 $ng \cdot ml^{-1}$ each of fluorescence-labeled saporin-S6 and ME_1 for 30 min. rRNAs were extracted with phenol/chloroform, treated with 1 M aniline, separated using a 4.5% urea-polyacrylamide gel electrophoresis, and stained with ethidium bromide. The presence (+) or absence (-) of aniline is denoted, and the arrow shows the presence of the diagnostic nucleotide cleavage product of rRNA. As a control, 100 $ng \cdot ml^{-1}$ of non-labeled ME_1 was used. **B,** Antifungal activity of NHS-fluorescein labeled saporin-S6 and ME_1 against *R. solani*. Filter-sterilized 100 $\mu g \cdot ml^{-1}$ of saporin-S6 (1), 50 $\mu g \cdot ml^{-1}$ (2), and 100 $\mu g \cdot ml^{-1}$ (3) of ME_1 were applied to the discs, and tested for antifungal activities as described in Materials and Methods. The control (4) consisted of 100 µl of 2 M NHS-Fluorescein dissolved in 25 mM $NaPO_4$ buffer, pH 7.5. After 96 h incubation, fungal hyphae were carefully collected from very near the discs to monitor RIPs-fungal interaction.

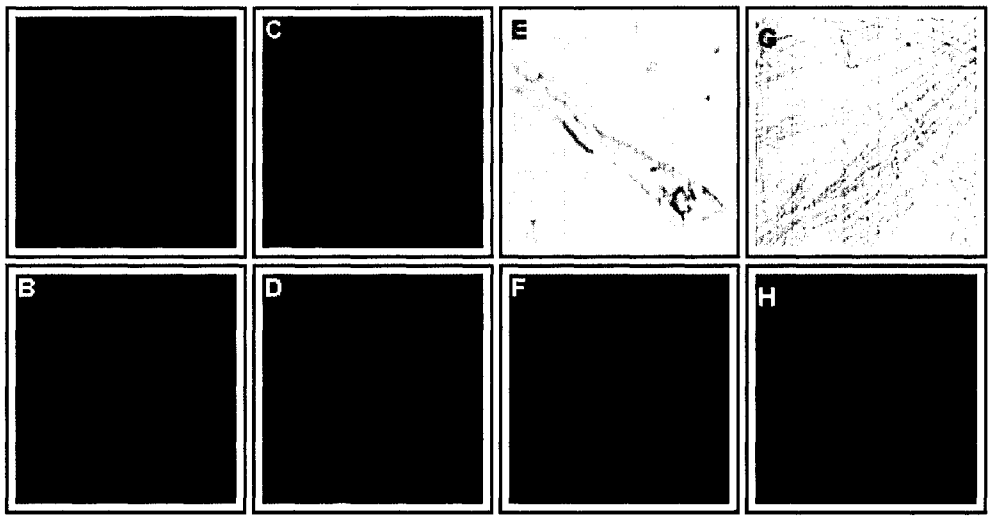

Figure 3.4. Fluorescence images monitoring interaction between RIPs and *R. solani.* The hyphae of *R. solani* were briefly washed with 10 % glycerol, and placed on a glass plate. Fluorescent images and phase images were taken using a fluorescent microscope (JEOL 2000 EXII). **A-F,** Interaction between ME_1 and *R. solani.* **G,** Phase-image was taken from the hyphae incubated with saporin-S6, and **H,** no fluorescence signaling was detected by interaction between saporin-S6 and *R. solani.* Control fungal hyphae images incubated with 50 μl of 2 M NHS-Fluorescein solution did not show fluorescent signal indicating that the signal is only detected by RIP-fungal interaction (data not shown).

DISCUSSION

Although several studies examined RIP antimicrobial properties such as antiviral and antifungal activities (Lodge et al., 1993; Tumer et al., 1997; Wang et al., 1998; Vivanco et al., 1999; Zoubenko et al., 2000), the role of RIP in plant defense is not yet clear. To explore the potential efficacy of RIPs as plant defense agents, I isolated ribosomes from various plant pathogenic fungi and characterized their sensitivity to three type I RIPs (RTA, saporin-S6 and ME_1). As summarized in table I, RTA, saporin-S6, and ME_1 exhibited depurination activity against fungal ribosomes in a substrate-specific manner. RTA showed overall the strongest activity toward fungal ribosomes.

In our studies comparing the catalytic activities of RTA, saporin-S6, and ME_1, each RIP clearly demonstrated enzymatic specificity (Fig.3.1 and Table 3.1) indicating that the depurination activity of RIPs depends on specific RIP-substrate interaction. The RIP-mediated substrate-specificity may be dependent on the flexibility of ribosomes and/or RIP structure (Monzingo et al., 1993; Chaddock et al., 1996; Maguire and Zimmermann, 2001). The RIP-ribosome interaction may contain a double step mechanism comprised of an initial interaction with ribosomal proteins and then the depurination of the rRNA (Hudak et al., 1999; Savino et al., 2000). Saporin showed covalent linkage to yeast ribosomal proteins (Ippoliti et al., 1992), and ricin was similarly linked to L9 and L10e proteins in mammalian systems (Valter et al., 1995). PAP was also shown to interact with *E. coli* L3 ribosomal protein (Hudak et al., 1999). These findings indicate that RIPs possess a structural domain involved in the recognition of specific ribosomal proteins. Recently, Savino et al. (2000) suggested the C-terminal region of saporin-S6 might be involved in this interaction. In addition, the conformational changes of the rRNA, which have been proposed to occur in the S/R loop during the elongation step, may enhance or interrupt RIP interaction with the target site (Marchant and Hartley, 1995). Therefore, substrate-specificity of RIPs may be caused by (1) the C-terminal region in RIPs that recognize and interact with ribosomal proteins, (2) unique ribosomal proteins from various ribosome sources that enhance or diminish interaction with RIPs, and (3) differential exposure of the S/R loop during the elongation step depending on different RIP-ribosomal conformations.

I found that the *N*-glycosidic activity of RIPs on fungal ribosomes did not completely account for their antifungal activity. RTA and saporin-S6 showed approximately 10 to 50-fold higher activity against isolated fungal ribosomes than did ME_1 (Fig.3.1 and Table 3.1). Nevertheless, RTA and saporin-S6 did not show antifungal activity in plate assays (Fig.3.2). In contrast, ME_1 showed inhibitory activity against *R. solani* growth at a dose as low as 10 $\mu g \cdot ml^{-1}$, although ME_1 was less active toward intact ribosomes of *R. solani* compared to RTA and saporin-S6 (Table 3.2). The potential function of RIPs as defense proteins has been supported by their enzymatic activity on ribosomal substrates isolated from several pathogenic microbes (for review, see Tumer et al., 1999; Neilson and Boston, 2001). However, in this communication, I show experimental evidence that certain type I RIPs have biological activity as defense proteins by directly inhibiting fungal growth, and this antifungal activity is independent of the level of their ribosome-depurinating activity.

To further our understanding of the antifungal mechanism of RIPs, I labeled ME_1 and saporin-S6 with NHS-fluorescein and monitored the interaction between labeled RIPs and *R. solani*. As shown in Figure 3.4, labeled ME showed strong interaction with *R. solani* hyphae, in contrast to no interaction between labeled saporin-S6 and *R. solani*. Furthermore, fluorescent signals were observed in the septa between two hyphal cells, and the density and thickness of signals shown within the septa and other cell barriers were similar, indicating that ME_1 not only interacted with the surface of cell walls but also was embedded in them. These results suggest that RIPs such as ME_1 interact with functional domains located in the fungal cell membranes and/or cell wall. Interestingly, I have also shown that ME_1 was internalized into fungal cytoplasmic space (Fig.3.4C-F). Type I RIPs lack the lectin chain contained in type II RIPs, and thus are believed to be incapable of penetrating undamaged cells. Here I report that ME_1, a type I RIP, is capable of penetrating undamaged fungal cells. Our results also showed that ME_1 selectively recognizes fungi and inhibits their growth, which leads us to hypothesize that a fungal membrane receptor is required for the action mechanism of ME_1, and that the internalization of ME_1 is necessary to exert its fungicidal activity. However, ME_1's mechanism of internalization is not clear at this point. As a possible explanation, posttranslational modifications may exist in ME_1

similar to some type I RIPs such as gelonin and dianthin (Stirpe et al., 1980; Stirpe et al., 1981), which may be utilized for binding to carbohydrate receptors on the fungal cell membrane (Lord and Roberts, 1996; Sandvig and van Deurs, 1996).

Internalization of ME_1 into the fungal cytoplasm accounts for the actual antifungal action mechanism of ME_1 by which it depurinates fungal ribosomes and causes protein synthesis to cease, thus causing cell death. Accordingly, fluorescent imaging reveals that ME bursts out of the mycelium cells through broken cell walls, causing fungal cell death (Fig.3.4). In contrast, fluorescence images taken after the incubation of labeled saporin-S6 with *R. solani* show no indication of interaction between saporin-S6 and the fungus (Fig.3.4G and H). This result correlates with the lack of antifungal activity of saporin-S6, although saporin did show higher depurination activity against *R. solani* ribosomes compared to ME_1.

In summary, I employed the ribosome depurination assay, the plate antifungal activity assay, and NHS-fluorescent labeling techniques to elucidate the antifungal role and function of several RIPs. Our findings provide experimental evidence that enzymatic activity of RIPs on certain substrates does not fully explain their inhibitory function against those pathogens. The RIP ME_1 did show direct inhibitory action against fungi. I hypothesize here that certain RIPs recognize specific fungi, are internalized into the cytoplasmic space, and kill the targeted cell by interrupting protein synthesis.

CHAPTER 4

The *N*-glycosidase activity of the ribosome-inactivating protein ME_1 targets single-stranded regions of nucleic acids independent of sequence or structural motifs

ASTRACT

ME_1, a type I RIP, belongs to a family of enzymes long believed to possess rRNA *N*-glycosidase activity directed solely at the universally conserved residue A_{4324} in the S/R loop of large eukaryotic and prokaryotic rRNAs. I have investigated the effect of structural modification of non-ribosomal RNA substrates on the interaction of those substrates with ME_1 and other RIPs. ME_1 was shown to depurinate a variety of partially denatured nucleic acids, randomly removing adenine residues from single-stranded regions and, to a lesser extent, guanine residues from wobble base-pairs in hairpin stems. A defined sequence motif was not required for recognition of non-paired adenosines and cleavage of the *N*-glycosidic bond. Substrate recognition and ME_1 activity appeared to depend on the physical availability of nucleotides, and denaturation of nucleic acid substrates increased their interaction with ME_1. Pretreatment of mRNA at 75°C rather than 60°C, for example, lowered the apparent K_D from 87.1 nM to 73.9 nM, making it more vulnerable to depurination by RIPs. Exposure to ME_1 completely abolished the infectivity of partially-denatured RNA transcripts of the potato spindle tuber viroid, suggesting that *in vivo* RIPs may target invading nucleic acids before they reach host ribosomes. The extensive folding of many potential substrates, however, interferes with their ability to interact with RIPs, thereby blocking their inactivation by ME_1 or other RIPs.

INTRODUCTION

RIPs are cytotoxic enzymes identified in plants, fungi and bacteria, which act as glycosidases that specifically cleave nucleotide N-glycosidic bonds (Endo et al., 1987). It has been proposed that RIPs inhibit protein synthesis by virtue of their enzymatic activity, selectively removing a specific adenine residue from the highly conserved and surface-exposed S/R loop in the large rRNA (Endo et al., 1987; Endo and Tsurigi, 1987; Hartley et al., 1991). This enzymatic cleavage prevents the binding of the EF-2/GTP complex to the ribosome, with the subsequent arrest of protein synthesis, and, eventually, cell death (Osborn and Hartley, 1990).

The universally conserved adenine residue A_{4324} of the eukaryotic 28S rRNA was long considered the only enzymatic substrate of RIPs, but several lines of evidence have recently

revealed alternative substrates to the S/R loop. For instance, it has been shown that several RIPs can release adenine from multiple sites in rRNA (Barbieri et al., 1992). Furthermore, saporin-L1 can release adenine residues from a variety of nucleic acid substrates - poly(A), mRNA, tRNA, and DNA (Barbieri et al., 1994, 1996). More than fifty other RIPs are active on DNA (Barbieri et al., 1997). Certain RIPs also display enzymatic activity toward RNA transcripts derived from various plant and animal viruses including the human immunodeficiency virus (Ussery et al., 1977; Aron and Irvin, 1980; McGrath et al., 1989; Zarling et al., 1990; Barbieri et al., 1994; Taylor et al., 1994; Rajamohan et al., 1999ab; Au et al., 2000). Enzymatic activity on these non-ribosomal substrates requires a high protein/substrate ratio, however, and the biological relevance of these observations is unclear.

Several studies using the RTA have suggested that RIP catalytic activity requires a specific substrate structure such as a tetraloop with the sequence $^{(1)}G^{(2)}A^{(3)}G^{(4)}A$ (Endo and Tsurugi, 1988; Marchant and Hartley, 1995, Orita et al., 1996). The stem of this structure possesses tilted Watson-Crick base-paring in the stem with an unusual $^{(1)}G:^{(4)}A$ base-pairing in the loop region (Szewczak et al., 1993; Orita et al., 1993). The depurination-site adenine ($^{(2)}A$) occupies an exposed position external to the solvent-accessible loop, while the other nucleotide bases are buried within the phosphodiester backbone by hydrogen-bonding and base-stacking. In contrast, PAP does not exhibit an absolute requirement for the tetraloop structure in order to exhibit enzymatic activity (Marchant and Hartley, 1995). Recent reports propose that PAP recognizes and binds to the cap structure of mRNAs, specifically depurinating downstream adenine residues (Hudak et al., 2000, 2002). Based on these results, PAP may bind to capped viral RNA, subsequently depurinating viral RNAs rather than host ribosomes during the infection process (Hudak et al., 2000). This hypothesis does not, however, explain the activity of PAP with substrates such as rRNA or DNA that lack a cap structure (Barbieri et al., 1997).

Possible explanations for this remarkable array of enzymatic activities include inherent differences among RIPs, the diversity of RNA substrates, or, as explored in this manuscript, differences in experimental conditions. Temperature, pH, and ionic composition of the assay buffer change not only the catalytic efficiency (k_{cat}/K_m) of RIPs but also their target sites (Barbieri

et al., 1996; Chen et al., 1998; Tang et al., 2001). Experimental conditions also determine the catalytic activities of different RIPs (Barbieri et al., 1997). Efficient catalysis may require that the substrate(s) assume a particular structural conformation induced by specific experimental conditions. These observations prompted us to ask whether the structural changes of substrates induced by experimental treatments such as heating could affect the enzymatic activity of RIPs.

RNAs are highly flexible molecules whose structures are influenced by such factors as the vectorial nature of transcription and translation, trans-acting factors, the presence of RNA-binding proteins or RNA chaperones, and the cellular environment, including ion homeostasis (Schroeder et al., 2002). Thus far, studies of RNA secondary structure have been carried out almost exclusively *in vitro*, and it remains to be proven whether conclusions from these studies also apply *in vivo*. For example, a recent study of telomerase RNA has shown that RNA structures can be different *in vitro* and *in vivo*, as exemplified by the *in vitro* formation of the phylogenetically conserved pseudo-knot in the 5' part of the telomerase RNA which was not observed *in vivo* (Antal et al., 2002). Importantly, changes in RNA structure *in vivo* can cause loss of the ability to interact with other molecules (Nikolcheva and Woodson, 1999). The structural differences occur due to the extensive folding of a single-stranded RNA *in vitro* transcript and/or to more minor factors. Experimental variables such as temperature or ionic concentration often trap RNAs in inactive conformations that interfere with their interactions with other molecules (Herschlag, 1995; Bonin et al., 2002).

In the present study, I have systematically perturbed the conformation of various nucleic acids to further understand the substrate specificity of RIPs. Our results demonstrate that the enzymatic activity of ME_1 on non-ribosomal substrates is highly structure-dependent. Extensive structural folding caused by experimental conditions was found to interfere with the interaction of ME_1 and non-ribosomal substrates. Enzymatic specificity and kinetics vary with the conformation of non-ribosomal substrates, and a specific motif was not found to be necessary for substrate recognition by ME_1.

MATERIALS AND METHODS

Proteins

ME_1 was purified from storage roots of *M. expansa* using immuno-affinity chromatography. A polyclonal antibody, previously raised in our laboratory against reverse-phase HPLC-purified ME_1 (Vivanco et al., 1999), was coupled to cyanogen bromide (CNBr)-activated sepharose at pH 8.0. Total root proteins of *M. expansa* were equilibrated with 75mM Tris-HCl, pH 8.0, to facilitate protein-ligand interaction, and immuno-bound proteins were then eluted with 100mM glycine-HCl, pH 2.7, containing 0.5M NaCl. ME_1 was further separated using cation-exchange chromatography (poros-HS; PE Biosystems), resulting in >99% pure protein as judged by SDS-PAGE with silver staining and sequence analysis. Purified RTA and saporin-S6 were purchased from Sigma. Their purities were checked by SDS-PAGE with silver staining, and protein concentration was determined as described by Bradford (1976) using a protein assay kit (Bio-Rad) and bovine serum albumin (BSA) as a standard.

DNA and Oligonucleotide

The ORF region of pap-h was amplified by polymerase chain reaction (PCR) from hairy roots of pokeweed using gene-specific primers (GSPs) 5E.30 (5'-ATGCATGTTCAT-CTGATCAATCATAAAAGT-3') and 3E.28 (5'-ATCAGAATCCCTGAAATAGATTACCAAG-3') designed from its cDNA sequence (GenBank accession no. AY071928). The PCR product was then subcloned into pGEM®T Easy vector (Promega). pGEM®T Easy recombinant plasmids encoding defense-related genes, *B26, Tom RP-O'b*, and *At2g14610*, were gifts of Dr. Christopher B. Lawrence (Depart. of Bioagricultural Sciences and Pest Management, Colorado State University).

The small oligonucleotide 23SSO-A_{12} (5'-GGGCCGGCGGUACCGCCGGCGCC-3') was synthesized from the Macromolecular Resources Facility (Department of Biochemistry, Colorado State University).

Isolation of Ribosomes

To isolate ribosomes, yeast cells (10g, *S. cerevisiae* strain YPH500) and leaves of *M. expansa* (50g) were ground in liquid N_2 with a mortar and pestle, and 100 ml of extraction buffer (200 mM KCl, 25 mM $MgCl_2$, 25 mM EGTA, 200 mM Sucrose and 25 mM ß-mercaptoethanol in 200 mM Tris-HCl, pH 9.0) was added. After centrifugation at 10,000 g for 20 min at 4 °C, the resulting supernatant was layered onto a sucrose cushion (1 M sucrose for yeast ribosomes and 2 M sucrose for *M. expansa* ribosomes, 20 mM KCl and 5 mM $MgCl_2$ in 25 mM Tris-HCl, pH 7.6) in 70 Ti tubes (Beckman), and centrifuged at 55,000 rpm for four hours at 4 °C (L-70 Ultracentrifuge, Beckman). The pellets were resuspended in 25mM Tris-HCl buffer (pH 7.6) with 25mM KCl and 5mM $MgCl_2$. Further preparation of protein-free rRNAs were extracted from ribosomes with phenol:chloroform (1:1, v/v) and precipitated with ethanol for two hours at –80 °C.

Preparation of Substrates

DNA fragments encoding the *pap-h* ORF were amplified from the corresponding pGEM®T Easy plasmids by PCR using GSP primers 5E.30 and 3E.28. After electrophoresis in a 1.5% [w/v] agarose gel and staining in 0.5 $mg \cdot ml^{-1}$ ethidium bromide, the DNA fragments were excised from the gel and recovered using the Quantum Prep Gel Slice Kit (Bio-Rad).

pap-h, *B26*, *Tom RP-O'b* and *At2g14610* mRNAs were transcribed from the corresponding pGEM®T Easy plasmid DNAs using T7 RNA polymerase (Promega). Template DNAs were linearized by *Spe*1 digestion and purified by phenol:chloroform extraction and ethanol precipitation. Transcription reactions containing 40 mM Tris-HCl, pH 7.5, 9 mM $MgCl_2$, 10 mM NaCl, 2 mM spermidine, 10 mM dithiothreitol, 20 units RNasin, 1.5 mM each of the four nucleoside triphosphates, 50 nM DNA templates, and 3 units/µl T7 polymerase were incubated at 37°C for one hour. PSTVd RNA transcripts were synthesized using SP6 RNA polymerase, plasmid pST64-B5 (Cress et al., 1983) as a template, and four nucleoside triphosphates with or without supplemental 5'-[□-^{32}P] UTP (3000 Ci/mmole; Amersham). Transcription reactions were subsequently extracted with phenol and chloroform, and the nucleic acids were precipitated with ethanol for two hours at –80°C before purification by electrophoresis on 6% [w/v] polyacrylamide

gels containing 1x TBE buffer-5M urea and elution in 500 mM ammonium acetate, 0.1% [w/v] SDS, 0.1 mM EDTA. RNA transcripts were then recovered by ethanol precipitation.

Heat Treatment and Depurination Analysis

Partial denaturation of DNA and RNA substrates carried out for 30 sec at various temperatures (30, 45, 60, 75 and 90°C). Each reaction (15 µl) contained approximately 150 nM of either DNA in incubation buffer PS-1 (10 mM Tricine-KOH, pH 8.7, 2.5 mM KCl, 3 mM $MgCl_2$, 3.75 µg/ml BSA, 0.005% [v/v] Tween-20) or RNA transcripts in buffer PS-2 (1.25 mM Tris-HCl, pH 7.4, 2.5 mM KCl, 1.25 mM $MgCl_2$, 0.01 mM EDTA). Reactions were quenched by placing the tubes on ice. Following addition of RIP incubation buffer PS-3 containing 10 mM Tris-HCl, pH 7.2, 40 mM KCl and 1 ng RIP (85µl), the reaction mixtures were incubated at 37 °C for 10 min. Nucleic acids incubated in the absence of RIPs served as negative controls. Following incubation, RIPs were removed by phenol:chloroform (1:1, v/v) extraction, and the aqueous phase containing the nucleic acids was divided in half. One aliquot was incubated for 30 min on ice with 1 M of aniline acetate (pH 4.5) before precipitation with ethanol; the second aliquot was precipitated directly. Both aniline-treated and untreated nucleic acids were fractionated by electrophoresis in 6% [w/v] polyacrylamide gels containing 7 M urea and stained with ethidium bromide.

A fluorescence assay of adenine release was carried out as described by Zamboni et al. (1989). Experiments were performed by pre-incubating SSO (10 nM) at 45°C for 30 sec in buffer PS-2, and, subsequently incubating the SSO in buffer PS-3 at 37°C for 20 min in the absence and presence of RIP. At the end of incubation, 1 vol. of cold ethanol was added and, after 10 min at –80°C, the ethanol-soluble fractions were recovered by centrifugation. Free adenine was then converted into its etheno derivative; 0.2 ml portion of the ethanol-soluble fractions was diluted to 1 ml with H_2O, 0.4 ml of 0.1 M sodium acetate buffer, pH5.1, containing 0.14 M chloroacetaldehyde was added, and the samples were heated in a water bath at 80°C for 40 min. Fluorescence was measured in an Aminco-Bowman spectrophoto-fluorimeter. Excitation and emission wavelengths were set at 280 and 400 nm respectively.

Temperature-Gradient Gel Electrophoresis

Temperature-gradient gel electrophoresis of ^{32}P-labeled PSTVd RNAs was carried out using a commercially available apparatus (Qiagen). The horizontal 5% polyacrylamide - 0.17% bisacrylamide gel and buffer reservoirs contained 0.2x TBE, 5 mM NaCl. Following pre-electrophoresis at 26°C (200 V, 30 min), PSTVd transcripts (approximately 40,000 cpm) were diluted with 165 µl loading buffer (18 mM NaCl, 17 mM sodium cacodylate, 3 mM cacodylic acid, 0.2 mM EDTA, pH 7.0) and 25 µl loading dye (50% glycerol, 1x TBE, 2% BPB-XC) and applied to the single 12 cm sample slot. Sixty minutes later, the current flow was stopped for 30 min while a 25-65°C temperature gradient was established across the gel. Upon resumption of electrophoresis, the voltage was increased to 350 volts, and 1 hr 45 min later, the gel was fixed in 10% [v/v] ethanol - 1 % [v/v] acetic acid and dried before overnight autoradiography.

Primer Extension

pap-h mRNA transcripts treated with ME_1 as described above were purified by extraction with phenol:chloroform and chloroform:isoamyl alcohol followed by ethanol precipitation. RNAs were resuspended in 5 µl 2x Primer Extension Buffer (100 mM Tris-HCl, pH 8.3, 100 mM KCl, 20 mM $MgCl_2$, 20 mM DTT, 1 mM spermidine, 2 mM dNTPs) and annealed for 20 min at 58°C with an oligonucleotide primer (5'-CTTTGGCTTGATTGCGTAGAG-3') complementary to sequences 200 bases downstream from the 5' end of pap-h mRNA. Primer extension by reverse transcriptase was carried out for 30 min at 42°C in a final reaction volume of 20 µl with the addition of 40 mM sodium phosphate buffer. RNA templates were destroyed by incubation with RNase A before the addition of formamide loading buffer (20 µl) to terminate the reaction. Following electrophoresis in 6% polyacrylamide gels containing 7 M urea, extension products were visualized by silver staining using the Silver Sequence™ DNA sequencing system (Promega). The position of the 5' end was verified by comparison with a DNA sequencing ladder from a pGEM®T Easy plasmid encoding pap-h prepared with the same primer used for primer extension.

In-Line Probing of RNA

Values for the half maximal apparent dissociation constant (apparent K_D) of each construct were determined by conducting in-line probing of RNA, wherein the concentration of the ME_1 was varied between zero and 100 μM. Composite plots of the fraction of RNA cleaved at specific sites versus the logarithm of the concentration of ME_1 were generated to provide an estimate of the apparent K_D. Fraction-cleaved values were normalized relative to the highest and lowest cleavage values measured for each site. Peaks corresponding to the identified bands are highlighted by colored lines. The graphs were generated and analyzed using Gel Doc 2000 gel documentation system and Quantification Software (Bio-Rad).

PSTVd Infectivity Assays

PSTVd transcripts incubated in the presence or absence of ME_1 after partial denaturation were diluted with 20mM $NaPO_4$, pH 7.0 to a final concentration of either 10 or 100 $pg \cdot \mu l^{-1}$. Aliquots (10 μl) were then placed on the carborundum-dusted cotyledons of seven-day-old tomato (*Lycopersicon esculentum* Mill cv "Rutgers") seedlings and gently rubbed with the side of a sterile micropipette tip. Control plants were inoculated with buffer alone. Inoculated seedlings were maintained for 4-6 weeks in a greenhouse under conditions suitable for viroid replication and periodically tested for the presence of PSTVd progeny by dot-blot hybridization using full-length, digoxygenin-labeled RNA probes specific for (+)PSTVd (Podleckis et al., 1993).

RESULTS

Immuno-Purification of ME_1

In order to obtain ME_1 with a high degree of purity in a single step, I used an affinity chromatography approach involving a polyclonal anti-ME_1 antibody. This antibody, previously raised in our laboratory (Vivanco et al., 1999), was used as a ligand to generate an affinity matrix via coupling to cyanogen bromide (CNBr)-activated sepharose. Total root proteins of *M. expansa*

were applied to the column, and immuno-bound proteins were eluted with pH linear gradients as outlined in Materials and Methods. As shown in Figures 4.1A and B, the single protein peak produced by the elution process contained two protein bands. These bands corresponded to ME_1 (30 kD; Vepachedu et al., 2003) and ME_2 (27 kD; Vivanco et al., 1999), two RIPs previously found to be present in *M. expansa* roots. ME_1 was further purified by cation-exchange chromatography, and its RNA *N*-glycosidase activity was confirmed with ribosomes prepared from *S. cerevisiae* as previously described (Park et al., 2002a). As shown in Figure 4.1C, the immuno-purified ME_1 depurinated the 28S rRNA and released the 367-nucleotide diagnostic fragments upon treatment with aniline, thereby demonstrating that immuno-purified ME_1 is enzymatically active as an RIP.

Activity of ME_1 on Partially Denatured Non-Ribosomal Substrates

As a first step in understanding the enzymatic activity of RIPs on nucleic acids, I examined the reaction catalyzed by ME_1 on various partially denatured non-ribosomal substrates including intact nucleic acids such as DNA and mRNA encoding *pap-h* (an RIP identified in the hairy roots of pokeweed; Park et al., 2002a), and rRNA isolated from yeast ribosomes. Before incubation with ME_1, each nucleic acid substrate was preheated to temperatures ranging from 30 to 90°C to induce structural modifications.

The non-covalent interactions such as hydrogen bonding and base stacking that stabilize double-stranded DNA (dsDNA) can be disrupted by simply raising the temperature (Fig. 4.2A). When a depurinated nucleic acid is treated with aniline, the phosphodiester backbone undergoes cleavage at the site(s) of depurination, and small nucleotide fragment(s) are released. As a result, the amount of intact nucleic acid quantitatively decreases. The fact that dsDNA levels were not affected by pre-incubation at 30°C followed by incubation with ME_1 and aniline treatment indicates that ME_1 does not enzymatically depurinate nor degrade dsDNA. Increasing the pre-incubation temperature to 45°C or even 75°C resulted in the release of single-stranded DNA (ssDNA), but the catalytic activity of ME_1 remained undetectable. In contrast, the quantitative decrease in intact ssDNA template visible in the electrophoretic profiles of dsDNA pre-incubated

at 90°C showed that ME_1 can depurinate ssDNA. As showed in Figure 4.2B, ssDNA produced at pre-incubation temperatures > 80°C became susceptible to ME_1. Note, however, that dsDNA was not susceptible to ME_1. These results indicate that ME_1 acts as an ssDNA *N*-glycosidase. Incubation of ssDNA released by pretreated at 90°C with as little 100 pg ME_1 resulted in detectable depurination (Fig. 4.2C). In addition, enzymatic activity of ME_1 is both rapid and spontaneous that ssDNA depurination was completely in ≤30 sec. (Fig. 4.2D). Throughout this study, aniline treatment of partially denatured nucleic acids alone did not result in cleavage (results not shown).

I next examined the catalytic action of ME_1 on two partially denatured RNA substrates. As shown in Figure 4.3A (lanes d and e), ME_1 was not active on deproteinized rRNAs stored at 0°C. Data presented in Figure 3B show, however, that pre-incubation of rRNAs at relatively low temperatures (i.e., 45°C and 60°C) resulted in the depurination of 26S rRNA following ME_1 exposure. Increasing the pre-incubation temperature to 75°C resulted in depurination of both 26S and 18S rRNA. Interestingly, the electrophoretic pattern showed that the ME_1-depurinated rRNAs released many different fragments after aniline treatment. Because rRNA templates were stable up to 90°C under the buffer conditions used (Fig. 4.3A, lanes f to m), the fragment patterns observed in Figure 4.3B indicate that ME_1 depurinates rRNAs at multiple sites. As shown in Figure 4.3C, heat-treated *pap-h* mRNA was also susceptible to ME_1. Taken together, these results indicate that i) onset of ME_1 enzymatic activity is closely related to the secondary structure of potential single-stranded nucleic acid substrates, and ii) ME_1 cleavage of physically available *N*-glycosidic bonds is random.

Activity of ME_1 on A Single-Stranded RNA with Multiple Adenines

To further examine the enzymatic activity and specificity of ME_1 on partially denatured mRNA substrates, *pap-h* mRNA synthesized *in vitro* was incubated with ME_1 and subjected to primer extension analysis using a primer annealing 200 bases downstream from its 5' terminus. Inspection of the electrophoretic profiles shown in Figure 4.4A reveal that *pap-h* mRNA fragmentation was highly temperature dependent. Pre-incubation of *pap-h* mRNA at temperatures

>45° C led to modification/cleavage at several sites. ME_1 activity was greater on mRNA pre-treated at 75°C than on those pre-incubated at lower temperatures. Several sites (e.g., A_{11}, A_{19}, A_{25}, A_{45}, A_{64}, A_{68} and A_{108}) were susceptible to ME_1 at all temperatures. None of the ME_1-targeted sites, however, showed any sequence homology, indicating that ME_1 recognition and catalysis do not require a defined sequence motif.

As shown in Figure 4.4B, the results of primer extension were largely congruent with the computationally predicted secondary structures of *pap-h* mRNA at various temperatures; i.e., depurination occurred most frequently at unpaired adenine residues in potential single-stranded regions and bulge loops. Only three of the adenine residues susceptible to depurination (A_{45}, A_{121} and A_{123}) were located in hairpin loops previously reported to be the structural motif required for RIP activity (Endo and Tsurugi, 1988). These results suggested that ME_1 acts mostly on adenine residues. Note, however, that two guanine residues (G_{117} and G_{133}) were also modified when the mRNA was pre-incubated at 60°C. Repeated experiments confirmed this same site-specific guanine removal, indicating that although ME_1 preferentially targets adenine residues, guanine residues are also potential targets. Susceptibility of guanine residues could involve formation of specific tertiary structure(s).

To further understand the interaction between ME_1 and potential mRNA substrates, enzymatic activity was analyzed by monitoring the extent of base removal at several ME_1-susceptible sites within *pap-h* mRNA. ME_1 activity was assessed by comparing the relative band-densities at four sites (i.e., A_{11}, A_{64}, A_{68} and A_{103}) that were consistently susceptible to ME_1 in mRNA pre-incubated at different temperatures. As shown in Figure 4.4C, the breakdown of mRNA structure led to increased ME_1 activity at all four positions.

The enzymatic specificity of ME_1 was further examined by determining the apparent dissociation constant (apparent K_D) over a range of ME_1 concentrations. When trace amounts of *pap-h* mRNA pre-treated at 60°C were incubated with 0 to 100 μM ME_1, half-maximal cleavage was observed in the presence of approximately 87.1 nM ME_1. Likewise, the probing of mRNA pre-treated at 75°C yielded an apparent K_D of 73.9 nM. The results presented in Figure 5A indicate that ME_1 activity increases with the degree of substrate denaturation. However, it is

worth noting that the K_D values for individual nucleotide-ME_1 interactions might differ from the overall apparent K_D values. As shown in Figure 4.5B, the K_D value of individual nucleotides varied, and ME_1 was more active at some sites present in RNA pre-treated at 60°C than at 75°C. For example, the apparent K_D values for positions A_{103} and A_{108} were lower for mRNAs pre-treated at 75°C than for those pre-treated at 60°C. Just the opposite behavior was observed for positions A_{11}, A_{64} and A_{68}.

ME_1 Depurinates a Variety of Uncapped mRNAs

To determine whether ME_1 activity on single-stranded RNA is a general phenomenon, RNA transcripts derived from three defense-related fungal and plant ORFs (i.e., *B26*, *Tom PR-O'b* and *At2g14610*) were partially denatured by heating and incubated with ME_1. These ORFs encode an acidic α-elicitin from *Phytophthora cryptogea* (*B26*; Panabieres et al., 1995), a β-1,3-glucanase from *L. esculentum* (*Tom RP-O'b*; Domingo *et al.*, 1994), and pathogenesis related protein-1 (PR-1) from *Arabidopsis thaliana* (*At2g14610*; Genbank accession no. AY117187). As shown in Figure 4.6A, heat treatment rendered all three RNAs susceptible to ME_1. RNAs pre-treated at 0°C were unaffected by incubation with ME_1 (data not shown), but depurination at selective sites could be seen at temperatures as low as 30°C. Interestingly, the enzymatic efficiency of ME_1 appeared to be mRNA dependent. ME_1 depurinated multiple sites on all three transcripts but was less active on *B26* RNA. Pre-incubation of *Tom PR-O'b* and *At2g14610* transcripts at high temperatures resulted in extensive depurination, and intact RNA was undetectable after aniline treatment (compare Figs. 4.6Ab and c). In contrast, intact *B26* transcripts were visible at all temperatures tested, even though the appearance of a "smear" of fragments after aniline treatment indicated that ME_1 acts at multiple sites (Fig. 4.6Aa). These results provided clear evidence that ME_1 can act in a structure-dependent fashion at multiple sites within a single-stranded RNA substrate.

Hudak et al. (2000, 2002) have recently proposed that recognition of luciferase mRNA by PAP requires the presence of a cap structure. Recognition is followed by depurination of downstream adenine residues. To determine whether or not a cap structure is required for recognition of luciferase mRNA, uncapped luciferase transcripts were pre-treated under various

conditions and then incubated with ME_1. As expected (see Hudak et al., 2000, 2002), depurination was not detectable with uncapped luciferase mRNAs stored at 0 °C (results not shown). Uncapped luciferase mRNAs that had been pre-treated at higher temperatures were clearly susceptible to ME_1, however. As shown in Figure 4.6Ba, multiple sites in uncapped luciferase transcripts became susceptible to ME_1 after pre-incubation at 45 °C, releasing a number of small fragments after aniline treatment. Note also that the catalytic efficiency of ME_1 increased with the ratio of substrate denaturation.

RIP activity on uncapped luciferase mRNA was not limited to ME_1. Parallel experiments involving several other well known RIPs such as RTA and saporin-S6 yielded RNA fragmentation patterns similar to those produced by ME_1, indicating that the cap structure is not absolutely required for mRNA depurination (Figs. 4.6Bb and c). In all cases, RIP activity appeared to be tightly regulated by mRNA conformation.

Activity of ME_1 on A Single-Stranded Plant Pathogenic RNA

To examine the possible biological effects of ME_1 activity on plant pathogenic RNAs, I tested the ability of ME_1 to depurinate the potato spindle tuber viroid (PSTVd). PSTVd is a small (359 nt), covalently closed circular RNA molecule whose ability to replicate in cultivated potato results in a disease known as spindle tuber. The temperature-dependent conversion of its rod-like native structure to an open circular form occurs via a series of discrete, well-characterized structural transitions (Riesner, 1990; Steger and Riesner, 2003). The possible role of these transitions in modulating the biological properties of PSTVd remains poorly understood.

This denaturation process is illustrated in Figure 4.7A where PSTVd RNA transcripts synthesized *in vitro* were analyzed by temperature gradient gel electrophoresis (TGGE) under low ionic strength conditions. Over a temperature range of 30-60°C, the transition of PSTVd from a highly base-paired, rapidly migrating structure to a more open, slowly migrating structure is clearly visible. Comparing these results with those from the depurination analysis shown in Figure 7B, ME_1 can be seen to act on PSTVd transcripts pre-incubated at temperatures $\geq$ 45°C. This result provides biochemical evidence that ME_1 can act directly on a pathogenic nucleic acid.

Finally, in order to examine the biological effects of ME_1 action, the ME_1-treated PSTVd RNAs were inoculated onto the cotyledons of young tomato (*L. esculentum*) seedlings. Five weeks post inoculation, epinasty and stunting symptoms typical of PSTVd infection began to appear in the foliage of plants inoculated with PSTVd RNAs incubated in the absence of ME_1 (Fig. 4.7C), and the inoculated plants were subsequently tested for the presence of PSTVd by dot-blot hybridization. As shown in Table 4.1, incubation of PSTVd RNA transcripts pretreated at temperatures greater than ≥ 75 °C with ME_1 completely abolished infectivity.

ME_1 Preferentially Targets A Non-Ribosomal Nucleic Acid Substrate

In order to further explore the affinity of ME_1 for various potential substrates *in vitro*, I examined i) the ability of ME_1 to act on ribosomes isolated from *M. expansa* leaf tissue and ii) the ability of such ribosomes to compete against a small synthetic oligonucleotide (SSO) substrate. As shown in Figure 4.8A, ME_1 depurinated *M. expansa* 28S ribosomal rRNA at a specific site, releasing a diagnostic fragment upon aniline treatment. The activity of ME_1 on *M. expansa* ribosomes did not exhibit the kinetics typical of an RIP, however. Although the diagnostic fragments were detectable after incubation with concentrations of ME_1 at as low as 0.1 nM, enzymatic activity did not increase with concentration (Fig. 4.8B). The relative band-densities of diagnostic fragments remained the same at each different concentration of ME_1 tested, up to 1 μM. In addition, the enzymatic reaction was not instantaneous; depurination was detectable only after relatively long incubation times (>15 min), and reaction time did not affect the enzymatic activity of ME_1 as shown by the amount of released fragments, which remained the same up to one hour (Fig. 4.8C). Survival of trace amounts of intact 28S rRNA indicates that ME_1 enzymatic activity did not reach saturation.

To determine whether or not *M. expansa* ribosomes could be the primary target for ME_1 action, I first investigated its activity with 23SSO-A_{12} (Fig. 4.8D). 23SSO-A_{12} contains only one adenine residue, and the activity was measured using a slight modification of a fluorimetric method previously described by Zamboni et al. (1989). At a fixed pre-incubation temperature and reaction time (45°C/ 20 min) with 10 nM of 23SSO-A_{12}, the apparent K_D was 105.9 nM.

Subsequently, I examined the activity of ME_1 toward *M. expansa* ribosomes in the presence of increasing concentrations of $^{23}SSO\text{-}A_{12}$ pre-incubated at 45°C. The reactions were carried out for 20 min. Data presented in Figure 4.8E showed that the presence of $^{23}SSO\text{-}A_{12}$ prevented the release the diagnostic fragments from *M. expansa* ribosomes. Longer reaction times (>40 min) did result in the release of detectable amounts of the diagnostic rRNA fragments, however (data not shown). These results indicate that ribosomes are unlikely be the primary target of RIP activity.

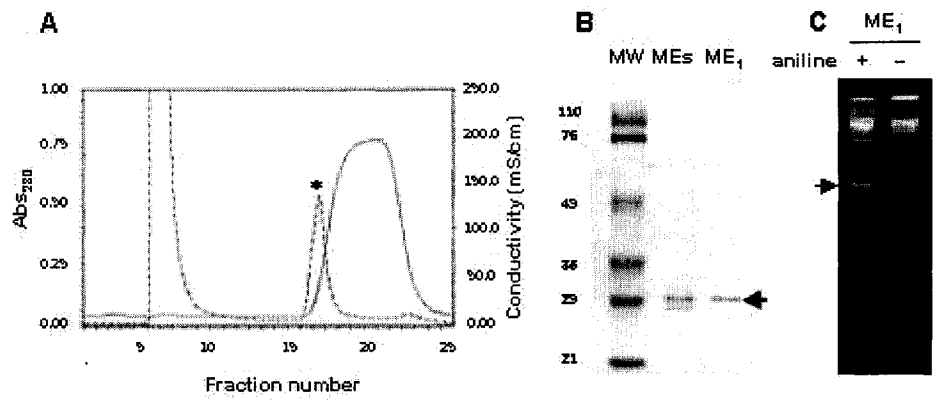

Figure 4.1. Immuno-affinity chromatography of ME_1. **A**, fractionation of total root protein from *M. expansa* on a sepharose-polyclonal anti-ME_1 antibody column. Proteins were equilibrated with 75mM Tris-HCl, pH 8.0, and loaded into the column. The asterisk indicates the peak of immuno-bound proteins eluted with 100mM glycine-HCl, pH 2.7, containing 0.5M NaCl. The affinity column was attached to a fast protein liquid chromatography (FPLC) system, and the chromatogram was monitored by a Bio-Rad BioLogic Duo-Flow system. The dotted line indicates A_{280} and the solid line conductivity. **B**, SDS-PAGE analysis of fractions resulting from affinity (MEs) followed by cation-exchange (ME_1) chromatography. Approximately 5 μg of protein was loaded per lane and visualized by silver staining. The arrow indicates the position of purified ME_1. **C**, enzymatic activity of purified ME_1 *in vitro*. Ribosomes isolated from *S. cerevisiae* were incubated with purified ME_1. Following phenol-chloroform extraction and ethanol precipitation, rRNAs were treated with aniline, fractionated on a 4.5% [w/v] urea-polyacrylamide gel, and stained with ethidium bromide. The arrow indicates the diagnostic 367-nucleotide product of 28S rRNA cleavage.

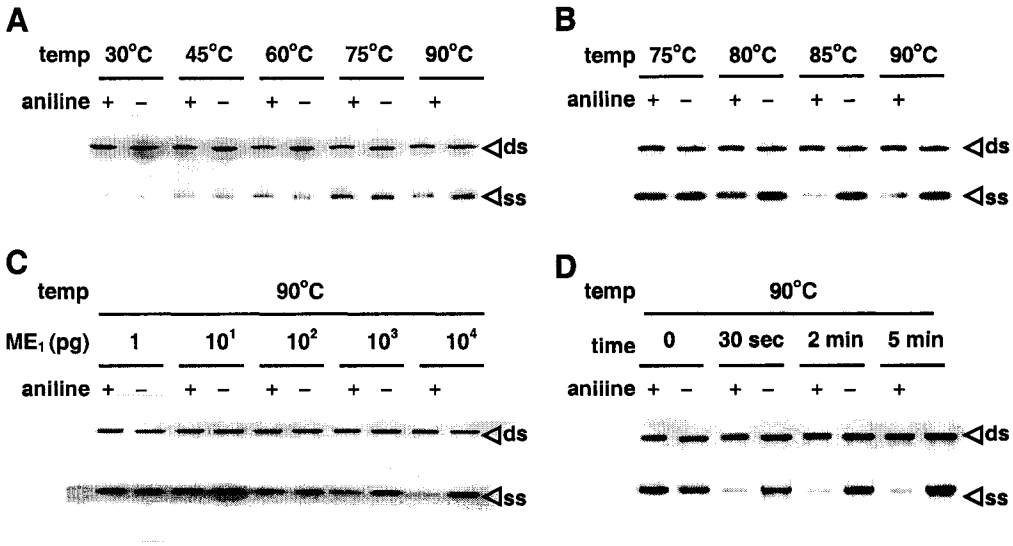

Figure 4.2. Enzymatic activity of ME_1 on heat-treated ssDNA substrates. **A** and **B**, the *N*-glycosidase activity of ME_1 on heat-treated DNA substrates (30-90°C). **C** and **D**, concentration and time-dependent *N*-glycosidase activity of ME_1 (1pg-10ng and 0-5min) toward ssDNAs produced at pre-incubation temperature 90°C. DNA substrates were heated before incubation with ME_1 as described in Materials and Methods. Nucleic acids were subsequently fractionated on 6% [w/v] polyacrylamide gels containing 7M urea and stained with ethidium bromide. Pre-incubation temperature and the presence (+) or absence (-) of aniline treatment are shown above each lane.

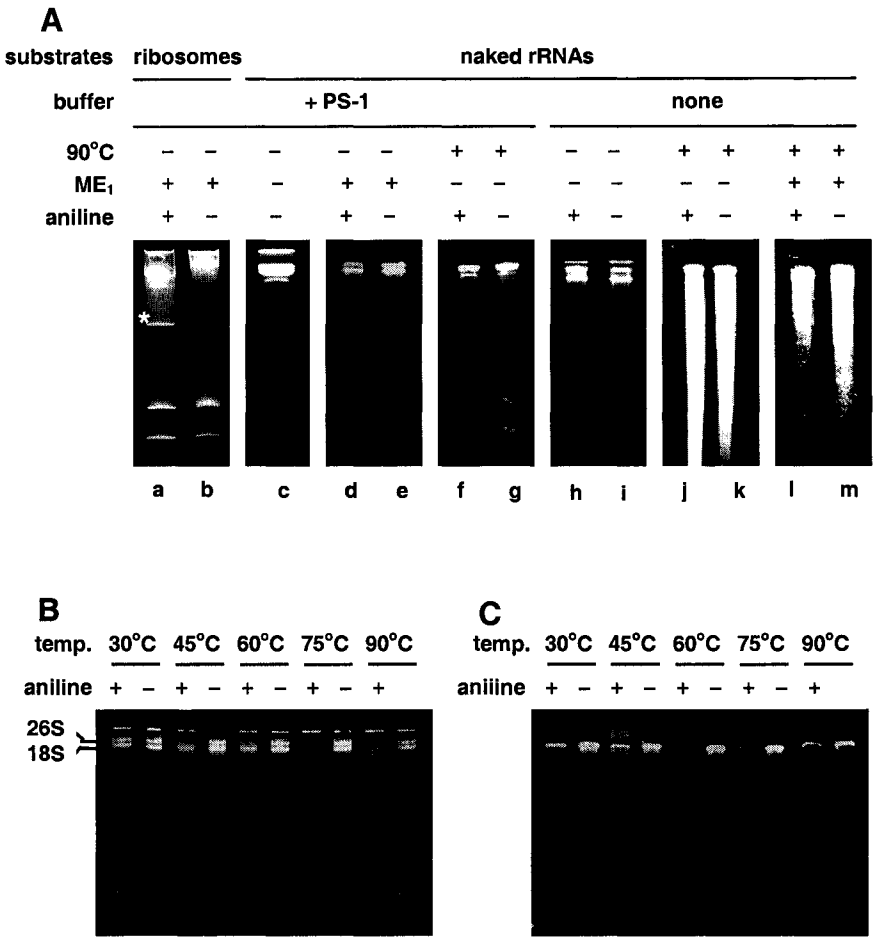

Figure 4.3. Enzymatic activity of ME_1 on heat-treated non-ribosomal substrates. The *N*-glycosidase activity of ME_1 on (**A**, lanes a and b) intact ribosomes, (**B**, lanes c-m and **C**) deproteinized rRNA, and (**D**) *pap-h* mRNA. Nucleic acids were heated before incubation with ME_1 as described in Materials and Methods. Nucleic acids were subsequently fractionated on 6% [w/v] polyacrylamide gels containing 7M urea and stained with ethidium bromide. Pre-incubation temperature and the presence (+) or absence (-) of aniline treatment are shown above each lane. The asterisk indicates the presence of a diagnostic 367-nucleotide product of rRNA cleavage.

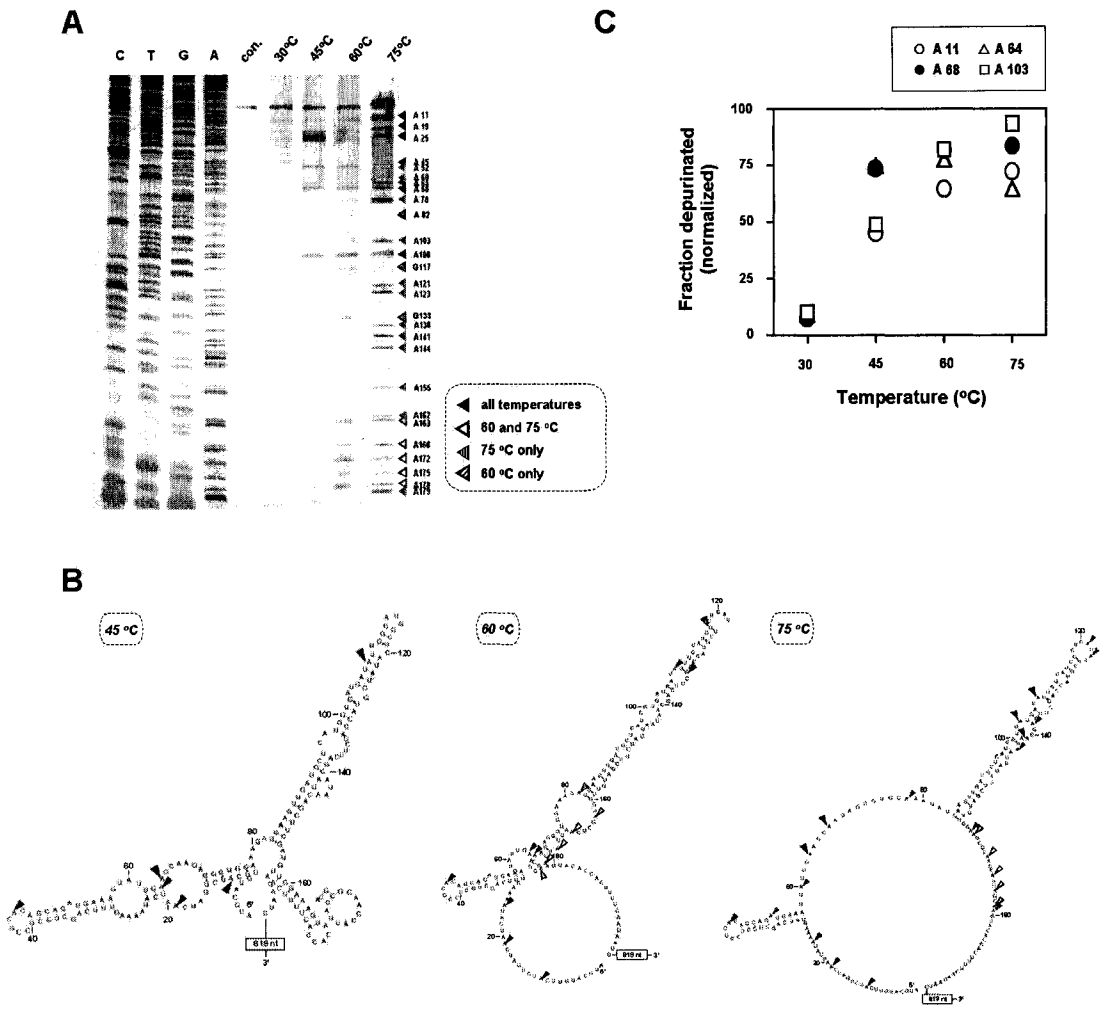

Figure 4.4. Identification of ME_1-susceptible sites in *pap-h* mRNA. **A**, primer extension analysis of the 5' portion of *pap-h* mRNA transcribed *in vitro* and pretreated at various temperatures before incubation with ME_1. A primer complementary to sequences located approximately 200 nt from the 5' terminus of *pap-h* mRNA was extended with reverse transcriptase. Extension products corresponding to various cleavage sites are numbered and identified by arrowheads. **B**, possible secondary structures of the 5' region of *pap-h* mRNA as predicted by a combination of computer modeling and ME_1-probing (Zuker et al., 1999; Mathews et al., 1999). Additional color coding details are described in box. **C**, the effect of pre-treatment temperature on the accessibility of specific adenosine residues in *pap-h* mRNA to modification by ME_1.

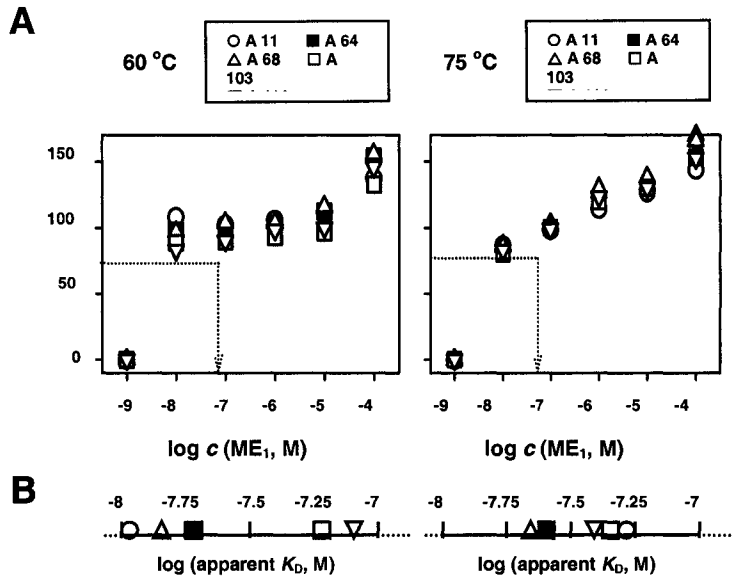

Figure 4.5. Affinity of ME_1 for partially denatured *pap-h* mRNA. **A**, relationship between ME_1 concentration and the extent of RNA cleavage at selected sites in *pap-h* mRNA pre-treated at 60°C (left) and 75°C (right). Dotted arrows reflect the estimated concentration of ME_1 needed to attain half maximal cleavage of RNA (apparent K_D). **B**, logarithm of the apparent K_D values for individual positions at the same temperatures.

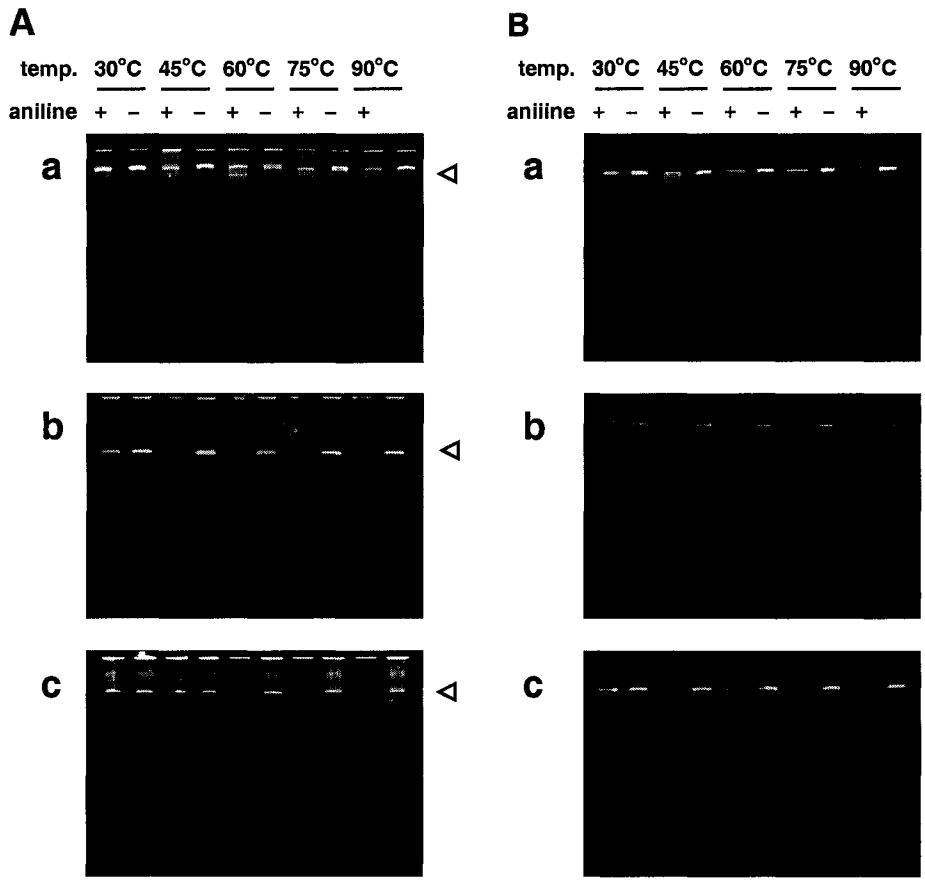

Figure 4.6. Enzymatic activity of RIPs on uncapped mRNAs after partial denaturation. **A**, *N*-glycosidase activity of ME_1 on mRNA *in vitro* transcripts of (a) acidic α-elicitin (*B26*) in *P. cryptogea*, (b) β-1,3-glucanase (*Tom RP-O'b*) in *L. esculentum*, and (c) pathogenesis related protein-1 (PR-1; *At2g14610*) in *A. thaliana*. The unfilled arrowhead indicates the position of intact RNA transcripts. **B**, *N*-glycosidase activity of (a) ME_1, (b) RTA, and (c) saporin-S6 on uncapped luciferease mRNAs after partial denaturation. mRNA templates were heat treated, incubated with RIPs, treated with aniline, and fractionated on a 7 M urea/ 6% [w/v] polyacrylamide gel.

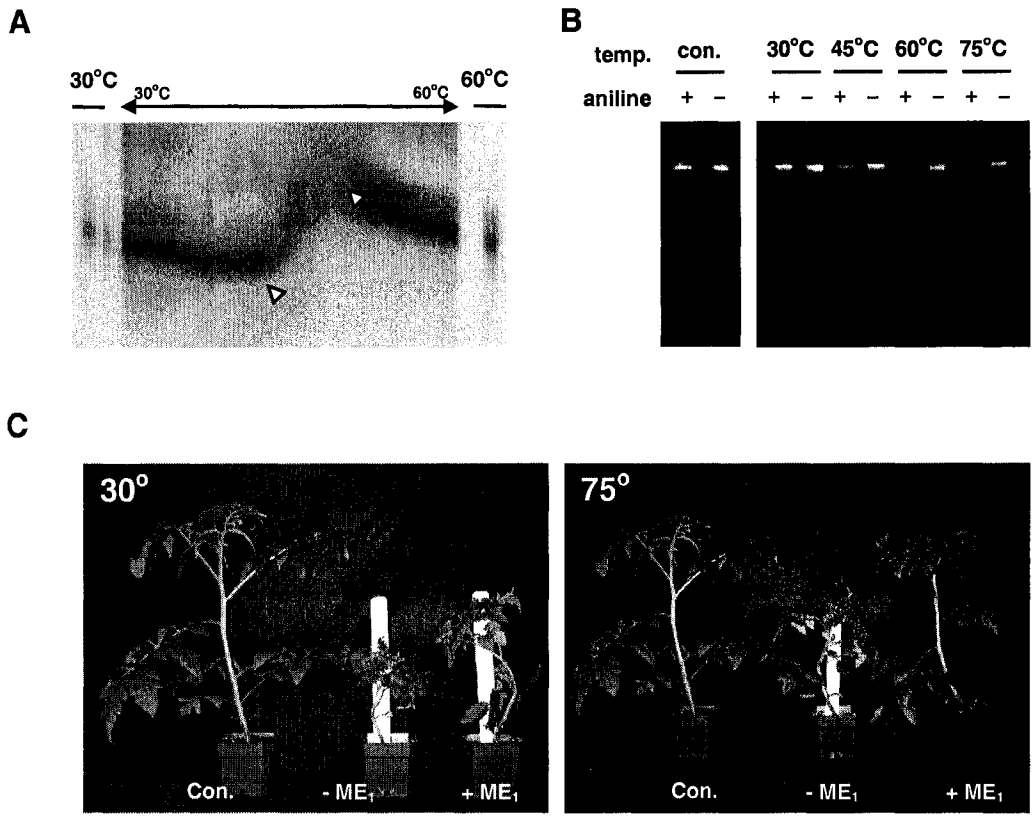

Figure 4.7. Direct action of ME_1 on a single-stranded plant pathogenic RNA. **A**, thermal denaturation of linear PSTVd under low ionic strength conditions. TGGE analysis of linear ^{32}P-labeled PSTVd RNA was carried out at temperatures ranging from 30 to 60°C. **B**, depurination of PSTVd. PSTVd *in vitro* transcripts were partially denatured, incubated with ME_1, treated with aniline, and fractionated on a 7 M urea/ 6% [w/v] polyacrylamide gel. **C**, infectivity of ME_1-treated PSTVd RNAs. Cotyledons of week-old tomato seedlings (*L. esculentum*) were dusted with carborundum and inoculated with aliquots (10 µl) of either untreated or ME_1-treated PSTVd RNA transcripts serially diluted in 20 mM Na phosphate, pH 7.0. Inoculated seedlings were maintained in a greenhouse and photographed 5 wks post inoculation.

Table 4.1. Effect of ME_1 treatment on PSTVd infectivity.

Pretreatment (°C)	Inoculum concentration[a]	Infectivity[b]
30	100	**6/10** (5/10)
	10	**2/10** (1/10)
	100 (+ ME_1)	**8/10** (5/10)
45	100	**3/5** (2/5)
	10	**1/5** (2/5)
	100 (+ ME_1)	**1/5**
60	100	**3/5** (2/5)
	10	**0/5**
	100 (+ ME_1)	**1/5**
75	100	**2/5**
	10	**0/5**
	100 (+ ME_1)	**0/5**

[a] Concentrations expressed as ng/ml.

[b] Infectivity expressed as **no. plants infected/ no. plants inoculated**. Values in parentheses, no. symptomatic plants / no. plants inoculated.

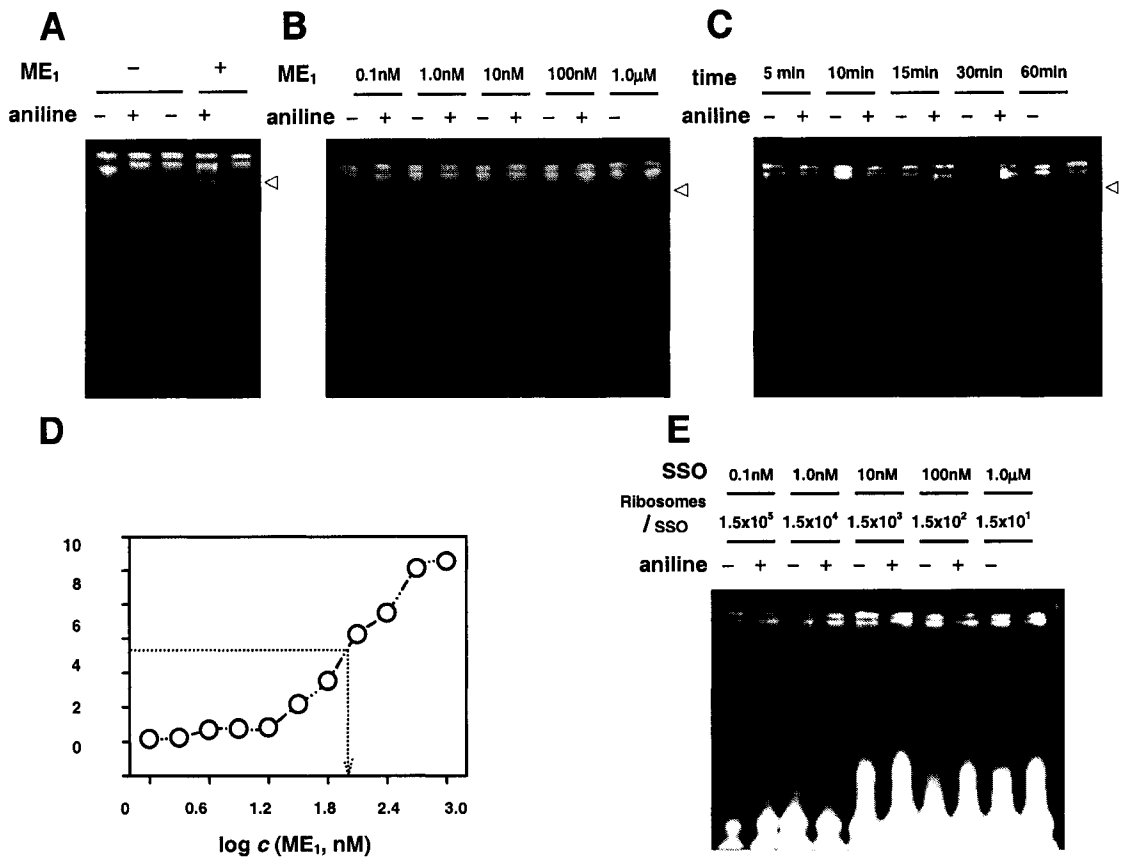

Figure 4.8. Relative affinity of ME_1 for ribosomal and non-ribosomal substrates. **A-C**, the *N*-glycosidase activity of ME_1 on *M. expansa* ribosomes. The left lane in (**A**) is protein-free rRNA. The presence (+) or absence (-) of ME_1, ME_1 concentrations (M), and reaction times (min) are indicated above each lane. The presence (+) or absence (-) of aniline is denoted. The unfilled arrowhead indicates the predicted product of 28S rRNA cleavage. **D**, relationship between ME_1 concentration and the extent of small oligonucleotide (SSO) cleavage. The SSO was pre-treated at 45°C, and adenine release from SSO was assayed using a fluorimetric method as described in Materials and Methods. Dotted arrows indicate the estimated concentration of ME_1 needed to attain half maximal cleavage of RNA (apparent K_D). **E**, inhibition of ME_1 activity on *M. expansa* ribosomes by SSO. Pretreated SSO was added to tubes containing ME_1 and *M. expansa* ribosomes, and resulting mixtures were incubated at 37°C for 20 min. rRNAs were then extracted, treated with aniline, and fractionated on 4.5% [w/v] urea-polyacrylamide gels. SSO concentrations (M), the concentration ratio of substrates (ribosome:SSO), and the presence (+) or absence (-) of aniline are indicated above each lane.

DISCUSSION

Previous studies have shown RIPs to possibly act on non-ribosomal substrates *in vitro*, but the biological significance of these observations remained unclear. To determine whether or not ME_1-substrate interaction could explain the exquisite specificity of RIPs for biological substrates, I have used as substrates mostly intact nucleic acids rather than the small synthetic oligonucleotides used by others (e.g., Endo et al., 1988; Nicolas et al., 1998). Our results clarify the role of secondary/tertiary structure in regulating the ability of ME_1, a type 1 RIP, to depurinate a wide range of non-ribosomal nucleic acids. RNA structure was unambiguously shown to play a key role in regulating the catalytic activity of ME_1.

RNA Structure Modulates The Enzymatic Activity of ME_1

RNA folding is stabilized by a combination of hydrogen bonds, metal ions, and tertiary interactions (Draper, 1996). The most stable structure of an RNA molecule, however, is not always optimal for RNA-protein interaction (Schroeder et al., 2002). The free energy of folding, under *in vitro* conditions, is considered small enough to facilitate RNA-protein interaction (Batey and Williamson, 1998; Ferré-D'Amaré and Doudna, 1999). I have shown that partial denaturation and structure modification of potential RNA substrates *in vitro* enhances the enzymatic activity of ME_1, possibly by optimizing RNA-RIP interaction. These results indicate that RIP activity could be quite different from that observed *in vitro* depending on the precise structure of a potential substrate *in vivo*.

Comparison of catalytic activities on *pap-h* mRNA pretreated to 60°C or 75°C indicated that ME_1-RNA interaction is controlled by the structure of the RNA molecules. This observation could be the explanation for previously reported non-specific depurination activity of RIPs under acidic pH conditions and/or in the absence of cofactors such as Mg^{2+} (Barbieri et al., 1997; Nicolas et al., 1997; Tang et al., 2001; He et al., 2002). Our assays contained only minimal concentrations of Mg^{2+} (approximately 1 mM), to stabilize RNA substrates upon heat treatment. Lowering either the pH or the concentration of Mg^{2+} causes the T_m of RNA molecules to decrease (Tanner and Cech, 1996; Bink et al., 2002). In addition, Mg^{2+} is not required for proper RNA

folding but its presence enhances the stability of those structure(s) that do form (Cole et al., 1972; Stein and Crothers, 1976). Therefore the presence of additional Mg^{2+} as reported in other studies may have inhibited RNA-RIP interaction instead of acting as a cofactor to increase enzymatic activity. Taken together, all these results suggest that RIPs are able to actively depurinate adenosines by interacting with specific structure of RNA.

At this time, I do not know whether the secondary or tertiary structure of an RNA molecule plays the most important role in its interaction with ME_1. However, changes in RNA tertiary structure may explain the activity of certain RIPs on guanine, a nucleotide considered to be a minor substrate site on both ribosome and non-ribosomal substrates (Endo et al., 1987; Hudak et al., 2000; Tang et al., 2001). Thus far, only ricin and PAP have been shown to have deguanylation activity (Peumans et al., 2001), and recent experiments using highly purified RIPs have ruled out deguanylation activity for gelonin, momordin, PAP-S, and saporin-S6 (Babieri et al., 2000). Our results indicate that ME_1 can only remove guanine residues from *pap-h* mRNA pre-treated at 60°C. As shown in Fig. 3C, computer predictions suggest that all three ME_1-susceptible guanine residues may be located in G:U wobble base-pairs next to internal loops. Because G_{117} and G_{133} are still predicted to be paired at 75°C, ME_1 activity appears to be regulated by more than just the secondary structure of a potential substrate.

Substrate recognition and enzymatic activity by ME_1 do not require specific sequence or structural motifs

Cleavage of small synthetic RNA substrates by RIPs requires specific sequence and structural motifs. Using such substrates, a GAGA tetraloop closed by C-G base-pairs was identified and proposed as the identity element required for RIP recognition and catalysis (Endo and Tsurugi, 1988; Endo et al., 1988, 1991; Glück et al., 1992, 1994; Chen et al., 1998). Furthermore, the second adenine residue in this motif was identified as the sole site of RIP activity, and similar size loop structures with different sequences were not recognized by RIPs (Orita et al., 1993). In addition to the adenosine at the depurination site, the guanosine on the 3' side ($^{(3)}G$) has also been proposed to play a critical role in RIP recognition (Orita et al., 1996).

pap-h mRNA contains only two potential enzymatic motifs, both with the sequence of GAGA, one starting at G_{451} and the second at G_{698}, which are predicted to be located in hairpin loops at 37°C. However, using a combination of primer extension assays and computational structure prediction, I have shown that ME_1 activity occurs not only at these sites but also at multiple adenine and guanine residues located in single-stranded regions. In addition, the sequences surrounding A_{45}, A_{121}, and A_{123} lack any obvious sequence homology, and the fact that denaturation leads to an increase of ME_1 activity is also consistent with the lack of a requirement for a specific motif for RNA recognition and catalytic activity. Recognition of an adenine residue by ME_1 does not require the presence of an adjacent guanine residue.

I have recently reported that ME_1 inhibits the translation of uncapped luciferase mRNA in a rabbit reticulocyte translation system (Vepachedu et al., 2003). The present study provides direct evidence that the cap analog, m7GpppG, is not necessary for ME_1 recognition. Additional experiments using RTA and saporin-S6 suggest that many RIPs can recognize and depurinate RNAs that lack a specific binding motif. Because I did not test the activity of PAP on uncapped luciferase transcripts, I cannot rule out the possibility that this RIP requires a cap structure for depurination activity (Hudak et al., 2000; 2002). RIP binding to the cap of mRNA may enhance the stability of the RIP-mRNA interaction, but the primary determinant of ME_1, RTA, and saporin-S6 enzymatic activity is the conformation of the mRNA.

ME_1 Can Directly Inactivate Pathogenic Nucleic Acids

An increasing body of evidence indicates that RIPs possess antimicrobial activity that is effective against a broad array of animal and plant viruses (for review, see Nielsen and Boston, 2001). The widely accepted mechanism for antiviral action identifies host ribosomes as the target of RIP activity. Viral infection is thought to alter the structure of the host cell, allowing RIPs to gain access to the ribosomes and leading to arrest of protein synthesis and cell death – thereby blocking viral replication and spread (Ready et al., 1986). Somewhat surprisingly, transgenic plants expressing PAP do not exhibit a hypersensitive response (HR) or other symptoms of spontaneous cell death in response to viral infection - even though they are resistant to a wide

range of viruses (Lodge et al., 1993; Zoubenko et al., 2000). Our results suggest that the enzymatic activity of ME_1 primarily targets pathogenic non-ribosomal substrates rather than the host ribosomes.

Because viral genomes must form single-stranded templates that are largely free of coat protein at some stage during the infection process, depurination of virus-related nucleic acids could provide direct protection against infection. The presence of high concentrations of RIPs within the cell wall (Ready et al., 1986; Vivanco et al., 1999; Park et al., 2002a) could facilitate RIP-viral nucleic acid contact; alternatively, RIPs could enter the cytoplasm together with the virions via mechanical damage to the cell wall and plasma membrane and act on viral RNA during co-translational disassembly (Shaw et al., 1986; Wu and Shaw, 1997). Because viroids lack the protein capsid that protects almost all conventional viruses, one might expect them to be particularly sensitive to RIPs.

I have shown that ME_1 can depurinate partially denatured PSTVd RNA, thereby leading to a dramatic decrease in infectivity. Detailed structural studies by Riesner and colleagues have characterized a series of rearrangements involving nucleotides within the central conserved region of PSTVd that are required for the cleavage/ligation of multimeric replicative intermediates into mature circular progeny (Baumstark et al., 1997; Schrader et al., 2003). One of these rearrangements results in the formation of a loop E motif very similar to those found in rRNAs. Several years ago, Wassenegger et al. (1996) reported that mechanical inoculation of tobacco (*Nicotiana tabacum* L.) plants with PSTVd-Intermediate strain results in the appearance of a novel variant containing a single C>U substitution at position 259 within this motif. More recently, Zhu et al. (2002) have shown that a U>A change at position 257 has similar effects on the ability of PSTVd to replicate in tobacco. The possible role of RIP(s) in restricting viroid host range remains to be determined.

In summary, our results throw new light on the biological function of RIPs in plants by which these enzymes potentially depurinate diverse nucleic acid substrates depending on their structure, and possibly at specific stages of plant development and/or pathogenic challenge.

CHAPTER 5

Conclusions

The present dissertation has focused on the isolation, characterization, antimicrobial mechanism, and enzymatic interactions of RIPs in order to begin understanding the biological function and role of RIPs *in planta*. RIPs have been considered to be endogenous plant defense proteins with broad-spectrum antimicrobial properties, making them highly desirable candidates to be characterized in order to facilitate plant-related disease control. In addition, the unique properties and activities of RIPs could potentially lead to diverse applications in veterinary and medical research including as an HIV and cancer reagent.

Since the enzymatic activity of RIPs, *N*-glycosidases, was first discovered approximately two decades ago, the functional studies for RIPs have been focused on and limited to their *in vitro* ribosome-inactivating activity, which is believed to lead the inhibition of protein synthesis and cell death. This hypothesis, however, has not been shown and/or proved in the case of any *in vivo* and *in planta* systems. Nevertheless, this hypothesis exclusively has been used to explain the biological role(s) of RIP for a long time. For example, the antimicrobial activity of RIPs has been long postulated only as the so-called "suicide-model". In the meantime, the field of RIP research has been rapidly expanding with identification of novel RIPs, although it has mainly been focused on isolation and biochemical characterization.

The present studies intend to further our understanding of the biological significance of RIPs. Based on the results of my studies, I propose that ribosomes, the substrate best studied *in vitro* examined and long believed to be the only substrate of RIPs, must be reconsidered as the actual target of RIPs within a host cell as well as in exogenous target cells. This finding would create new insights into the defense mechanisms of RIPs and their additional non-ribosomal substrates which have also begun to increase our understanding of properties important for protecting organs and regulating cellular functions of host cells. Such varied approaches will likely accelerate our knowledge of the biological function of RIPs and establish their fundamental significance for medicinal applications.

The major findings in this dissertation are the following:

1. The identification, purification and characterization of a novel type I RIP, PAP-H, from *A. rhizogenes*-transformed hairy roots of *P. americana*. The N-terminus region of PAP-H amino acid was further sequenced, and, subsequently, cDNA corresponding to the PAP-H protein was cloned and sequenced using rapid amplification of cDNA ends. PAP-H has a molecular weight of 29.5 KD and its isoelectric point was determined to be 7.8. The cDNA sequence (Genebank, accession number AY071928) of PAP-H contains 1125 bp with an open reading frame of 1074 bp. The deduced translated amino acid sequence indicated that PAP-H cDNA has a putative signal peptide sequence of 47 amino acids, and a coding sequence of 292 amino acid residues.

2. The localization of PAP-H was found to be embedded in the cell wall matrix of hairy roots. In addition, PAP-H was also found to be localized in the cell walls of root border cells, and constitutively secreted into the rhizosphere as water-drop-shaped exudates. The secretion of PAP-H was found to be significantly enhanced by exogenously challenged—as well as endogenously produced—ethylene. To our knowledge, PAP-H is the first RIP shown to be secreted from the root exudates, as well as the first shown to be compartmentalized in secreted root border cells.

3. By co-incubating PAP-H with fungal cells, it was observed that PAP-H is capable of penetrating into fungal cells with the aid of other PR proteins within the root exudates such as chitinase, β-1,3-glucanase, and proteases. In addition, PAP-H showed direct interaction and enzymatic activity toward fungal ribosomes, suggesting that PAP-H is constitutively produced as a host defense protein, and secreted into the rhizosphere as a barrier against soil-borne microbe infection. The secretion of PAP-H is regulated in response to endo- and exogenous stresses. Based on present results, PAP-H may prevent the multiplication of pathogens in the soil, acting in an additive effect with other PR proteins.

4. Comparing the catalytic activities of RTA, saporin-S6, and ME_1 toward four different fungal ribosomes (*Rhizoctonia solani*, *Alternaria solani*, *Trichoderma reesei* and *Candida*

albicans), each RIP clearly demonstrated enzymatic specificity, indicating that the depurination activity of RIPs depends on specific RIP-substrate interaction. This RIP-mediated substrate-specificity may be dependent on the flexibility of ribosomes and/or RIP structure; (a) the C-terminal region in RIPs that recognize and interact with ribosomal proteins, (b) unique ribosomal proteins from various ribosome sources that enhance or diminish interaction with RIPs, and (c) differential exposure of the S/R loop during the elongation step depending on different RIP-ribosomal conformations.

5. Comparing the catalytic specificity of three type I RIPs, RTA, saporin-S6, and ME_1, with the antifungal activity, it has been found that the ribosome-inactivating activity of RIPs does not completely account for their antifungal activity. RTA and saporin-S6 showed approximately 10 to 50-fold higher activity against isolated fungal ribosomes than did ME_1. In contrast, just the opposite behavior was observed for antifungal activity. The potential function of RIPs as defense proteins has been long supported by their enzymatic activity on ribosomal substrates isolated from several pathogenic microbes. However, in the present studies, we showed experimental evidence that certain type I RIPs have biological activity as defense proteins by directly inhibiting fungal growth, and this antifungal activity is independent of the level of their ribosome-depurinating activity.

6. Monitoring RIP-fungi interactions using NHS-fluorescein labeled-ME_1 and saporin-S6 with *Rhizoctonia solani*, it has been found that ME_1 strongly interacts with target fungal hyphae, in contrast to no interaction between saporin-S6 and the fungi. Furthermore, fluorescent signals were observed in the septa between two hyphal cells and cytoplasmic space, indicating that ME_1 not only interacted with the surface of cell walls but also was embedded in them followed by internalization. These results suggest that RIPs such as ME_1 selectively interact with functional domains located in the fungal cell membranes and/or cell wall, and are incapable of penetrating undamaged cells.

7. The enzymatic interaction of the RIP ME_1 with non-ribosomal nucleic acids was investigated upon structure modification of substrates through thermodynamic challenge. The partial structure denaturation of substrates was found to optimize nucleic acid-RIP interactions, indicating that the enzymatic activity of RIPs is different from that observed *in vitro* depending on the precise structure of a potential substrate *in vivo*. Comparing the catalytic activity of RIP on various forms of mRNA structure demonstrated that RIP-RNA/ RIP-DNA interactions are modulated by the secondary/tertiary structure of the RNA and DNA molecules.

8. Using the primer extension and computational structure analysis, the enzymatic target sites of RIP were determined to be multiple adenine residues from single-stranded regions and, to a lesser extent, guanine residues from a certain secondary conformation of substrate structure. The computer predictions suggest that RIP-susceptible guanine residues be located in G:U wobble base-pairs next to internal loops.

9. In contrast to our earlier understanding, it has been found that target-recognition and nucleotide cleavage of RIPs do not require sequence and structure motifs such as a GAGA with its tetraloop. Further, the target-site specificity of RIP upon different substrate structures was examined by determining the apparent dissociation constant (apparent K_D) over a range of protein concentrations. The results determined that RIP activity increases with the degree of substrate denaturation. However, individual nucleotide-RIP interactions differed from the overall apparent K_D values, and were very specific upon physical availability.

10. Exposure to ME_1 completely abolished the infectivity of RNA transcripts of the potato spindle tuber viroid, suggesting that RIPs target and are biologically active toward invading pathogenic nucleic acids. Subsequently, we examined the enzymatic affinity of ME_1 toward *M. expansa* ribosomes in competition with increasing concentrations of small synthetic oligonucleotides ($^{23}SSO\text{-}A_{12}$). The presence of $^{23}SSO\text{-}A_{12}$ completely prevented RIP affinities

toward ribosomal substrates indicating that ribosomes are unlikely to be the primary target of RIP activity.

Taken together, these observations could be an opportunistic indication that RIPs may not target endogenous ribosomes upon infection, leading to cell death, but that rather RIPs may act directly against invading pathogens. Since viral nucleic acids form single-stranded templates freed from protein coats at some stage of infection, depurination of virus-derived nucleic acids may give direct protection against infecting viruses. In addition, localization of RIPs in high concentrations within cell walls should allow for RIP-viral nucleic acid contact. We have also reported the direct antimicrobial activity of RIPs against fungal and bacterial pathogens. Therefore, we hypothesize here that RIPs pursue their defense role through direct inhibition of infected pathogens.

CHAPTER 6

References

Abeles FB, Bosshart RP, Forrence LE, Habig WH (1971) Preparation and purification of glucanase and chitinase from bean leaves. Plant Physiol **47:** 129-134

Andresen I, Becker W, Schlűter K, Burges J, Parthier B, Apel K (1992) The identification of leaf thionin as one of the main jasmonate-induced protein of barley (*Hordeum vulgare*). Plant Mol Biol **19:** 193-204

Anderson PM, Meyers DE, Hasz DE, Covalcius K, Saltzman D, Khanna C, Uckun FM (1995) In vitro and in vivo cytotoxicity of an anti-osteosarcoma immunotoxin containing pokeweed antiviral protein. Cancer Res **55:** 1321-1327

Antal M, Boros E, Solymosy F, Kiss T (2002) Analysis of the structure of human telomerase RNA *in vivo*. Nucleic Acids Res **30:** 912-910.

Aron GM, Irvin JD (1980) Inhibition of herpes simplex virus multiplication by the pokeweed antiviral protein. Antimicrob Agents Chemother **17:** 1302-1303

Au TK, Collins RA, Lam TL, Ng TB, Fong WP, Wan DCC (2000) The plant ribosome inactivating proteins luffin and saporin are potent inhibitors of HIV-1 integrase. FEBS Lett **471:** 169-172

Bais HP, Loyola-Vargas VM, Flores HE, Vivanco JM (2001) Root-specific metabolism: the biology and biochemistry of underground organs. In Vitro Cell Dev-PLANT **37:** 730-741

Barbieri L, Aron GM, Irvin JD, Stirpe F (1982) Purification and partial chracterization of another form of the antiviral protein from the seeds of *Phytolacca americana* L. (Pokeweed). Biochem J **203:** 55-56

Barbieri L, Ferreras JM, Barraco A, Ricci P, Stirpe F (1992) Some ribosome-inactivating proteins depurinate ribosomal RNA at multiple sites. Biochem J **286:** 1-4

Barbieri L, Battelli MG, Stirpe F (1993) Ribosome-inactivating proteins from plants. Biochem Biophys Acta **1154:** 237-282

Barbieri L, Gorini P, Valbonesi P, Castiglioni P, Stirpe F (1994) Unexpected activity of saporins. Nature **372:** 624

Barbieri L, Valbonesi P, Gorini P, Pession A, Stirpe F (1996) Polynucleotide:adenosine glycosidase activity of saporin-L1: effect on DNA, RNA and poly(A). Biochem J **319:** 507-513

Barbieri L, Valbonesi P, Bonora E, Gorini P, Bolognesi A, Stirpe F (1997) Polynucleotide:adenosine glycosidase activity of ribosome-inactivating proteins: effect on DNA, RNA and poly (A). Nucleic Acids Res **25:** 518-522

Barbieri L, Valbonesi P, Righi F, Zuccheri G, Monti F, Gorini P, Samori B, Stirpe F (2000) Polynucleotide:adenosine glycosidase is the sole activity of ribosome-inactivating proteins on DNA. J Biochem **128:** 883-889

Barbieri L, Brigotti M, Perocco P, Carnicelli D, Ciani M, Mercatali L, Stirpe F (2003) Ribosome-inactivating proteins depurinate poly (ADP-ribosyl)ated poly(ADP-ribose) polymerase and have transforming activity for 3T3 fibroblasts. FEBS Lett **538:** 178-182

Bass HW, Webster C, OBrian GR, Roberts JKM, Boston RS (1992) A maize ribosome-inactivating protein is controlled by the transcriptional activator *Opaque-2*. Plant Cell **4:** 225-234

Batey RT, Williamson JR (1998) Effects of polyvalent cations on the folding of an rRNA three-way junction and binding of ribosomal protein S15. RNA **4:** 984-997

Battelli MG, Polito L, Bolognesi A, Lafleur L, Fradet Y, Stirpe F (1996) Toxicity of ribosome-inactivating proteins-containing immunotoxins to a human bladder carcinoma cell line. Int J Cancer **65**: 485-490

Baumstark T, Schröder AW, Riesner D (1997) Viroid processing: a switch from cleavage to ligation driven by a change from a tetraloop to a loop E conformation. Nucleic Acids Res **23:** 4246-4254

Beker W, Apel K (1992) Isolation and charaterization of a cDNA encoding a nevel hasmonate-induced protein of barley (*Hordeum vulgare* L.). Plant Mol Biol **19:** 1065-1067

Bink HH, Hellendoorn K, van der Meulen J, Pleij CWA (2002) Protonation of non-Watson-Crick base pairs and encapsidation of turnip yellow mosaic virus RNA. Proc Natl Acad Sci USA **99:** 13465-13470

Bolognesi A, Barbieri L, Abbondanza A, Falasca AI, Carnicelli D, Battelli MG, Stirpe F (1990) Purification and properties of new ribosome-inactivating proteins with RNA N-glycosidase activityt. Biochim Biophys Acta **1087:** 293-302

Bolognesi A, Tazzari PL, Olivieri F, Polito L, Falini B, Stirpe F (1996) Induction of apoptosis by ribosome-inactivating proteins and related immunotoxins. Int J Cancer **68:** 349-355

Bonin M, Zhu R, Klaue Y, Oberstrass J, Oesterschulze E, Nellen W (2002) Analysis of RNA flexibility by scanning force spectroscopy. Nucleic Acids Res **30:** *e*81.

Bowles DJ (1990) Defense-related proteins in higher plants. Annu Rev Biochem **59:** 873-907

Bradford MM (1976) A rapid and sensitive method for the quantitation of microgram quantities of protein utilizing the principle of protein-dye binding. Anal Biochem **72:** 248-254

Bruland OS, Fodstad O, Funderud S, Pihl A (1986) New monoclonal antibodies specific for human sarcomas. Int J Cancer **38:** 27-31

Bruland OS, Fodstad O, Stenwig AE, Pihl A (1988) Expression and characteristics of a novel human osteosarcoma-associated cell surface antigen. Cancer Res **48:** 5302-5309

Cawley DB, Hedblom ML, Hoffman EJ, Houston LL (1977) Differential ricin sensitivity of rat liver and wheat germ ribosomes in polyuridylic acid translation. Arch Biochem Biophys **182:** 690-695

Chaddock JA, Monzingo AF, Robertus JD, Lord JM, Roberts LM (1996) Major structural differences between pokeweed antiviral protein and ricin A-chain do not account for their differing ribosome specificity. Eur J Biochem **235:** 159-166

Chaudhry B, Műller-Uri F, Cameron-Mills V, Gough S, Simpson D, Skriver K, Mundy J (1994) The barley 60 kDa jasmonate-induced protein (JIP60) is a novel ribosome-inactivating proteins. Plant J **6:** 815-824

Chen X-Y, Link TM, Schramm VL (1998) Ricin A-chain: Kinetics, mechanism and RNA stem-loop inhibitors. Biochemistry **37:** 11605-11613

Chen Y-F, Randlett MD, Findell JL, Schaller GE (2001) Ethylene receptor ETR1 localizes to the ER of *Arabidopsis*. In Proceeding of Plant Biology 2001, Providence, RI, Poster No. 959, American Society of Plant Biology, Rockwille, MD, p 190

Cho GH, Kim DI, Pedersen H, Chin CK (1988) Ethaphon enhancement of secondary metabolite synthesis in plant cell cultures. Biotechnol Prog **4:** 184-188

Cole PE, Yang SK, Crothers DM (1972) Conformational changes of transfer ribonucleic acid. Equilibrium phase diagrams. Biochemistry **11:** 4358-4368

Cress D, Kiefer MC, Owens RA (1983) Construction of infectious potato spindle tuber viroid cDNA clones. Nucleic Acids Res **11:** 6821-6835

Day PJ, Lord JM, Roberts LM (1998) The deoxyribonuclease activity attributed to ribosome-inactivating proteins is due to contamination. Eur J Biochem **258:** 540-545

Del Vecchio Blanco F, Bolognesi A, Malorni A, Sande MJW, Savino G, Parente A (1997) Complete amino acid sequence of PD-S2, a new ribosome-inactivating protein from seeds of *Phytolacca dioica* L. Biochim Biophy Acta **1338:** 137-144

Domingo C, Conejero V, Vera P (1994) Genes encoding acidic and basic class III bata-1,3-glucansases are expressed in tomato plants upon viroid infection. Plant Mol. Biol **24:** 725-732

Dong X (1998) SA, JA, ethylene, and disease resistance in plants. Curr Opin Plant Biol **1:** 316-323

Draper DE (1996) Parallel worlds. Nat Struct Biol **3:** 397-400

Dunaeva M, Goebel C, Wasternack C, Parthier B, Goerschen E (1999) The jasmonote-induced 60 kDa protein of barley exhibits *N*-glycosidase activity in vivo. FEBS Lett **452:** 263-266

Ek O, Waurzyniak B, Myers DE, Uckun FM (1998) Antitumor activity of TP3(anti-p80)-pokeweed antiviral protein immunotoxin in hamster cheek pouch and severe combined immunodeficient mouse xenograft models of human osteosarcoma. Clin Cancer Res **4:** 1641-1647

Endo Y, Mitsui K, Motizuki M, Tsurugi K (1987) The mechanism of action of ricin and related toxic lectins on eukaryotic ribosomes: the site and the characteristics of the modification in 28S ribosomal RNA caused by the toxins. J Biol Chem **262:** 5908-5912

Endo Y, Tsurugi K (1987) RNA N-glycosidase activity of ricin A-chain: mechanism of action of the toxic lectin ricin on eukaryotic ribosomes. J Biol Chem **263:** 8735-8739

Endo Y, Chan Y-L, Lin A, Tsurugi K, Wool IG (1988) The cytotoxins α-sarin and ricin retain their specificity when tested on a synthetic oligoribonucleotide (35-mer) that mimics a region of 28 S ribosomal ribonucleic acid. J Biol Chem **263:** 7917-7920

Endo Y, Tsurugi K (1988) RNA N-glycosidase activity of ricin A-chain. The characteristics of the enzymatic activity of Ricin A-chain with ribosomes and with rRNA. J Biol Chem **263:** 8735-8739

Endo Y, Glück A, Wool IG (1991) Ribosomal RNA identity elements for ricin A-chain recognition and catalysis. J Mol Biol **254:** 848-855

Ferré-D'Amaré AR, Doudna JA (1999) RNA folds: Insights from recent crystal structures. Annu Rev Biophys Biomol Struct **28:** 57-73.

Flores HE, Curtis WR (1992) Approaches to understanding and manipulating the biosynthetic potential of plant roots. Ann NY Acad Sci **665:** 188-209

Flores HE, Vivanco JM, Loyola-Vargas V (1999) "Radicle" biochemistry: the biology of root-specific metabolism. Trends in Plant Sci **4**: 220-226

Frankel A, Schlossman D, Welsh P, Hertler A, Withers D, Johnston S (1989) Selection and characterization of Ricin toxin A-chain mutation in *Saccharomyces cerevisiae*. Mol Cell Biol **9**: 415-420

Funatsu G, Islam MR, Minami Y, Sung-Sil K, Kimura M (1991) Conserved amino acid residues in ribosome-inactivating proteins from plants. Biochimie **73:** 1157-1161

Glück A, Endo Y, Wool IG (1992) Ribosomal RNA identity elements for ricin A-chain recognition and catalysis: Analysis with tetraloop mutants. J Mol Biol **226:** 411-424

Glück A, Endo Y, Wool IG (1994) The ribosomal RNA identity elements for ricin and for □-sarcin: Mutations in the putative CG pair that closes a GAGA tetraloop. Nucleic Acids Res **22:** 321-324

Hall AE, Findell JL, Schaller GE, Sisler EC, Bleecker AB (2000) Ethylene perception by the ERS1 protein in *Arabidopsis*. Plant Physiol **123:** 1449-1458

Hammond-Kosack KE, Jones JDG (1996) Resistance gene-dependent plant defense responses. Plant Cell **8:** 1773-1791

Hartley MR, Legname G, Osborn RW, Chen Z, Lord JM (1991) Single chain ribosome inactivating proteins from plants depurinate *Escherichia coli* 23S ribosomal RNA. FEBS Lett **290:** 65-68

Hatley MR, Lord JM (1993) Structure, function and applications of ricin and related cytotoxic proteins. *In* D Griesson, eds, Biosynthesis and Manipulation of Plant Products, New York, Chapman & Hall, pp 210-239

Hawes MC, Cunawardena U, Miyasaka S, Zhao X (2000) The role of root border cells in plant defense. Trends Plant Sci **5:** 128-133

Helmy M, Lombard S, Pieroni G (1999) Ricin RCA_{60}: evidence of its phospholipase activity. Biochem Biophys Res Commun **258:** 252-255

He W-J, Liu WY (2004) Both N- and C-terminal regions are essential for cinnamomin A-chain to deadenylate ribosomal RNA and supercoiled couble-stranded DNA. Biochem J **377:** 17-23

He W-J, Tang S, Liu W-Y, Stirpe F (2002) Nonspecific deadenylation of sarcin/ricin domain RNA catalyzed by gelonin under acidic conditions. Arch Biochem Biophys **399:** 181-187

Herschlag D (1995) RNA chaperones and the RNA folding problem. J Biol Chem **270:** 20871-20874

Hey TD, Hartley M, Walsh TA (1995) Maize ribosome-inactivating protein (b-32) homologs in related species, effects on maize ribosomes, and modulation of activity by pro-peptide deletions. Plant Physiol **107:** 1323-1332

Hudak KA. Dinman JD, Tumer NE (1999) Pokeweed antiviral protein accesses ribosomes by binding toL3. J Biol Chem **274:** 3859-3864

Hudak KA, Wang P, Tumer NE (2000) A novel mechanism for inhibition of translation by pokeweed antiviral protein: depurination of the capped RNA template. RNA **6:** 369-380

Hudak KA, Bauman JD, Tumer NE (2002) Pokeweed antiviral protein binds to the cap structure of eukaryotic mRNA and depurinates the mRNA downstream of the cap. RNA **8:** 1148-1159

Ippoliti R, Lendaro E, Bellelli A, Brunori M (1992) A ribosomal protein is specifically recognized by saporin, a plant toxin which inhibits protein synthesis. FEBS Lett **298:** 145-148

Irvin JD (1975) Purification and partial characterization of the antiviral protein from *Phytolacca americana* which inhibits eukaryotic protein synthesis. Arch Biochem Biophys **169:** 522-528

Irvin JD, Kelly T, Robertus JD (1980) Purification and properties of a second antiviral protein from *Phytolacca americana* which inactivates eukaryotic ribosomes. Arch Biochem Biophy **200:** 418-425

Jach G, Gornhardt B, Munday J, Logemann J, Pinsdorf E, Leah R, Schell J, Maas C (1995) Enhanced quantitative resistance against fungal disease by combinatorial expression of different barley antifungal proteins in transgenic tobacco. Plant J **8:** 97-109

Jansen B, Uckun FM, Jaszcz WB, Kersey JH (1992) Establishment of a human t(4;11) leukemia in severe combined immunodeficient mice and successful treatment using anti-CD19 (B43)-pokeweed antiviral protein immunotoxin. Cancer Res **52:** 406-412

Joshi CP (1987) Putative polyadenylation signals in nuclear genes of higher plants: a compilation and analysis. Nucl Acids Res **15**: 9627-9640

Koiwa H, Bressan RA, Hasegawa PM (1991) Expression of protease inhibitor genes – host plant/ insect interaction. Trends Plant Sci **2:** 379-384

Kombrink E, Schroder M, Hanbrock K (1988) Several "pathogenesis-related" proteins in potato are 1,3-β-glucanase and chitinases. Proc Natl Acad Sci USA **85:** 782-786

Kragh KM, Jacobsen S, Mikkelsen JD (1990) Induction, purification and characterization of barley leaf chitinase. Plant Science **71:** 55-68

Krawetz JE, Boston RS (2000) Substrate specificity of a maize ribosome-inactivating protein differs across diverse taxa. Eur J Biochem **267:** 1966-1974

Laemmli UK (1970) Cleavage of structural proteins during the assembly of the head of bacteriophage T4. Nature **227:** 680-285

Lam SK, Ng TB (2001a) Hypsin, a novel thermostable ribosome-inactivating protein with antifungal and antiproliferative activities from fruiting bodies of the edible mushroom Hyprizigus marmoreus. Biochem Biophys Res Commun **285:** 1071-1075

Lam SK, Ng TB (2001b) First simultaneous isolation of a ribosome inactivating protein and an antifungal protein from a mushroom (*Lyophyllum shimeji*) together with evidence for synergism of their antifungal effects. Arch Biochem Biophys **393:** 271-280

Lee-Huang S, Kung HF, Huang PL, Bourinbaiar AS, Morell JL, Brown JH, Huang PL, Tsai WP, Chen AY, Huang HI, Chen HC (1994) Human immunodeficiency virus type 1 (HIV-1) inhibition, DNA binding, RNA binding, and ribosome inactivation activities in the N-terminal segments of the plant anti-HIV protein GAP31. Proc Natl Acad Sci USA **91:** 12208-12212

Lee-Huang S, Huang PL, Huang PL, Bourinbaiar AS, Chen HC, Kung HF (1995) Inhibition of the integrase of human immunodeficiency virus (HIV) type 1 by anti-HIV plant proteins MAP30 and GAP31. Proc Natl Acad Sci USA **92:** 8818-8822

Leubner-Metzger G, Meins F Jr (1999) Functions and regulation of plant β–1,3-glucanase (PR-2). *In* SK Datta, S Muthukrisknan, eds, Pathogenesis-Related Proteins in Plants. CRC Press, Boca Raton, FL, pp 49-76

Ling J, Liu WY, Wang TP (1994) Cleavage of supercoiled double-stranded DNA by several ribosome-inactivating proteins in vitro. FEBS Lett **345:** 143-146

Ling J, Liu WY, Wang TP (1995) Simultaneous existence of two types of ribosome-inactivating proteins in the seeds of *Cinnamonum camphora* –characterization of the enzymatic activities of these cytotoxic proteins. Biochim Biophys Acta **1252:** 15-22

Lin Q, Chen ZC, Antoniw JF, White RF (1991) Isolation and characterization of a cDNA clone encoding the anti-viral protein from *Phytolacca americana*. Plant Mol Biol **17:** 609-614

Linthorst HJM (1991) Pathogenesis-related proteins of plants. CRC Crit Rev Plant Sci **10:** 305-308

Li X-D, Chen W-F, Liu W-Y, Wang G-H (1997) Large-scale preparation of two new ribosome-inactivating proteins-Cinnamomin and Camphorin from the seeds of *Cinnamomum camphora*. Pretein Express Purif **10:** 27-31

Lodge JK, Kaniewski WK, Tumer NE (1993) Broad-spectrum virus resistance in transgenic plants expressing pokeweed antiviral protein. Proc Natl Acad Sci USA **90:** 7089-7093

Lodish H, Berk A, Zipursky SL, Matsudaira P, Baltimore D, Darnell JE (2000) Molecular Cell Biology: 4th edn, WH Freeman and Company, New York, pp 675-750

Lord JM, Roberts LM (1996) The intracellular transport of ricin. Why mammalian cells are killed and how *Ricinus* cells survive. Plant Physiol Biochem **34:** 253-261

Maddaloni M, Forlani F, Balmas V, Donini G, Stasse L, Corazza L, Motto M (1997) Tolerance to the fungal pathogen *Rhizoctonia solani* AG4 of transgenic tobacco expressing the maize ribosome-inactivating protein b-32. Transgenic Res **6:** 393-402

Maguire BA, Zimmermann RA (2001) The ribosome in focus. Cell **104:** 813-816

Marchant A, Hartley MR (1995) The action of pokeweed antiviral protein and ricin A-cahin on mutant in the □-sarcin loop of *Escherichia coli* 23S ribosomal RNA. J Mol Biol **254:** 848-855

Mathews DH, Sabina J, Zuker M, Turner DH (1999) Expanded sequence dependence of thermodynamic parameters improves prediction of RNA secondary structure. J Mol Biol **288:** 911-940

Mauch F, Hadwiger LA, Boller T (1988) Antifungal hydrolases in pea tissue. I. Purification and characterization of two chitinases and two *ß*-1,3-glucanases differentially regulated during development in response to fungal infection. Plant Physiol **87:** 325-333

McGrath MS, Hwang KM, Caldwell SE, Gaston I, Luk KC, We P, Ng VL, Crowe S, Danials J, Deinhart T, Lekas PV, Vennary IC, Yeung H-W, Lifwon JD (1989) GLQ223: an inhibitor of human immunodeficiency virus replication in acutely and chronically infected cells of lymphocyte and mononuclear phagocyte lineage. Proc Natl Acad Sci USA **86:** 2488-2484

Messinger Y, Yanishevski Y, Avramis VI, Gunther R, Myers DE, Irvin JD, Evans W, Uckun FM (1996) Treatment of human B-cell precursor leukemia in SCID mice using a combination of the investigational biotherapeutic agent B43-PAP with cytosine arabinoside. Clin Cancer Res **2:** 1533-1542

Mirjalili N, Linden JC (1995) Gas phase composition effects on suspension cultures of *Taxus cuspidata*. Biotechnol Bioeng **48:** 123-132

Monzingo AF, Collins EJ, Ernst SR, Irvin JD, Robertus JD (1993) The 2·5 Å structure of pokeweed antiviral protein. J Mol Biol **233:** 705-715

Murashige T, Skoog F (1962) A revised medium for rapid growth and bioassays with tissue cultures. Physiol Plant **15:** 473-397

Neuhaus J-M (1999) Plant chitinases. *In* SK Datta, S Muthukrisknan, eds, Pathogenesis-Related Proteins in Plants, CRC Press, Boca Raton, FL, pp 77-105

Ng TB, Parkash A (2002) Hispin, a novel ribosome-inactivating protein with antifungal activity from hairy melon seeds. Protein Expr Purif **26:** 211-217

Ng TB, Lam YW, Wang H (2003) Calcaelin, a new protein with translation-inhibiting, antiproliferative and antimitogenic activities from mosaic puffball mushroom *Calvatia caelata.* Planta Med **69:** 212-217

Nicolas E, Beggs JM, Haltiwanger BM, Taraschi TF (1997) Direct evidence for the deoxyribonuclease activity of the plant ribosome-inactivating protein gelonin. FEBS Lett **406:** 162-164

Nicolas E, Beggs JM, Haltiwanger BM, Taraschi TF (1998) A new class of DNA glycosylase/apurinic/apyrimidinic lyase that act on specific adenines in single-stranded DNA. J Biol Chem **273:** 17216-17220

Nielsen K, Boston RS (2001) Ribosome-inactivating proteins: a plant perspective. Annu Rev Plant Physiol Plant Mol Biol **52:** 785-816

Nikolcheva T, Woodson SA (1999) Facilitation of group I splicing *in vivo*: Misfolding of the *Tetrahymena* IVS and the role of ribosomal RNA exons. J Mol Biol **292:** 557-567

Ogasawara T, Sawasaki T, Morishita R, Ozawa A, Madin K, Endo Y (1999) A new class of enzyme acting on damaged ribosomes: ribosomal RNA apurinic site specific lyase found in wheat germ. EMBO J **18:** 6522-6531

Ohme-Takagi M, Suzuki K, Shinshi H (2000) Regulation of ethylene-induced transcription of defense gene. Plant Cell Physiol **41:** 1187-1192

Orita M, Nishikawa F, Shimayama T, Taira K, Endo Y, Nishikawa S (1993) High-resolution NMR study of a synthetic oligoribonucleotide with a tetranucleotide GAGA loop that is a substrate for the cytotoxic protein, ricin. Nucleic Acids Res **21:** 5670-5678.

Orita M, Nishikawa F, Kohno T, Senda T, Mitsui Y, Endo Y, Taira K, Nishikawa S (1996) High-resolution NMR study of a GdAGA tetranucleotide loop that is an improved substrate for ricin, a cytotoxic plant protein. Nucleic Acids Res **24:** 611-618.

Osborne RW, Hartley MR (1990) Dual effects of the ricin A chain on protein synthesis in rabbit reticulocyte lysate. Inhibition of initiation and translocation. Eur J Biochem **193:** 401-407

Ozawa A, Sawasaki T, Takai K, Uchiumi T, Hori H, Endo Y (2003) RALyase; a terminator of elongation function of depurinated ribosomes. FEBS Lett **555:** 455-458

Panabieres F, Marais A, Le Berre JY, Penot I, Fournier D, Ricci P (1995) Characterization of a gene cluster of *Phytophthora cryptogea* which codes for elictins, proteins inducing a hypersensitive-like reponse in tobacco. Mol Plant Microbe Interact **8:** 996-1003

Park S-W, Lawrence CB, Linden JC, Vivanco JM (2002a) Characterization of a novel ethylene-inducible ribosome-inactivating protein exuded from root cultures of *Phytolacca americana*. Plant Physiol **130:** 164-178

Park S-W, Stevens NM, Vivanco JM (2002b) Enzymatic specificity of three ribosome-inactivating proteins against fungal ribosomes, and correlation with antifungal activity. Planta **216:** 227-234

Peterson GL (1977) A simplification of the protein assay method of Lowry et al. which is more generally applicable. Anal Biochem **83:** 346-356

Peumans WJ, Hao QH, Van Damme EJM (2001) Ribosome-inactivating proteins from plants: more than RNA N-glycosidases? FASEB **15:** 1493-1506

Phisalaphong M, Linden JC (1999) Kinetic studies of paclitaxel production by *Taxus canadensis* cultures in batch and semicontinuous with total cell recycle. Biotechnol Prog **15**: 1072-1077

Podleckis EV, Hammond RW, Hurtt SW, Hadidi A (1993) Chemiluminescent detection of potato and pome fruit viroids by digoxygenin labelled dot blot and tissue blot hybridization. J Virol Methods **43:** 147-158

Qiu J, Hallmann J, Kokalis-Burelle N, Weaver DB, Rodriguez-Kabana R, Tuzun S (1997) Activity and differential induction of chitinase lsozymes in soybean cultivars resistant or susceptible to root-knot nematodes. J Nematol **29:** 523-530

Rajamohan F, Venkarachalam TK, Irvin JD, Uckun FM (1999a) Pokeweed antiviral protein isoforms PAP-I, PAP-II, and PAP-III depurinate RNA of human immunodeficiency virus (HIV)-1. Biochem Biophys Res Commun **260:** 453-458

Rajamohan F, Kurinov IV, Venkatachalam TK, Uckun FM (1999b) Deguanylation of human immunodeficiency virus (HIV-1) RNA by recombinant pokeweed antiviral protein. Biochem Biophys Res Commun **263:** 419-424

Rajamohan F, Pugmire MJ, Kurinow IV, Uckun F (2000) Modeling and alanine scanning mutagenesis studies of recombinant Pokeweed antiviral proteins. J Biol Chem **275:** 3382-3390

Ramakrishnan S, Houston LL (1984) Inhibition of human acute lymphoblastic leukemia cells by immunotoxins: potentiation by chloroquine. Science **223:** 58-61.

Ready MP, Brown DT, Robertus JD (1986) Extracellular localization of pokeweed protein. Proc Natl Acad Sci USA **84:** 5053-5056

Reinbothe C, Tewes A, Lehmann J, Parthier B, Reinbothe S (1994) Induction by methyl jasmonate of embryogenesis-related proteins and mRNAs in *Nicotiana plumbaginifolia*. Plant Sci **104:** 59-70

Reinbothe C, Parthier B, Reinbothe S (1997) Temporal pattern of jasmonate-induced alterations in gene expression of barley leaves. Planta **201:** 281-287

Reinbothe S, Machmudova A, Wasternack C, Reinbothe C, Parthier B (1992a) Jasmonate-induced proteins in cotton: Immunological relationship to the respective barley proteins and homology of transcripts to late embryogenesis abundant (Lea) mRNAs. J Plant Growth Regul **11:** 7-14

Reinbothe S, Reinbothe C, Lehmann J, Rarthier B (1992b) Differential accumulation of methyl jasmonate-induced mRNAs in response to abscisic acid and desiccation in barley (*Hordeum vulgare*). Physiol Plant **86:** 49-56

Reinbothe S, Reinbothe C, Parthier B (1993) Methyl jasmonate represses translation initiation of a specific set of mRNAs in barley. Plant J **4:** 459-467

Reinbothe S, Reinbothe C, Lehman J, Becker W, Apel K, Parthier B (1994) JIP60, a methyl jasmonate-induced ribosome-inactivating protein involved in plant stress reactions. Proc Natl Acad Sci USA **91:** 7012-2016

Remi Shih NR, McDonald KA, Jackman AP, Girbes T, Lglesias R (1997) Bifunctional plant defense enzymes with chitinase and ribosome inactivating activities from *Trichosanthes kirilowii* cell cultures. Plant Sci **130**: 145-150

Reymond P, Farmer EE (1998) Jasmonate and Salicylate as global signals for defense gene expression. Curr. Opin. Plant Biol **1:** 404-411

Riesner D (1990) Structure of viroids and their replication intermediates. Are thermodynamic domains also functional domains? Sem Virology **1:** 83-99

Rippmann JF, Michalowski CB, Nelson DE, Bohnert HJ (1997) Induction of a ribosome-inactivating protein upon environmental stress. Plant Mol Biol **35:** 701-709

Ryan CA, Pearce G(1998) Systemin: a polypeptide signal for plant defensive genes. Annu Rev Cell Dev Biol **14:** 1-17

Sandvig K, van Deurs B (1996) Endocytosis, intracellular transport, and cytotoxic action of Shiga toxin and ricin, Physiol Rev **76:** 949-966

Savary BJ, Flores HE (1994) Biosynthesis of defense-related proteins in transformed root cultures of *Trichosanthes kirilowii* Maxim. Var *japonicum* (Kitam.) Plant Physiol **106:** 1195-1204

Savary BJ, Flores HE, Hill JJ (1997) Isolation of a class III chitinase produced in root cultures of *Trichosanthes kirilowii* and assessment of accumulation patterns and antifungal activity. Plant Physiol Biochem **35:** 543-551

Savino C, Federici L, Ippoliti R, Lendaro E, Tsernoglou D (2000) The crystal structure of saporin SO6 from *Saponaria officinalis* and its interaction with the ribosome. FEBS Lett **470:** 239-243

Schaller A, Ryan CA (1995) Systemin: a polypeptide defense signal in plants. BioEssays **18:** 27-23

Schaller GE, Ladd AN, Lanahan MB, Spanbauer JM, Bleecker AB (1995) The ethylene response mediator ETR1 *Arabidopsis* forms a disulfide-linked dimer. J Biol Chem **270:** 12526-12530

Schlumbum A, Mauch F, Vogeli U, Boller T (1986) Plant chitinases are potent inhibitors of fungal growth. Nature **324:** 36-367

Schrader O, Baumstark T, Riesner D (2003) A mini-RNA containing the tetraloop, wobble-pair and loop E motifs of the central conserved region of potato spindle tuber viroid is processed into a minicircle. Nucleic Acids Res **31:** 988-998

Schroeder R, Grossberger R, Pichler A, Waldsich C (2002) RNA folding *in vivo*. Curr Opin Sutruct Biol **12:** 296-300.

Sharma N, Park S-W, Vepachedu R, Barbieri L, Ciani M, Stirpe F, Savary BJ, Vivanco JM (2004) Isolation and characterization of an RIP-like protein from *Nicotiana tabacum* with dual enzymatic activity. Plant Physiol **134:** 171-181

Shaw JG, Plaskitt KA, Wilson TMA (1986) Evidence that tobacco mosaic-virus particles disassemble cotranslationally *in vivo*. Virology **148:** 326-336

Smirnov S, Shualev V, Tumer NE (1997) Expression of pokeweed antiviral protein in transgenic plants induces virus resistance in grafted wild-type plants independently of salicylic acid accumulation and pathogenesis-related protein synthesis. Plant Physiol **114:** 1113-1121

Song S-K, Choi Y, Moon YH, Kim S-G, Choi YD, Lee JS (2000) Systemic induction of a Phytolacca incularis antiviral protein gene by mechanical wounding, jasmonic acid, and abscisic acid. Plant Mol Biol **43:** 439-450

Steger G, Riesner D (2003) Molecular characteristics. In Hadidi,A. Flores,R. Randles,J.W. and Semancik,J.S. (ed.), *Viroids*. CSIRO Publishing, Collingwood, Australia, pp. 15-29

Stein A, Crothers DM (1976) Equilibrium binding of magnesium (II) by *Escherichia coli* $tRNA^{fMet}$. Biochemistry **15:** 157-160

Steeves RM, Denton ME, Barnard FC, Henry A, Lambert JM (1999) Identification of three oligosaccharide binding sites in ricin. Biochemistry **38:** 11677-11685

Stirpe F, Olsnes S, Pihl A (1980) Gelonin, a new inhibitor of protein synthesis, nontoxic to intact cells. J Biol Chem **255:** 6947-6953

Stirpe F, Williams DG, Onyon LY, Legg RF, Stevens WA (1981) Diathins, ribosome-damaging proteins with anti-viral properties from *Dianthus caryophyllus* L. (carnation). Biochem J **195**: 399-405

Stirpe F, Barbieri L, Battelli MG, Ralasca AI, Abbondanza A, Lorenzoni E, Stevens WA (1986) Bryodin, a ribosome-inactivating protein from the roots of *Bryonia dioica* L. (white bryony). Biochem J **240:** 659-665

Stirpe F, Barbieri L, Batelli MG, Soria M, Lappi DA (1992) Ribosome inactivating proteins from plants: present status and future prospects. Bio/ Technology **10:** 405-412

Stripe F, Barbieri L, Gorini P, Valbonesi P, Bolognesi A, Polito L (1996) Activities associated with the presence of ribosome-inactivating proteins increase in senescent and stressed leaves. FEBS Lett **382:** 309-312

Surolia N, Misquith S (1996) Cell surface receptor directed targeting of toxin to human malaria parasite, Plasmodium falciparum. FEBS Lett **396:** 57-61

Szewczak AA, Moore PB, Chan YL, Wool IG (1993) The conformation of the sarcin/ricin loop from 28S ribosomal RNA. Proc Natl Acad Sci USA **90:** 9581-9585

Taiz L, Zeiger E (1991) Ethylene and abscisic acid. *In* L Taiz, E Zeiger, eds, Plant Physiology. The Benjamin/Cummings Publishing Company, Redwood City, CA, pp 473-489

Tang S, Sie L, Hou F, Liu W-Y, Ruan K (2001) Non-specific deadenylation and deguanylation of naked RNA catalyzed by ricin under acidic condition. Biochim Biophys Acta **1519:** 192-198

Tanner MA, Cech TR (1996) Activity and thermostability of the small self-splicing group I intron in the pre-tRNA^{Ile} of the purple bacterium *Azoarcus*. RNA **2:** 74-83

Taylor S, Massiah A, Lomonossoff G, Roberts LM, Lord JM, Hartley M (1994) Correlation between the activities of five ribosome-inactivating proteins in depurination of tobacco ribosomes and inhibition of tobacco mosaic virus infection. Plant J **5:** 827-835

Tomlinson JA, Walker VM, Fleweet TH, Barclay GR (1974) The inhibition of infection by cucumber mosaic virus and influenza virus by extracts from *Phytolacca americana.* J Gen Virol **22:** 225-232

Tumer NE, Hwang DJ, Bonness M (1997) C-terminal deletion mutant of pokeweed antiviral protein inhibits viral infection but does not depurinate host ribosomes. Proc Natl Acad Sci USA **94:** 3866-3871

Tumer NE, Hudak K, Di R, Coetser C, Wang R, Zoubenko O (1999) Pokeweed antiviral protein and its applications. Curr Top Microbiol Immunol **240:** 139-158

Uchiumi T, Sato N, Wada A, Hachimori A (1999) Interaction of the sarcin/ricin domain of 23 S ribosomal RNA with proteins L3 and L6. J Biol Chem **274:** 681-686

Uckun FM, Yanishevski Y, Tumer N, Waurzyniak B, Messinger Y, Chelstrom LM, Lisowski EA, Ek O, Zeren T, Wendorf H, Langlie MC, Irvin JD, Myers DE, Fuller GB, Evans W, Gunther R (1997) Pharmacokinetic features, immunogenicity, and toxicity of B43(anti-CD19)-pokeweed antiviral protein immunotoxin in cynomolgus monkeys. Clin Cancer Res **3:** 325-337.

Ussery MA, Irvin JD, Hardesty B (1977) Inhibition of poliovirus replication by a plant antiviral peptide. Ann NY Acad Sci **284:** 431-440

Valbonesi P, Barbieri L, Bolognesi A, Bonora E, Polito L, Stirpe F (1999) Preparation of highly purified momordin II without ribonuclease activity. Life Sci **65:** 1485-1491

Valter CA, Bartle LM, Leszyk JD, Lambert JM, Goldmacher (1995) Ricin-A chain can be chemically cross-linked to the mammalian ribosomal-proteins L9 and L10E. J Biol Chem **270:** 12933-12940

Van Damme EJM, Hao Q, Chen Y, Barre A, Vandenbussche F, Desmyter S, Rouge R, Peumans WJ (2001) Ribosome-inactivating proteins: A family of plant proteins that do more than inactivate ribosomes. Critic Rev Plant Sic **20:** 359-465

Vepachedu R, Bais HP, Vivanco JM (2003) Molecular characterization and post-transcriptional regulation of ME1, a type I ribosome-inactivating protein from *Mirabilis expansa.* Planta **217:** 498-506

Verveliet G, Holsters M, Teuchy H, Van Montagu M, Schell J (1975) Characteristics of different plaque forming and defective temperate phages in *Agrobacterium* strains. J Gel Virol **26**: 33-48

Vivanco JM, Savary BJ, Flores HE (1999) Characterization of two novel type I ribosome-inactivating proteins from the storage roots of the Andean crop *Milabilis expansa*. Plant Physiol **119:** 1447-1456

Vivanco JM, Flores HE (2000) Control of Root Formation by Plant Growth Regulators. *In* AS Basra, ed, Plant Growth Regulators in Agriculture and Horticulture: Their Role and Commercial Uses. Food Products Press, An imprint of The Haworth Press, New York, pp 1-25

Vögeli U, Meins F Jr, Boller B (1988) Co-ordinated regulation of chitinase and β-1,3-glucanase in bean leaves. Planta **174:** 364-372

Wang J-H, Nie H-L, Huang H, Tam S-C, Zheng Y-T (2003) Independency of anti-HIV-1 activity from ribosome-inactivating activity of trichosanthin. Biochem Biophys Res Commun **302:** 89-94

Wang P, Zoubenko O, Tumer NE (1998) Reduced toxicity and broad spectrum resistance to viral and fungal infection in transgenic plants expressing pokeweed antiviral protein II. Plant Mol Biol **38:** 957-964

Wang P, Tumer NE (1999) Pokeweed antiviral protein cleaves double-stranded supercoiled DNA using the same active site required to depurinate rRNA. Nucleic Acids Res **27:** 1900-1905

Wassenegger M, Spieker RL, Thalmeir S, Gast F-U, Riedel L, Sänger HL (1996) A single nucleotide substitution converts potato spindle tuber viroid (PSTVd) from a noninfectious to an infectious RNA for *Nicotiana tabacum*. Virology **226:** 191-197

Wasternack D, Parthier B (1997) Jasmonate-signalled plant gene expression. Trends Plant Sci **2:** 302-307

Wirth SJ, Wolf GA (1992) Micro-plate colourimetric assay for endo-acting cellulase, xylanase, chitinase, 1.3-β–glucanase and amylase extracted from forest soil horizons. Soil Biol Biochem **24:** 511-519

Wong R, Ng TB, Chan SH, Dong TX, Xeung HW (1992) Chracterization of *Mirabilis jalapa* antiviral protein: a ribosome inactivating protein from *Mirabilis jalapa* L. Biochem Int **28:** 585-593

Wu X, Shaw JG (1997) Evidence that a viral replicase protein is involved in the disassembly of tobacco mosaic virus particles *in vivo*. Virology **239:** 426-434

Wyatt SE, Pan SQ, Kuć J (1991) β–1,3-glucanase, chitinase, and peroxidase activities in tobacco tissues resistant and susceptible to blue mould as related to flowing, age and sucker development. Physiol Mol Plant Pathol **39:** 433-440

Zamboni M, Brigotti M, Rambelli F, Montanaro L, Sperti S (1989) High-pressure-liquid-chromatographic and fluorimetric methods for the determination of adenine released from ribosomes by ricin and gelonin. Biochem J **259:** 639-643

Zarling JM, Moran RA, Haffar O, Sias J, Richmann DD, Spina CA, Myers DE, Kuelbeck V, Ledbetter JA, Uckun FM (1990) Inhibition of HIV replication by pokeweed antiviral protein targeted to $CD4^+$ cells by monoclonal antibodies. Nature **347:** 92-95

Zoubenko O, Uckun F, Hur Y, Chet I, Tumer NE (1997) Plant resistance to fungal infection induced by nontoxic pokeweed antiviral protein mutants. Nat Biotechnol **15:** 992-996

Zoubenko O, Hudak K, Tumer NE (2000) A non-toxic pokeweed antiviral protein mutant inhibits pathogen infection via a novel salicylic acid-independent pathway. Plant Mol Biol **44:** 219-229

Zhu Y, Qi Y, Xun Y, Owens R, Ding B (2002). Movement of *Potato spindle tuber viroid* reveals regulatory points of phloem-mediated RNA traffic. Plant Physiol **130:** 138-146

Zuker M, Mathews DH, Turner DH (1999) Algorithms and thermodynamics for RNA secondary structure prediction: A practical guide. In Barciszewski,J. and Clark,B.F.C. (ed.), *RNA Biochemistry and Biotechnology*. NATO ASI series, Kluwer Academic, Dordrecht, NL, pp 11-43

LIST OF ABBREBIATION

1. ABA : abscisic acid
2. BA : benzonic acid
3. CM : carboxymethyl
4. DMSO : dimethyl sulfoxide
5. ER : endoplasmic reticulum
6. GSP : gene specific primer
7. HIV : human immunodeficiency virus
8. HR : hypersensitive response
9. JA : jasmonic acid
10. JIPs : jasmonate-induced proteins
11. LBB : labeling-blocking buffer
12. LOX : lipoxygenase
13. MCP : methylcyclopropane
14. ME : *Mirabilis expansa* proteins
15. MeJA : methyl-jasmonate
16. ORF : open reading frame
17. PAP : poweed antiviral protein
18. PDA medium : potato-dextrose-agar medium
19. PR protein : pathogenesis-related protein
20. PSTVd : potato spindle tuber viroid
21. RACE : rapid amplification of cDNA ends
22. PCR : polymerase chain reaction
23. RIP : ribosome-inactivating protein

24. RTA : ricin A-chain
25. SA : salicylic acid
26. SAR : systemic acquired resistance
27. SDS-PAGE : sodium-dodecyl sulfate-polyacrylamide gel electrophoresis
28. SOD : superoxide dismutase
29. SPB : sorenson's phophate buffer
30. S/R loop : sarcin/ricin loop
31. SSO : small synthetic oligonucleotide
32. TCS : trichosanthin
33. TGGE : temperature gradient gel electrophoresis
34. YPD medium : yeast extract-peptone-dextrose medium